AD-A127 340 A STUDY OF LOW LEVEL LASER RETINAL DAMAGE(U) JOHNS HOPKINS UNIV LAUREL MD APPLIED PHYSICS LAB B F HOCHHEIMER 15 MAR 83 N00024-83-C-5301 1/2

UNCLASSIFIED F/G 20/5 NL

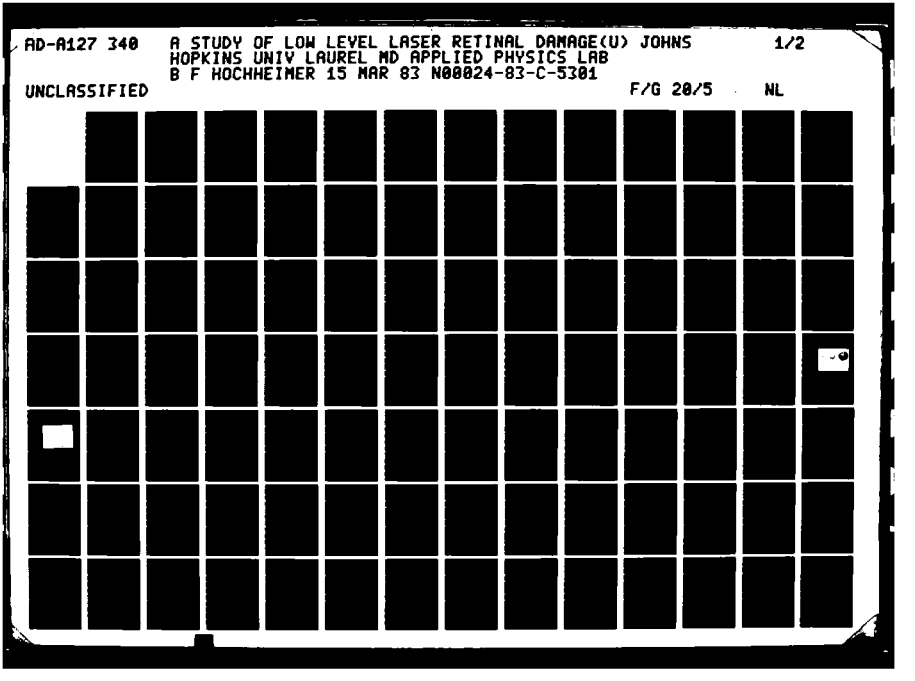

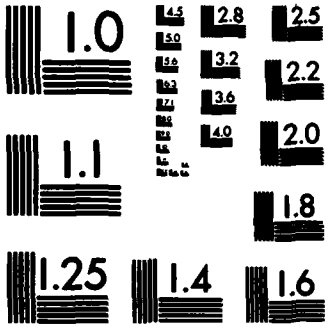

(12)

AD_____

ANNUAL

PROGRESS REPORT

for

U.S. ARMY MEDICAL RESEARCH AND DEVELOPMENT COMMAND
Fort Detrick, Frederick, Maryland 21701

from

RC-RCS-030
The Johns Hopkins University
Applied Physics Laboratory
Johns Hopkins Road
Laurel, Maryland 20707

on

A STUDY OF LOW LEVEL LASER RETINAL DAMAGE

Approved for public release; distribution unlimited

B. F. Hochheimer

March 15, 1983

AD_____

ANNUAL

PROGRESS REPORT

for

U.S. ARMY MEDICAL RESEARCH AND DEVELOPMENT COMMAND
Fort Detrick, Frederick, Maryland 21701

from

RC-RCS-030
The Johns Hopkins University
Applied Physics Laboratory
Johns Hopkins Road
Laurel, Maryland 20707

on

A STUDY OF LOW LEVEL LASER RETINAL DAMAGE

B. F. Hochheimer

March 15, 1983

SECURITY CLASSIFICATION OF THIS PAGE (When Data Entered)

REPORT DOCUMENTATION PAGE

READ INSTRUCTIONS BEFORE COMPLETING FORM

1. REPORT NUMBER: RC-RCS-030	2. GOVT ACCESSION NO.: AD A127 340
3. RECIPIENT'S CATALOG NUMBER:	
4. TITLE (and Subtitle): A Study of Low Level Laser Retinal Damage	5. TYPE OF REPORT & PERIOD COVERED: Annual Progress Report 5/1/81-12/31/82
	6. PERFORMING ORG. REPORT NUMBER:
7. AUTHOR(s): Bernard F. Hochheimer	8. CONTRACT OR GRANT NUMBER(s): N00024-83-C-5301
9. PERFORMING ORGANIZATION NAME AND ADDRESS: The Johns Hopkins University, Applied Physics Laboratory, Johns Hopkins Road, Laurel, Maryland 20707	10. PROGRAM ELEMENT, PROJECT, TASK AREA & WORK UNIT NUMBERS:
11. CONTROLLING OFFICE NAME AND ADDRESS: U.S. Army Medical Research & Development Command, Fort Detrick, Maryland	12. REPORT DATE: March 15, 1983
	13. NUMBER OF PAGES: 134
14. MONITORING AGENCY NAME & ADDRESS (if different from Controlling Office): Non-Ionizing Radiation Division, Letterman Army Institute of Research, Presido of San Francisco, California 94129	15. SECURITY CLASS. (of this report): Unclassified
	15a. DECLASSIFICATION/DOWNGRADING SCHEDULE:

16. DISTRIBUTION STATEMENT (of this Report)

Approved for public release, distribution unlimited.

17. DISTRIBUTION STATEMENT (of the abstract entered in Block 20, if different from Report)

18. SUPPLEMENTARY NOTES

19. KEY WORDS (Continue on reverse side if necessary and identify by block number)

Laser Retinal Damage

20. ABSTRACT (Continue on reverse side if necessary and identify by block number)

The general objective of this program is to document changes in the retina due to very low laser irradiation. We have two primary aims. One is to develop and improve methods that can be used, in vivo, to objectively determine changes that occur in the retina from laser irradiation. The second is to determine the mechanisms that cause these retinal changes.

During this past year we have:

DD FORM 1 JAN 73 1473 EDITION OF 1 NOV 65 IS OBSOLETE

SECURITY CLASSIFICATION OF THIS PAGE (When Data Entered)

1) Modified our equipment to do small retinal area reflectivity measurements;

2) Measured the internal light scatter in the eye for wavelengths from 450 to 850 nm;

3) Our fluoresence measurements project has proceeded to the point where we can measure many fluoresence parameters after a single injection of fluorescence;

4) Accurate measurement of spectral reflectivities of small areas of a laser damaged monkey retina have been proven to be feasible;

5) A photographic technique to improve the resolution and contrast of fluorescence angiograms ~~has been perfected~~;

6) Several dyes ~~are recommended~~ for use as dyed tear films for retinal protection from laser radiation.

FOREWORD

In conducting the research described in this report, the investigator(s) adhered to the "Guide for Laboratory Animal Facilities and Care", as promulgated by the Committee on the Guide for Laboratory Animal, Resources, National Academy of Sciences-National Research Council.

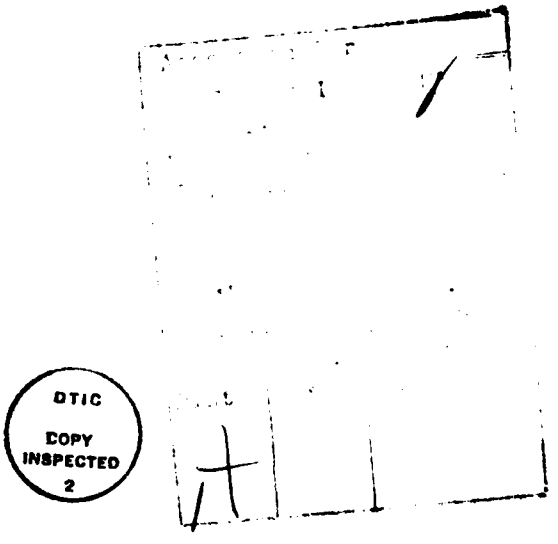

DISTRIBUTION:

Commander
U. S. Army Medical Research and Development Command
ATTN: SGRD-RMS
Fort Detrick, Frederick, Maryland 21701
4 copies

Defense Documentation Center (DDC)
ATTN: DDC-TCA
Cameron Station
Alexandria, VA 22314
12 copies

Superintendent
Academy of Health Sciences, U. S. Army
Fort Sam Houston, TX 78234
1 copy

Dean, School of Medicine
Uniformed Services University of Health Sciences
Office of the Secretary of Defense
4301 Jones Bridge Road
Bethesda, MD 20014
1 copy

Commander
Letterman Army Institute of Research
ATTN: SGRD-ULZ-RCM/Dr. Neville
Presido of San Francisco, CA 94129
5 copies

TABLE OF CONTENTS

LIGHT SCATTER IN THE EYE

INTRODUCTION

Light scatter in the eye is important in the project for two reasons. First we are using the measured reflectivity of the retina to infer the progression of light induced damage, the onset of retinal changes, and the damaged layers in the retina. In any measurement of retinal reflectivity, the quantity measured is energy reflected into the measuring system plus any energy that is scattered that reaches the measuring system. For accurate determination of retinal reflectivity the scattered components must either be reduced to an amount below our measurement accuracy or else be compensated for in post measurement calculations.

The second reason that scattered light is important is that it itself may be damaging to the eye when a laser beam is focused on the retina. When a high power laser beam impinges on the retina it may not only damage the area it hits, but it may damage a much larger area or possibly the whole retina.

For these reasons, we measured the scattered light in the eye and compared the scattering for coherent and incoherent light.

BACKGROUND

Boynton et al[1,2,3,4] in a study of glare in the eye, measured the scattered light in several animal species, mostly steer eyes but also cat and human eyes. The eyes studied were all enucleated eyes and corrections were made for post-mortem changes. Their results indicated that the amount of scattered light in the eye is proportional to the illuminated area and not the shape of that area. They also found that the amount scattered did not vary greatly with wavelength from 500 to 600nm nor did it depend on pupil size.

Their measurements showed that much of the incoming light is scattered, 70% of this from the cornea, 20% from the lens and 10% from the vitreous. They did not find any scattered component coming from the retina.

Vos et al [5,6,7] also in a study of glare sources in the eye concluded that the cornea contributes 30% of all scattered light and that the retina contributes an equivalent amount. Miller and Benedek[8] estimate that 25% of the total light scatter in the eye is from the cornea, 50% from the lens and 25% from the retina. They also quote LeGrand's[9] data indicating that 10% of all incoming light is scattered over the whole retina, this may be an incorrect quotation.

De Mott[10] and Campbell et al[11,12,13] measure the optical properties of the eye as it presents an image on the retinal surface. De Mott[10] quotes Hartridge[14] whose theoretical study of the optical property of the eye indicates that at the retinal image of a sharp edge the light levels should fall by two log units in two minutes of arc. De Mott, using images of wires or edges surrounded or bounded by a uniform light source, does not find this rapid fall in intensity; he used very large retinal illuminated areas and consequently had high internal light scatter in the eye. Campbell et al[11,12,13] used very narrow line sources of light (filament images) which are the inverse of De Mott's wires. He found that the retinal reflection showed a fall in light to 1% of the peak value at 6 1/2 minutes of arc away from the filament retinal image in one test and 16 minutes in another. He also showed that the fundus is a diffuse reflector which retains 80% of the polarizability, similar to an aluminized projection screen. Campbell's measurements of retinal spectral reflectivity indicates no evidence of any maximum or minimum from the reflection spectrum of hemoglobin except in albino rabbits. (This conclusion was also reached by Kornup[15]). Kraushopf[16] also used the data obtained from reflected line images on the retina to infer the eye's optical quality. He states that the scattered light falls

one log unit for every 4 1/2 minutes of arc and the drop in intensity is linear on a log plot.

Geeraets et al [17,18] have measured the spectral reflectivity of the retina as well as absorption and scattering in human, monkey and rabbit enucleated eyes. Hochheimer[19] and Flower et al[20] used a fundus photographic technique to measure spectral reflectivity. Their results are open to question because, as found by Flower[21], any area of the retina has 50% internal light scattered on it compared with the directly illuminated energy when the area measured is illuminated by a 30° cone of light. Alpern and Campbell[12] also measured the spectral reflectivity of the retina using the same techniques as did Brindley and Willmer[22]. All these methods give different results because the same area of the retina was not measured, different illumination area sizes were used and because of the variability of individual species.[20]

Boettner and Wolter[23] have measured the total transmission, including scattered light, and the direct, non-scattered transmission of the retina and choroid. They used enucleated eyes separated into its various components.

Fuek[24,25,26] has made a detailed study of the transmission and scattering of the rabbit cornea. His data shows an inverse wavelength to the 5th. power dependence, that is, the corneal scattering is greater in the blue than in the red by a factor of 10x. The angular dependence of forward scatter is also reported but only from 40 to 90° off the axis.

Boynton and Vos are measuring the properties of glare light in the eye and De Mott, Campbell and Krauskopf are concerned with the image forming optical properties of the eye. Geeraets, Hochheimer, Flower, Brindley and Wilmer, and Alpern and Campbell have all measured the spectral reflectivity of the eye and report widely varying spectral curves. Geeraets and Boettner have data on the absorption and reflectivity of the retina. Fuek (and many others including

Benedek,[27] Maurice[28] and Farrell[29])have reported on the corneal transmission and light scatter. Even with all of this data available, it is difficult to arrive at a thorough understanding of the light scattering properties of the eye. Most of the retinal light scatter measurements were done with "white" light and often in enucleated eyes. From any of the spectral data of Fuek, Geeraets, or Flower it is obvious that wavelength variations must be important. Boynton, Enoch and Bush[1] and others show wide variations between animal and human eyes. Measurements are often taken with variable, and sometimes not reported, areas of the retina illuminated. Nowhere is there reported any effect due to scatter of light inside the retinal, choroidal or scleral tissue.

Since almost all of the reports on light scatter in the eye were published prior to the discovery of the laser, no properties of the scatter of coherent radiation are even considered.

REQUIREMENTS

We wish to know the amount of light scattered in the eye especially for small angles and for coherent light. The scattering source in the eye may be the cornea, aqueous, lens, vitreous or the retina. In order to predict the amount and distribution of scattered light from any arbitrary source, it is necessary that the total scattering process is understood. This includes certain properties of the eye; how these vary with wavelength and how they interact with light. The transmission, absorption, reflection and scatter are all important. Since we are concerned with in-vivo situations, all experiments should be done in live animals to avoid changes that may occur in enucleated eyes.

In the experiments of Krauskopf[16] and De Mott[10] and Campbell[11] a small source is imaged on the retina and the retinal reflected and scattered light is measured. "White" light was used. Our experiments will be similar to these in that a small area of the retina is illuminated with monochromatic light and the

retinal reflected energy measured. For these measurements, it is important that back scattered light from the cornea, lens, aqueous and vitreous be eliminated and that back-scattered light in the optical system that is used is extremely low. It is also necessary that the retina be illuminated with a well-defined spot of light and the electronic recording equipment have very wide dynamic range. The elimination of back-scatter, wide dynamic range recording and the use of monochromatic light was not done in the above mentioned experiments.

METHODS

We use a modified Zeiss fundus camera to illuminate the retina and collect the return reflected energy. The light to illuminate the retina (See Fig. 1) is from a fiber optic light source. The end of the fiber is imaged at a reduced size in a plane conjugate to the retina. It is relayed by several lenses and mirrors to the cornea. There is a stop, conjugate to the cornea, which limits the light at the cornea to a ring 7mm OD and 3 1/2 mm ID. All of the original lenses in the Zeiss camera illumination system have been replaced with high quality photographic objectives so that the image of the fiber optics on the retina has negligible residual spherical and chromatic aberrations.

The reflected light from the retina is collected through an aperture whose image at the cornea is 1.5 mm in diameter. The input and return beams are thus separated at the cornea and also in the aqueous and at the lens. They are separated in the vitreous until they are within 1mm of the retina. Since the total vitreous contributes only a small measurable component of scattered light[2], this small region of interaction does not seem to be of any consequence.

There is only one lens common to both the input and reflected light paths. The incoming light reflected from the surface of this lens nearest the eye is imaged at a small internal black dot in this lens. The light reflected

from the rear surface of the lens images a central stop in the incoming light at the hole in the mirror that introduces the incoming light. Thus this lens does not contribute to optical system scattered light. We also have introduced a stop conjugate to the dot in the incoming light path so that it is not illuminated from the rear and we have a stop in the reflected light path to remove any residual effect of this dot.

The image of the fiber optic on the retina is approximately 75 microns in diameter and the quality of the edges is limited by aberrations and diffraction of the eye.

The energy reflected from the retina is collected by the first lens of the Zeiss camera and is limited by a stop just back of the perforated mirror. It is reimaged by a high quality enlarging lens to an aperture at the rear of the camera. At this aperture the retina is enlarged approximately 10x. The light going through the aperture can be viewed with a low power microscope; the aperture size is set so that it just encompasses the illuminated retinal area. The light from the aperture is relayed by an optical system through a rotating interference monochrometer to an S-20 response photomultiplier tube. The monochrometer has a spectral resolution of 17 nm from 400 to 700 nm and 35 nm from 700 to 1200 nm. The aperture relay lens system images the retinal relay enlarging lens on to the photomultiplier tube. This ensures that a constant area of the PMT tube face is used.

The last aperture, its relay lens system, the rotating interference monochrometer,and the photomultiplier tube and housing are all mounted on an X-Y positioning stage. The Y axis is changed with a high quality lab-jack table and the X axis with a lathe cross-slide. Thus the aperture can be moved anywhere over a 4 mm diameter area referred to the retina.

The PMT is powered with a regulated supply of 0 to 2000 volts and can be cooled thermoelectrically. The signal output is amplified with a Princeton Applied Research Model 113 low level preamplifier. The preamplifier has high accuracy,variable stepped,gain settings from 10 to 10,000. The preamplifier output is recorded on a strip chart recorder.

The optical-mechanical-electrical system meets all of our requirements for illuminating the retina and collecting and measuring the reflected light from the retina. It has no measurable back-scattered light and back-scattered light from the eye is negligible. A sharp image is formed on the retina, any wavelength from 400 to 850 nm can be selected,and a dynamic range of over 100,000 can be accomodated.

Measurements

1) Pre-Test

Although retinal distances and areas are given in this report, these are only approximately correct. We have measured only angular quantities, i.e., the angle subtended at the pupil of the eye. Retinal distances are computed assuming a 15 mm focal length monkey eye and correcting for the index of refraction of the vitreous, this was assumed to be 1.33. Angular calibration was done by placing a 50 cm focal length lens at the position normally occupied by the cornea and a millimeter scale at the lens focal plane. The low power microscope, used to view the retinal image plane,was focused on the scale and aperture diameter and cross slide distances were calibrated against the millimeter scale.

An artificial eye with a grey "retina" was illuminated with a small spot of light approximately 1° in diameter. The rear aperture was centered on this spot and closed until it was the same size as the spot image. The aperture was then scanned across the "retina" and intensity readings taken at discrete intervals. A plot of this data is shown in Fig. 2. There are two things to

note about this data, one, the ratio of the maximum to the minimum is over 1600, and two,that the convolution curve approximately fits the data at the top of the curve. The convolution curve is the convolution of two circles, it is the curve that would be expected if no scatter occurs. These two items will be compared with similar data on real eyes. This artificial eye was a cylinder 6 cm in diameter and 5 cm in length. It was painted black on the inside. The lens was new, with no scratches, and was clean.

This same lens was used with a grey paper at the focus and no artificial eye enclosure, the maximum to minimum ratio increased by over an order of magnitude.

The fiber optics "retinal" image was imaged in air using the same 5 cm focal length lens. Using a very small fiber optics tip and a radiometer the energy in the image was compared to the energy just outside the image, this ratio was over 10^6 to 1.

These tests show that our source image is sharp; it does not show spread at the edges. They also show that under suitable condition a minimum value of less than 10^{-4} of the maximum can be measured with our optical system.

2) Animal preparation

All of our tests were made using young cynomolgus monkeys. No previous experiments had been done with these animals and their eyes were very clear. The monkeys were sedated with Ketamine so that they could be handled. They were anesthetized with Halothane and positioned in front of the camera in a stereotaxic holder. The eyelids were held open with a child's lid retractor and a contact lens placed on the cornea. The contact lens prevents corneal drying.

White light was used to illuminate the retina for focusing. The forward and backward position of the animal was carefully done to eliminate reflected light from the cornea. The image of the fiber optics cable was focused on the retina and the white light turned off. The rear aperture was positioned over the retinal fiber optics illuminated area and closed so that it just encompassed this area.

3) Animal Tests

The rotating interference filter monochrometer (calibrated with a low pressure mercury arc and narrow bandwidth interference filters) was set for the desired wavelength and the photomultiplier voltage set to give near 100% strip chart reading with the preamplifier set to a gain of ten. The PMT voltages used were between 800 and 1200 volts.

The lathe cross slide, which holds the aperture, relay lens, monochrometer and PMT, was moved in 1/100 inch steps across the retinal image. Measurements were made at every 50mm from 500 to 800mm. All focusing was done using visible light, no corrections were made for chromatic abberations. One set of the strip chart measurements are shown in Fig. 3. Fig. 4 shows the resultant data curves for 500, 550, 600 and 650 nm. The data has not been normalized. Fig. 5 shows the same thing for 700, 750 and 800 nm.

4) Laser Tests

Similar tests were also done with the monochrometer center frequency set at 633 nm with white light illumination of the retina. The end of the fiber was then illuminated with a 632.8 nm HeNe laser and the test repeated. The laser was then positioned so that the microscope objective formed a focused laser spot instead of an image of the fiber optics. Without changing the retinal image aperture size, readings were again taken of intensity versus aperture position. This data is shown in Fig. 6.

Theoretical model for light reflected in the eye

The following derivation is similar to that used by Gouffe[30] to predict the blackbody characteristics of hollow cones and cylinder and Hochheimer[31] to predict the light emitted from jet aircraft engines.

Consider light incident on an area A of the retina; this area has a reflectivity R_A. The irradiance is W_A. Reflected from A is power P_A.

$$P_A = W_A A R_A$$

Some of this energy leaves through the pupil of the eye, this is given by

$$W_A A R_A \Omega_A \cos \Theta_A / \pi$$

where Ω_A is the solid single subtended by the pupil at A and Θ_A is the angle between the normal to A and a line from the center of A through the center of the pupil.

$$\Omega_A = \pi r^2 / D^2$$

$$K_A = \Omega_A \cos \Theta_A / \pi$$

where r is the pupil radius and D the diameter of the eye. The amount remaining in the eye is

$$W_A A R_A (1-K_A)$$

this amount is distributed uniformly over the inside of the such that

$$W_{a,1} = W_A A R_A (1-K_A)/S \qquad (1)$$

Where S is the area of the inside of the eye and $W_{a,1}$ is the reflected power per unit area a anywhere in the eye. If s is the pupil area and Y the area weighted reflectivity of the inside of the eye such that

$$Y = (AR_A + BR_B + CR_C + \text{---})/(S-s)$$

$W_A A R_A (1-K_A)Y$ is reflected, s/S times this value leaves the eye and (1- s/S)

remains. This amount is $W_{a,2} = W_A\ A\ R_A\ (1-K_A)\ Y\ (1-s/S)/S$ (2)

and it is distributed over the inside of the eye. Some of this is reflected and some leaves the eye. The amount remaining is

$$W_{a,3} = W_A\ A\ R_A\ (1-K_A)\ Y^2\ (1-s/S)^2/S \quad (3)$$

If we collect the terms (1), (2), (3)..... we get

$$W_A\ A\ R_A\ (1-K_A)\ [1 + Y\ (1-s/S) + Y^2\ (1-s/S)^2 + ...]$$

The bracketed section converges to $1/(1-Y(1-s/S))$. This implies that the power per unit area at any area a inside the eye due to internally reflected light is given by

$$Wa = \frac{W_A\ A\ R_A\ (1-K_A)}{S\ [1-Y\ (1-s/S)]}$$

while the power per unit area at A is

$$W_A\ \text{Total} = \frac{W_A A}{A} + \frac{W_A A\ R_A\ (1-K_A)}{S\ [1-Y\ (1-s/S)]}$$

$$= W_A\ \frac{1 + A\ R_A\ (1-K_A)}{S\ [1-Y\ (1-s/S)]} = W_A\ 1 + \frac{AR_A\ (1-K_A}{S\ \ 1-Y(1-s/S)}$$

The ratio of W_A Total to W_a

$$\frac{W_{A\ \text{Total}}}{W_a} = 1 + \frac{S\ [1-Y\ (1-s/S)]}{A\ [R_A\ (1-K_A)]}$$

Now consider some typical values for a monkey eye

$S = \pi D^2$ $\quad$ d = 1.5 cm = 15 mm

$s = \pi r^2$ $\quad$ r = 3.5 mm

$s/S \simeq \frac{1}{20}$ or $(1-s/S) \simeq 1$

$\Omega_A \simeq 0.17$

$\cos \Theta_A \simeq 1$

$K_A = 0.05$ or $(1-K_A) \simeq 1$

R_A is in the range of 1 to 10%.

Y is in the range of 1 to 10%.

$$\frac{W_{A\ Total}}{W_a} = 1 + \frac{S\ (1-Y)}{A\ R_A} = \frac{A\ R_A + S\ (1-Y)}{A\ R_A}$$

A for our experiments $\simeq 4 \times 10^{-5}$ cm^2

$R_A \simeq 0.05$

$A\ R_A = 2 \times 10^{-6}$

while

$S \simeq 7$ cm^2

$(1-Y) \simeq 0.95$

$S(1-Y) \simeq 7$ cm^2

so that A R_A is negligible with respect to S(1-Y), therefore

$$\frac{W_{A\ Total}}{W_a} \simeq \frac{S\ (1-Y)}{A\ R_A}$$

$$W_a = \frac{W_{A\ Total}\ A\ R_A}{S\ (1-Y)} = \frac{W_A\ A\ R_A}{S\ (1-Y)} + \frac{W_a\ A\ R_A}{S\ (1-Y)}$$

$$W_a << W_A$$

$$W_a \simeq (W_A\ A\ R_A)/[S\ (1-Y)]$$

To obtain approximate values assume $R_A = Y$ and R_A is in the range of 1 to 10%.

$$\frac{Wa}{WA} = \frac{A}{S}\ \frac{R_A}{1-Y} = 6 \times 10^{-8} \text{ if } R_A = 1\%$$

$$= 6 \times 10^{-7} \text{ if } R_A = 10\%$$

so that if W_A A is the total input power then

$$W_a = \text{Total input power x} \begin{cases} 10^{-3} \text{ if } R_A = 1\% \\ 10^{-2} \text{ if } R_A = 10\% \end{cases}$$

If the area used to measure W_a and W_A is A and if the total power measured at A is Q_A and at a is Q_a then

$Q_A = W_A A$ total input power and

$Q_a = W_a A$

or $Q_a = Q_A \times 6 \times 10^{-8}$ if $R_A = 1\%$

$= Q_A \times 6 \times 10^{-7}$ if RA = 10%

In our experiments the ratio of $Q_a / Q_A = \delta$ is the measured quantity with the maximum value normalized to one. The theoretical value of δ then should be

$$\delta = 6 \times 10^{-8} \text{ if } R = Y = 1\%$$
$$= 6 \times 10^{-7} \text{ if } R_A = Y = 10\%$$

when the area of the inside of eye that is illuminated is approximately one part in 10^5 of the total area of the eye. The only basic assumption that was made for this derivation is that the inside of the eye is a diffuse, completely scattering surface. It does not take into account any scattering in the cornea, lens, aqueous or vitreous.

Discussion

1) Retinal Reflectivity

The theoretical model for light scatter includes a term for the reflectivity of the retina over the illuminated area and the area weighted average retinal reflectivity. Both of these terms probably lie in the range of 1 to 10% and vary with wavelength. The reflectivity of the retina has been measured by Hochheimer,[19] Vos, et al[43] Geeraets and Berry,[18] Brindley and Willmer,[22] Alpern and Campbell[12] and Flower et al[20] for both monkey and human eyes. This data, plotted in Fig. 7, has wide variations. Our most recent results are also plotted in Fig. 7, our curve seems to fall approximately in the midst of all the rest of the data.

2) Discussion of our Data

The total scattered light curves show a fall off in energy from the central peak leveling off at approximately 3 or 4°. Consider first the data for 500 nm as shown in Fig. 8. The dotted curve shows what would be expected if no scatter occurred, it is just the convolution of two circles as they are separated. Although these curves are both normalized to coincide at zero it is

not necessarily true that all of the energy at zero degrees is due to direct illumination.

When the retina is illuminated with light, some of this light is scattered by the lens, cornea, vitreous and aqueous, some is internally scattered by the partially reflecting retina and some is internally scattered in the retina, pigment epithelum, choroid and sclera. Corneal scattering curves have been measured by Kikkawa[32] and his data is also indicated in Fig. 8. It is assumed that the cornea scatters approximately 10% of the total input energy and the lens contributes about the same amount,and that the convolution data should make up 80% of the total. When these are added together they should approximate our data. This approximation is shown in Fig. 9 for our data at 500 nm. At 500 nm, the fit is not too bad. When a constant energy term, (.006 x the maximum value) is added to the corneal scatter-convolution term the fit to the 500 nm data is very good except near the peak of the curve.

My interpretation of these results is that most of the energy can be accounted for by the convolution term at the center and optical element scatter in the wings. Some energy (.006 x the maximum value) is internal reflected energy and the remaining energy near the peak is internal scattered light in the choroid and sclera. Any computation of this last mentioned internal scattered light is impossible to do with any accuracy because it involves the subtraction of two large numbers to yield a small value. A similar analysis can be done for the 550, 600, 650 and 700 nm curves however, for the 700 nm data, this results in a large internal contribution term.

Corneal scatter is proportional to the inverse third power of the wavelength[29] and small particle scattering proportional to the inverse fourth power.[33] Scattering at 800 nm should therefore be less than 25% of that at 500 nm. With this in mind, the same analysis that was used with our 800 nm data that was used at 500 nm. See Fig. 10. The combination of convolution-

corneal scattering produces a curve which is not even close to the actual data. With a constant (10% of peak value) term added so that the predicted and actual data curves meet at 3° off axis, there is a very large discrepancy at all other angles. The same thing happens if the actual data at 750 nm is used.

It was suggested by several physicist here at APL (Richard Farrell and Russel McCally) that my data did not go to large enough field angles. With a different monkey than was originally used, a second set of data was taken. This data is shown in Fig. 11. The curves are similar in shape to our other data, they level off at 3 or 4°. The lowest values are lower than the previous set, this is probably due to animal to animal variations.

3) A Comparison with the Theoretical Model

Our theoretical model is similar to that of Gouffe[30] who used his derivation to successfully predict the emission from blackbody sources and to that of Hochheimer[31] who used his derivation to successfully predict the power radiated by jet aircraft engines. When our derivation is applied as a limiting case of an integrating sphere, the results are correct. We therefore have some confidence in the theoretical predictions. However, when applied to our data there seems to be no correlation. The theoretical model predicts a low value leveling off of our curves at 10^{-6} to 10^{-7} of the maximum value for internal retinal reflectivities of 10 to 1%. These values of reflectivity seem reasonable even with the spread in values shown in Fig. 7. Our data indicates a low value of 10^{-1} for 800 nm and 10^{-2} to 10^{-3} for shorter wavelengths.

4) Transmission of the eye

If we knew the amount of light transmitted by the eye directly, that is not scattered, we could deduce an upper limit for the amount of scattered light. Wiesinger et al[34] measured the transmission of rabbit eyes and found it to be 85% at 450 nm and rising to 95% at 680 nm and falling to 91% at 860 nm. They used

a 5 mm diameter opening in the back of the rabbit eye, this amounts to a 15° collection angle, hardly the directly transmitted light. Geeraets et al[17] did similar measurements, they used a 9 mm diameter opening. Geeraets and Berry[18] did measurements on monkey, human and rabbit eyes again with a 9 mm diameter opening.

Boettner and Wolter[23] measured the direct (within 1°) and total(direct + scattered) transmission of various sections of enucleated eyes. For the cornea they show a total transmission of about 90% from 400 to 850 nm and a direct transmission of 40% at 400 nm rising to 70% at 800 nm. It is difficult to imagine that the energy scattered at angles greater than 1° from the cornea is approximately 1/2 the incident energy. Their measurements for the total light reaching the retina indicate a value of 80% from 450 to 850 nm and the direct transmittance 35% at 450 and 50% at 850 nm.

5) Other Measurements of Scattered Light in the Eye

Boynton et al[1] measured the stray light in excised steer, cat and human eyes by scanning a light source over the retina and measuring the light going through a hole cut in the back of the retina. They illuminated an area 4.76° in diameter and used an aperture of 1.5 mm diameter, the aperture subtended about 4° in a steer eye. The stray energy vs. angle graphs look similar to our data except that the low energy value occurs at over 20° and amounts to 1 part in 10^3 of the maximum value. Their experimental procedure differs from ours in that they use a single pass through the eye and we use a double pass, that is we measure the return energy. When they cut a second hole in the back of the eye to let the image out, not hit the retina, they coul. detect no change in stray light. They concluded that reflected light is unimportant.

These experiments were repeated by DeMott and Boynton[3] with essentially the same results. They also did scattering measurements at 5° as a function of wavelength, the wavelength going from 460 to 640 nm. Some eyes showed small variations, others showed none.

Fry and Alpern[35] measured the effect on visual brightness from a glare source. They concluded that the stray energy on the retina from a glare source of light varied as the inverse of the angle between the glare source and the fovea to the 2.5 power. They quote Stiles and Dunbar[36] as determining the exponent to be 2 instead of 2.5.

Vos [5,6,7] in a series of papers on entoptic stray light concluded that the cornea contributes 25%, the retina 25% and the other optical components of the remainder. He also concluded that the entoptic stray light is independent of the eccentricity of incidence.

Westheimer and Campbell[13] and Kraushopf[16] measured the image forming characteristic of the eye by imaging a line source on the retina and measuring the distribution of light in the retinal reflected image. Their technique was very similar to what was used in the project. It is unfortunate that their data is all plotted on linear scales and low energy values at large angles are therefore not obtainable. DeMott[10] used the inverse of a line source, a black line on a bright background. His experiments indicate a very large value for scattered light because of the large area of the retina is illuminated. The energy in the image of an edge falls by one log unit in 0.5° and does not agree with theoretical calculations of the image quality of the eye performed by Hartridge.[14]

6) Comparison of our data with other published data.

Fig. 12 shows the scattered light data of DeMott and Boynton for a human eye. Also plotted on this curve is the fall off that would be expected if stray light had the $1/\theta^2$ distribution predicted by LeGrand.[9] Our data for 500 nm is also shown. As can be seen from Fig. 12 our data for visible light (500-700nm) agrees fairly well with that of Boynton or Fry. It also agrees with Boynton's conclusion that there is little variation with wavelength over the visible spectrum.

When our data for 500 nm is compared with what could be expected from a combination of a convolution of two circles combined with the corneal scatter predicted by Kikkawa and a small amount of internal retinal scatter as predicted by Vos or LeGrand the agreement is also quite good.

If the value for constant glare, as predicted by LeGrand,[9] is corrected for the illuminated area difference, that is

$$E\ (\text{glare}) = 800\ E\ (\text{Illumination})\ (0.5^\circ\ \text{field})$$

$$E\ (\text{glare}) = 800 \times \left(\frac{0.5}{0.836}\right)^2\ E\ (\text{Illumination})\ (0.835^\circ\ \text{field})$$

$$E\ (\text{glare}) = 287\ (\text{Illumination})\ (0.835^\circ\ \text{field})$$

then the predicted glare value is 0.003 of the maximum value. Our measured constant energy term is 0.006 of the maximum value. This agreement is excellent considering the different approaches taken and the different types of eyes measured.

For visible wavelengths, our data seems in reasonable agreement with what was found by others with the exception of the lack of retinal reflected light found by Boynton et al. Because of this agreement, we believe our data for 750 and 800 nm also to be correct.

7) The Total Amount of Scattered Light in the Eye.

LeGrand says that for a 1/2 degree source there is uniform scatter

over the retina equal to 1/800 of the power at the illuminated area. A 1/2 degree diameter area is about 1 part in 10^5 of the total retinal area. If the total area is illuminated with 1 part in 10^3 of the directly illuminated area there must be 100 times as much energy spread over the whole retina as is in the directly illuminated area.

Boynton indicates from his curves that the scattered light over the inside of the eye could be 1 part in 1000 of the value of the illuminated area. His illuminated area is one part in 500 of the total retina. This indicates that 1/2 the total energy may be scattered light.

Flower[37] determined that with a normal Zeiss fundus camera, which illuminates a 30° angle in the eye, that of the total light coming from the illuminated area 50% is scattered energy. He found this value by comparing the retinal photographs of large area and small area illuminated photographs. A 30° angle illuminates about 10% of the total retina. The total light scattered over the retina could be 5x the directly illuminated energy on the retina.

De Mott[10] in his measurements of the reflected energy from the retina when an edge is illuminated or with a black bar-white background target also indicates that a great deal of the energy impinging on the retina is scattered over large angles.

Our theoretical calculations indicate that for a retinal illumination of 10^{-4} of the total retinal area only one to 10% ought to be reflected over the entire inside of the eye. Our experimental data (500 nm) would indicate that the retinal illumination is 1 part in 200 of the illuminated area. This would imply 50 times as much total scattered energy as direct energy. The theory accounts only for reflected energy, it does not include scattered light.

The fact that transmission measurements in the eye indicate a high (~90%) transmission does not conflict with any of the above data since large

solid angles were used in the measurements, 15 or 20° included angles were often used.

While the data of Boettner and Wolter is in conflict with that of Farrell et al[29] in that Farrell measures a direct transmission of the cornea of well over 90% and Boettner a much lower value, our data is in agreement with Boettner and Wolter.

Miller and Benedek[8] say that the cornea scatters 10% of the incident energy. They also say that the cornea contributes 25% of the scatter, the fundus 25% and the lens 50%. If the cornea scatters 10% then the fundus must also scatter 10% and the lens 20%. If a 10% value is assigned to all other scattering sites then 50% of incident light on the eye is scattered.

Thus even considering only visible light if a small area of the retina is directly illuminated the total amount of light impinging on the rest of the retina may be 1/2 to over 10 times the directly illuminated power.

We have no data from other sources to compare with ours for 750 or 800 nm. Since corneal scatter should be almost negligible here, we must conclude that the retinal reflected energy combined with the scattered energy from the lens is very high. The shape of the curves (Fig. 5) would also indicate a large internal retina-choroid-sclera scatter, covering several degrees.

8) Comparison between Coherent and Incoherent Illumination

Since the fiber optics illuminated curves (Fig. 6) from filtered white light and 632.8 nm HeNe laser light are almost identical, within our measurement accuracy, temporal coherence seems to have no effect. When the laser illuminates the retina directly the curves fall off to a much lower value. This is to be expected since the illuminated area is small compared to the measuring area.

We therefore believe that spatial coherence is of no consequence in entoptic light scatter.

9) Color of Small areas in a Retinal Photograph

Hochheimer[19] and Flower et al[20] have both used bandwidth limited retinal photographs to determine the spectral reflectivity of retina. Flower made measurements on the arteries and veins of three human and one monkey retina. His curves would indicate that the arteries (or veins) of all of these retinas vary widely in color. We have examined color photographs of all of these subjects.[38] Over or near the disc all of the arteries (or veins) are the same color for all of the different subjects. Over the rest of the retina the arteries (or veins) seem to take on the same color as the background, pigmented color, of the retina.

In order to determine if the color change is due to internal scattered light, a series of color retinal photographs were taken with large to small retinal illuminated areas. These are shown in Fig. 13. The flash exposure for the largest illuminated area is setting 1 on a 260P power supply and is setting 4 for the smallest illuminated area. The total scattered light in the eye should be proportional to the illuminated area and if the reflected light from a small retinal area is measured as the illuminated area is increased, the measured energy value will also increase and can be expressed as

$$E_{\text{energy}} = \text{Constant}\ (1 + \text{Constant} \times \text{Area})$$

In the last yearly progress report we described an experiment to test this hypothesis. The retina was illuminated with white light over areas that were varied over wide values, the maximum retinal area was $3\ mm^2$. The sampled retinal area was small and centered with respect to the illuminated area.

The data was plotted and a straight line drawn through the largest energy values. This supplied constants for the equation.

$$\text{Energy} = 91\ (1 + 0.004\ \text{Area})$$

The accuracy was such that the 0.004 value is not well known, it lies between 0.003 and 0.006.

From flash 1 to flash 4 for the Zeiss power supply the energy output varies by about a factor of 5. The smallest area differs from the largest area by a factor of 400. The theoretical expression, with measured constants, would predict a difference in retinal reflected energy due to scattering from the largest to the smallest areas of 2.6X. The photographic exposures of smallest and largest areas are probably the same within a factor of 2. Flower's statement that over one half the reflected light in a retinal photograph is scattered is true. This again verifies that the scattering in the eye is very high.

Boynton et al[1] in his steer eye experiments found a similar increase in what was essentially the same type experiment that we did. The illuminated area was increased by 19X and the energy through the illuminated hole increased by 14%. Our formula would predict an 8% increase.

Fig.14 is a composite photograph that shows the change in color of a vein as the illuminated area is decreased. On the original positive slides, the color change is somewhat more pronounced than is seen in the reproduction. Even with this small of an area of illumination, the vein still has some of the color of the background indicating that scatter still exists.

In Fig. 13, when the illuminated area is a considerable fraction of the area photographed, a large amount of flare energy can be detected as background in the non-illuminated area. The blue color is likely due to the high blue film sensitivity at low exposure levels and the high blue content of the

xenon flash lamp.

10) Consequences of high valves of scattered light

If the total scattered light in the eye really is as high as it seems to be from the data of LeGrand, Bounton, Fry, Vos or ours and does increase dramatically in the near infrared there are several consequences.

A. The quantum efficiency of the eye has been determined to be only several percent.[39] Scattering could account for this low value.

B. The energy needed to cause laser retinal damage rises in the near infrared.[40] If much of the input light is scattered away from the laser impact area, this rise would be accounted for.

C. It is very surprising that our vision is as good as it is.

Conclusions

1) There are no differences in entoptic scatter between coherent and incoherent illumination.

2) A very large percentage of light impinging on the cornea is scattered before and after reaching the retina.

3) Because of the large acceptance angles the data for light transmission in the eye is unreliable.

4) Because of light scatter in the eye retinal reflectance measurements are inconsistent and unreliable.

5) The scatter in the eye due to retinal reflectance is low in the visible but probably very high in the near infrared.

6) The shape of gallium arsenide laser burns, as found by Beatrice and Lund,[41] could be accounted for by entoptic light scatter.

7) Gallium arsenide or neodymium laser energy is much more likely to effect the whole retina, not just where it is directly illuminating, than is a visible laser.

8) Color indications of small retinal areas from retinal photographs are likely to be misleading, the pigment epithelium exerts a large influence.

9) Laser pan-retinal photocoagulation may have an effect over the whole retina because of the very large number of individual burns.

10) Focal ERG measurements are greatly influenced by scattered light even for very small areas of illumination (see also ref. 42).

Future Areas of Research

It is expected that our laboratory at Wilmer Institute will be moved to a different room in the very near future. When this occurs, we will adapt our argon ion laser to make scattering measurements when the laser energy is impinging on a coagulated area.

We are also exploring the possibility of using a silicon diode detector in place of the photomultiplier in order to go to longer wavelengths. We will then investigate in more detail the 700 to 1000 nm region to see if there are any unexpected changes with wavelength.

Figure Captions

Fig. 1

A. Optical, Mechanical and electronic system for recording light scatter in the eye.

B. Optical paths for illumination and recording beams in the eye. For simplicity all refraction was considered to take place at the cornea. The overlapping beams are shown only for centered beams, non-co-axial beams will also overlap but only partially so.

Fig. 2

Scattering data in an artificial eye. Also shown is the expected curve if only the convolution curve of the overlapping of two circles occurred.

Fig. 3

A typical strip chart record of the light scattering data for 650 nm.

Fig. 4

Non-normalized scattering curves for 500, 550, 600 and 650 nm.

Fig. 5

Non-normalized scattering curves for 700, 750 and 800 nm.

Fig. 6

Scattering curves for filtered white light at 633 nm and for HeNe (633 nm) fiber optics retinal illumination. Shown also is the curve where the laser directly illuminates the retina.

Fig. 7

Retinal reflection curves taken from many sources for monkey or human subjects. Note the wide variation in the data.

Fig. 8

Data for 500 nm scattering plus the corneal scattering as predicted by Kikkawa and the curve for the convolution of two circles.

Fig. 9 — The curve is the scattering data for 500 nm. The data points are for terms made up of 80%. convolution curve, 20% corneal scattering and 0.6% constant term. The data points fit the curve very well except near the peak. This difference is believed to be due to internal retinal, choroidal and scleral scattering.

Fig. 10 — This curve is for 800 nm, similar to Fig. 9. 95% convolution curve, 5% corneal scattering and a 10% constant term make up the data points. Note the large discrepancy.

Fig. 11 — Curves similar to fig. 4 and 5 for 500, 600, 700 and 800 nm. Data is normalized and is extended to 7°. This data is not for the same animal used for fig. 4 and 5.

Fig. 12 — The 500 nm data from Fig. 11 along with the curve of De Mott and Boynton for a human eye and a $1/\Theta^2$ fall off in glare as predicted by LeGrand or Fry. Fry predicted a $1/\Theta^{2.5}$ fall off.

Fig. 13 — A composite of color monkey retinal photographs with different areas of the retina illuminated. The large area of illumination was taken with Flash 1 while the smallest area was taken with Flash 4, a factor of five variation in retinal energy per unit area.

Fig. 14 — A side by side comparison of a vein taken with large and small area illumination. Note the color shift and the variation in color of the veins and arteries over the disc and over the rest of the retina.

1. Boynton, R. M., Enoch, J. M. and Bush, W. R.

"Physical Measures of Stray Light in Excised Eyes"
JOSA 44, 879, (1954)

2. Boynton, R. M. and Clarke, F. J. J.

"Sources of Entoptic Scatter in the Human Eye"
JOSA, 54, 110, (1964)

3. DeMott, D. W. and Boynton, R. M.

"Retinal Distribution of Entoptic Stray Light"
JOSA 48, 13, (1958)

4. DeMott, E. W. and Boynton, R. M.

"Sources of Entoptic Stray Light"
JOSA 48, 120, 1958

5. Vos, J. J. and Boogaard, J.
"Contribution of the Cornea to Entoptic Scatter"
JOSA 53, 869, (1963)

6. Vos, J. J. and Bouman, M. A.

"Contribution of the Retina to Entoptic Scatter"
JOSA 54, 95, (1964)

7. Vos, J. J.

"Contribution of the Fundus Oculi to Entoptic Scatter"
JOSA 53, 1449, (1963)

8. Miller, D. and Benedek, G.

Intraocular Light Scattering
Charles C. Thomas, Springfield, Ill. 1973

9. LeGrand, Y.

"Essai sur la diffusion de la lumiere dans l'oeil"
Rev Opt 16, 201 and 241,(1937)

10. DeMott, D. W.

"Direct Measure of the Retinal Image"
JOSA 49, 571,(1959)

11. Campbell, F. W. and Gubisch, R. W.

"Optical Quality of the Human Eye"
J. Physiol. 186, 558, (1966)

12. Alpern, M. and Campbell F. W.

"The Spectral Sensitivity of the Consensual Light Reflex"
J. Physiol. 164, 478, (1962)

13. Westheimer, G. and Campbell, F. W.

"Light Distribution in the Image Formed by the Living Human Eye"
JOSA 52, 1040, (1962)

14. Hartridge, H.

Phil. Trans. Roy. Soc. London B232, 519, (1947)

15. Kornerup, T.

"An Investigation, in Successively Variable Monochromatic Light, of Vessels of the Human Eye in Diseased Conditions"

Acta Ophthal. Supp XXVIII, Vol. 4.

16. Krauskopf, J.

"Light Distribution in Human Retinal Images"
JOSA 52, 1046, (1962)

17. Geeraets, W. J., Williams, R. C., Chan G., Ham, W. T., Guerry, D., and Schmidt, F. H.

"The Loss of Light Energy in Retina and Choroid".
Arch Opthal. 64, 158/606, (1960)

18. Geeraets, W. J. and Berry, E. R.

"Ocular Spectral Characteristics as Related to Hazards from Lasers and Other Light Sources".

AJO 66, 15, (1968)

19. Hochheimer, B. F.

"Light Reflected from Small Areas of a Monkey Retina".
J. Bio. Photo. Assn. 45, 146,(1977)

20. Flower, R. W., McLeod, D. S. and Pitts, S. M.

"Reflection of Light by Small Areas of the Ocular Fundus"
Invest Opthal. and Vis. Sci. 16, 981,(1977)

21. Flower, R. W.

"Wide Field versus Small Field Fundus Photography"
J. Bio. Photo Assn. 46, 15,(1978)

22. Brindley, G. S. and Willmer, E. N.

"The Reflexion of Light from the Macular and Peripheral Fundus Oculi in Man"
J. Physiol. 116, 350,(1952)

23. Boettner, E. A. and Wolter, J. R.

"Transmission of the Ocular Media"
Invest Ophth. 1, 776,(1962)

24. Fuek, T.

"On the Transparency of the Stroma in the Manmalian Cornea"
IEEE Trans. Bio. Med. Eng. 17, 186, (1970)

25. Fuek, T.

"The Wavelength Dependence of Scattered Light Intensity in the Rabbit Cornea"
IEEE Trans. Bio. Med. Eng. 18, 92, (1971)

26. Fuek, T. and McQueen, D.

"The Angular Dependence of Light Scattered from Rabbit Corne
Invest Ophthol. 10, 294, (1971)

27. Benedek, G.

"Theory of Transparency of the Eye"
Appl. Optics 10, 459,(1971)

28. Maurice, D. M.

"The Structure and Transparency of the Cornea"
J. Physiol 136, 263, (1957)

29. Farrell, R. A., McCally R. L. and Tatham P.E.R.

"Wave-Length Dependencies of Light Scattering in Normal and Cold Swollen Rabbit Corneas and their Structural Implications"

J. Physiol 233, 589,(1973)

30. Gouffe A.

"Corrections d'Ouverture des Corps-noirs Artificiels Compti tenu des Diffusions Multiples Internes"

Rev Opt 24, 1, (1945)

31. Hochheimer, B. F.

"Radiation Pattern for A Diffuse Wall Cavity, Nonuniform in Temperature and Emissivity"

Appl. Opt. 16, 2038,(1977)

32. Kikkawa, Y.

"Light Scattering Studies of the Rabbit Cornea"

Jap J. Physiol 10, 292, (1960)

33. Born, M. and Wolf, E.

Principles of Optics
Pergamon Press, N. Y., 1959.

34. Wiesinger, H., Schmidt, F. H., Williams, R.C., Tiller C.O. Ruffin, R. S. Guerry, D., Ham, W. T.

"The Transmission of Light Through the Ocular Media of the Rabbit Eye"

A. J. O. 42, 907,(1956)

35. Fry, G. A. and Alpern M.

"The Effect of a Peripheral Glare Source upon the Apparent Brightness of an Object"

JOSA 43, 189, (1953)

36. Stiles, W. S. and Dunbar C.

Illum Res Comm (Great Britain) Tech Paper No. 16, (1935)

37. Flower, R. W.

"Wide Field versus Small Field Fundus Photography"
J. Bio. Photo Assn. 46, 15, (1978)

38. Flower, R. W. private communication

39. Rose, A.

Vision, Human and Electronic

Plenum Press, New York 1974

40. Sliney,D. and Wolbarsht,M.

Safety with Lasers and Other Optical Sources

Plenum Press, N. Y., 1980

41. Beatrice E. S. and Lund, D. J.

"Characteristics of Damage Produced by Non-Circular Retinal Laser Radiation"

LAIR Report #31

42. Armington, J. C.

The Electroretinogram

Academic Press, New York 1974

43. Vos, J.J., Munnik, A.A. and Boogaard, J.

"Absolute Spectral Reflectance of the Fundus Oculi"

JOSA, 55, 573, (1965)

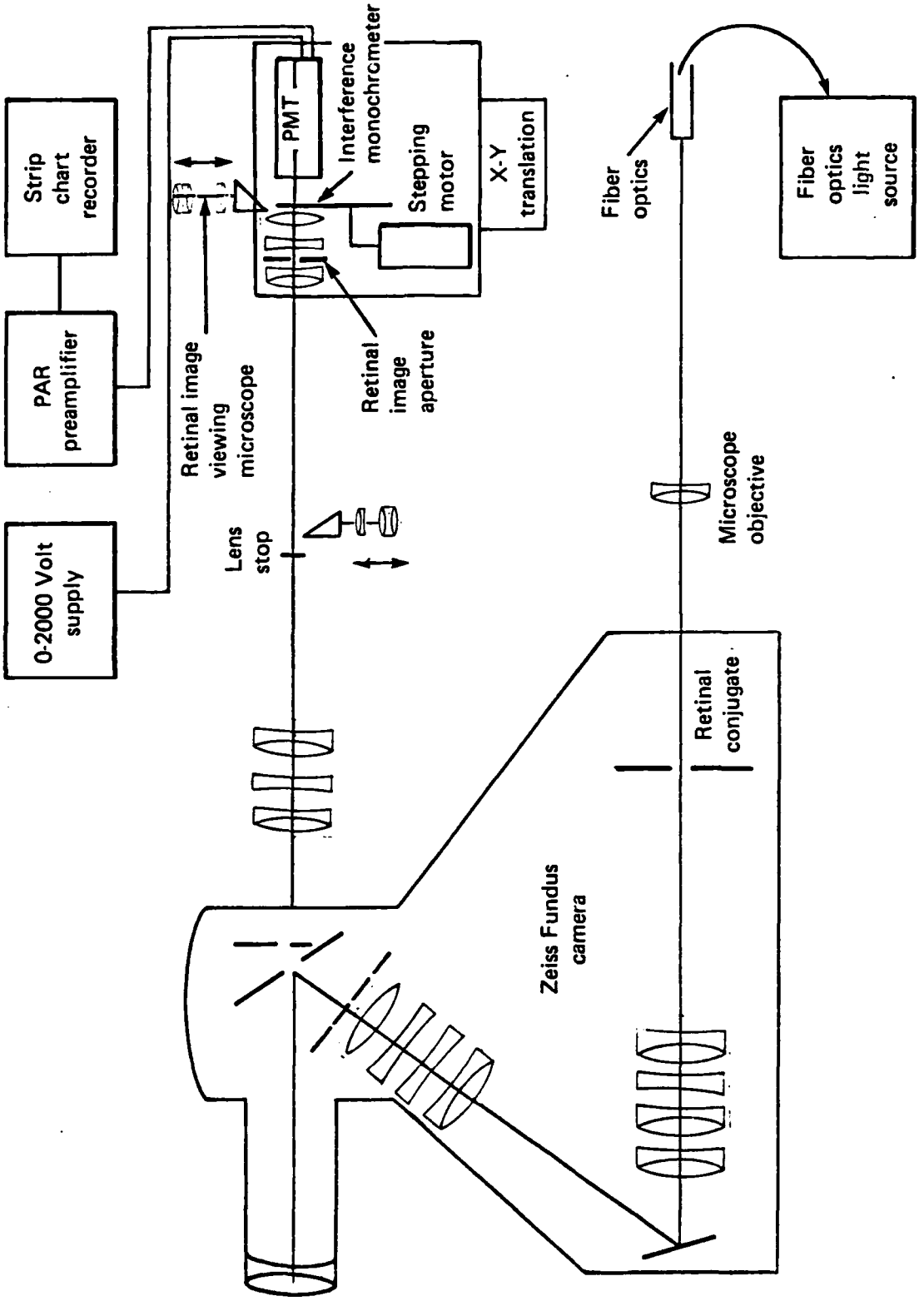
Strip chart recorder
PAR preamplifier
0-2000 Volt supply
Retinal image viewing microscope
PMT
Interference monochrometer
Stepping motor
X-Y translation
Retinal image aperture
Lens stop
Fiber optics
Fiber optics light source
Microscope objective
Retinal conjugate
Zeiss Fundus camera

Fig. 1A

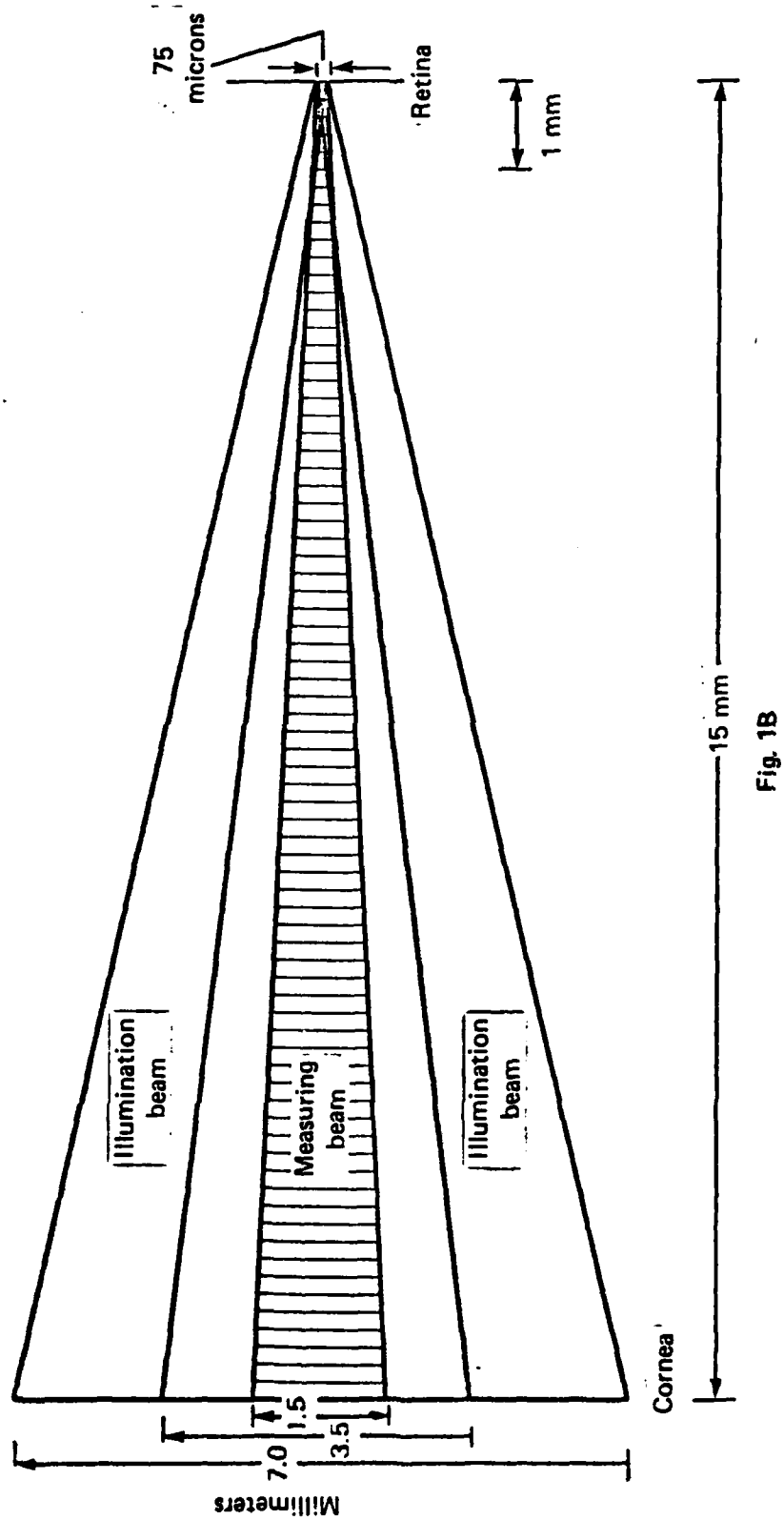
75 microns
Retina
1 mm
15 mm
Illumination beam
Measuring beam
Illumination beam
Cornea
1.5
3.5
7.0
Millimeters

Fig. 1B

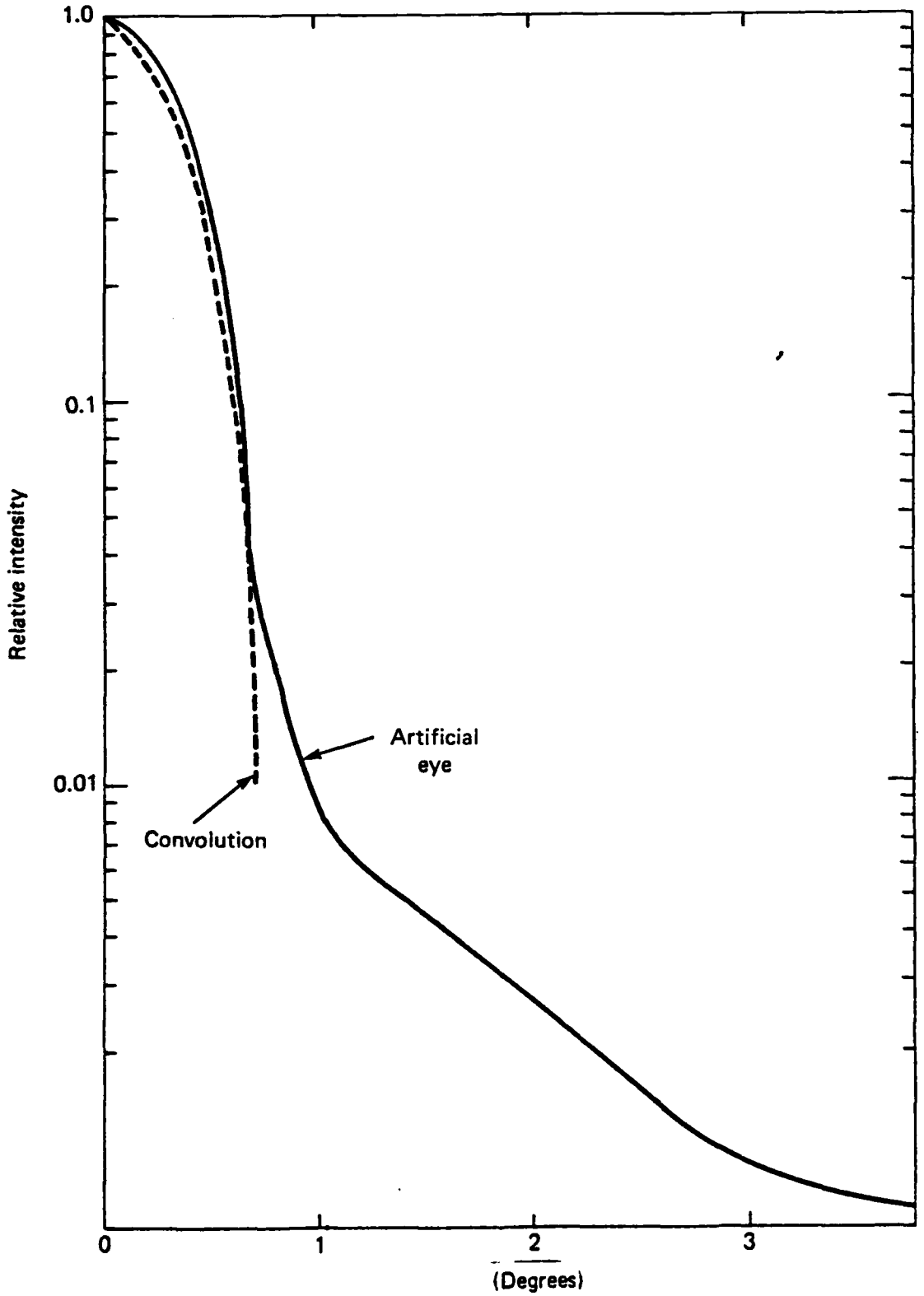
1.0
0.1
0.01
Relative intensity
Artificial
eye
Convolution
0
1
2
3
(Degrees)

Fig. 2

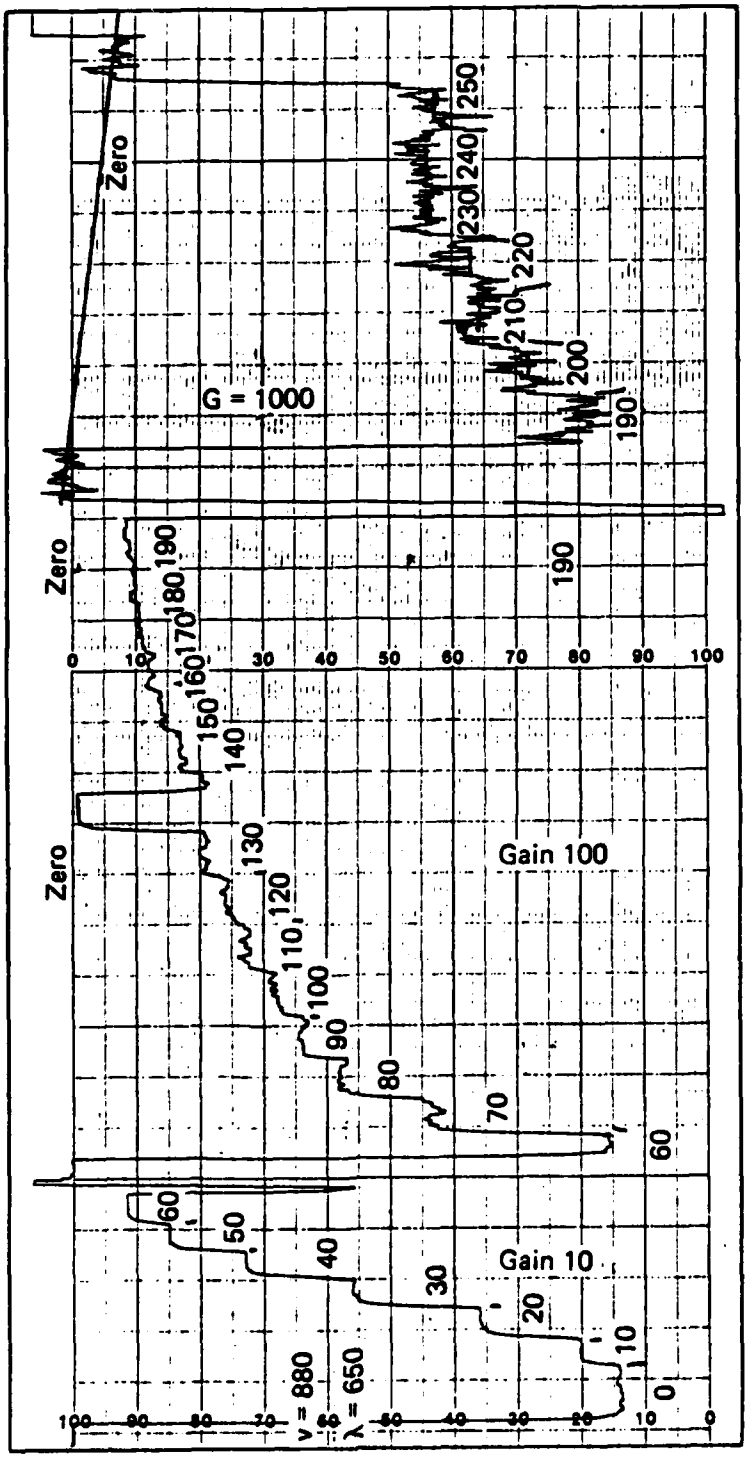

Fig. 3 Typical strip chart recording.

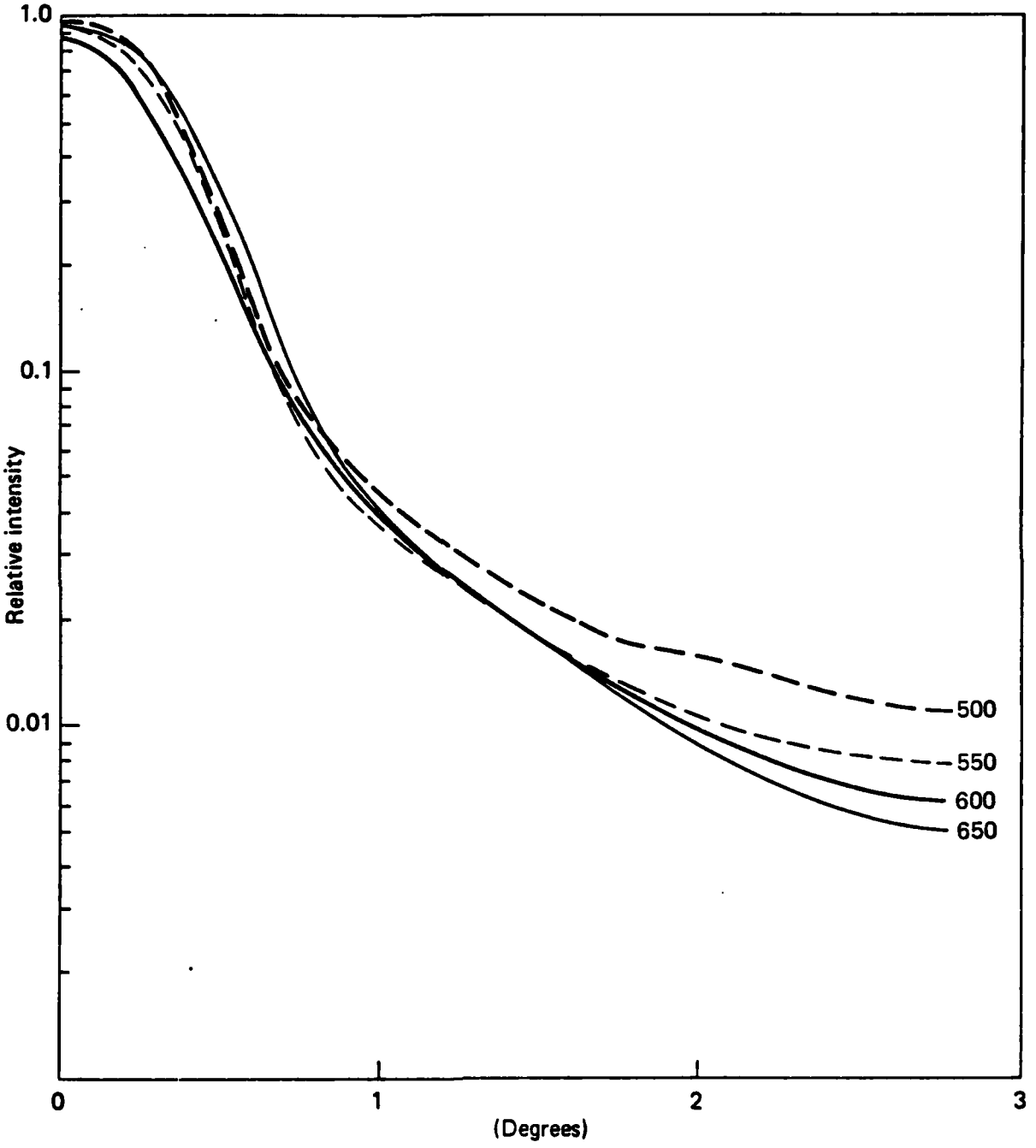

Fig. 4

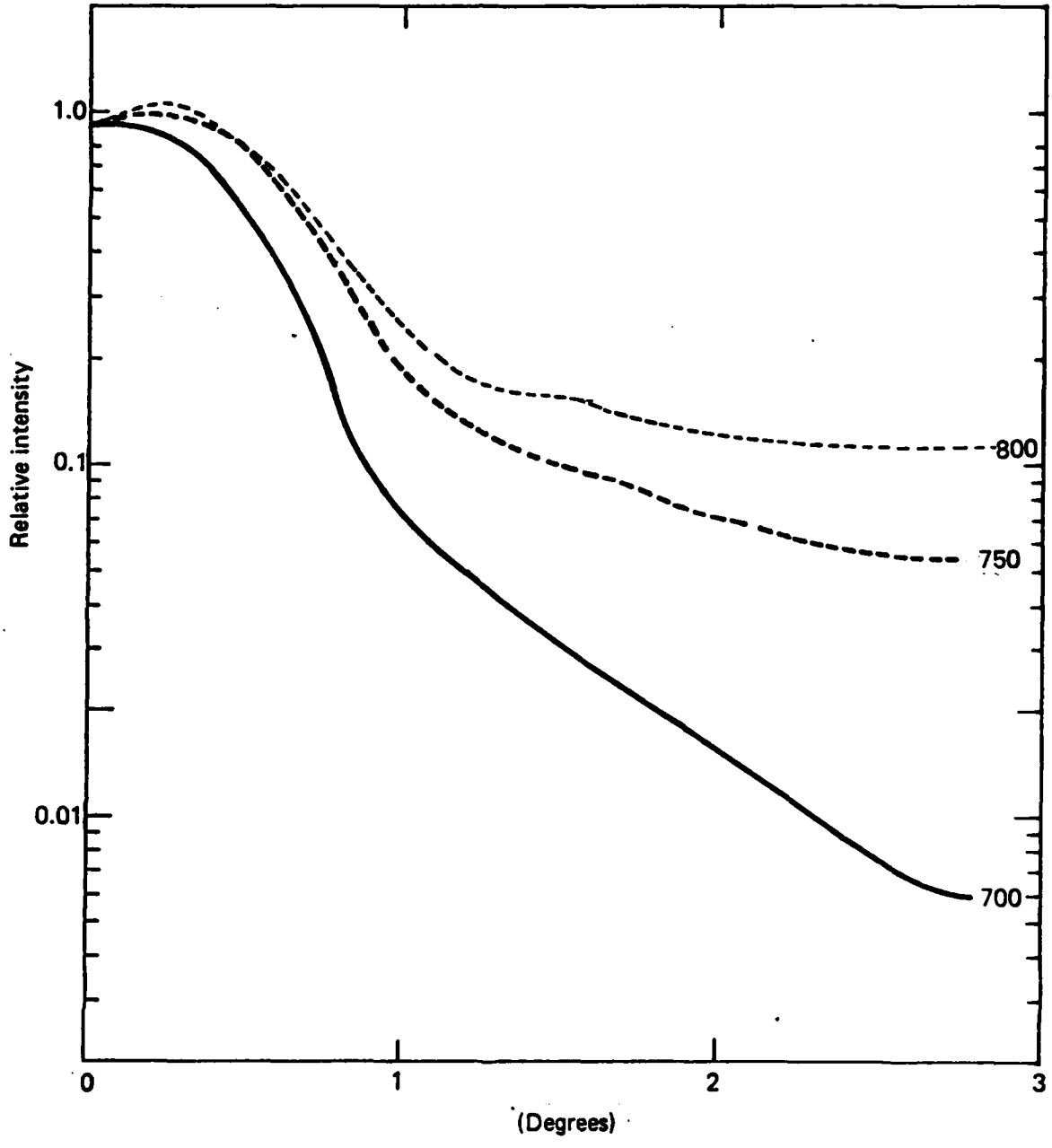

Fig. 5

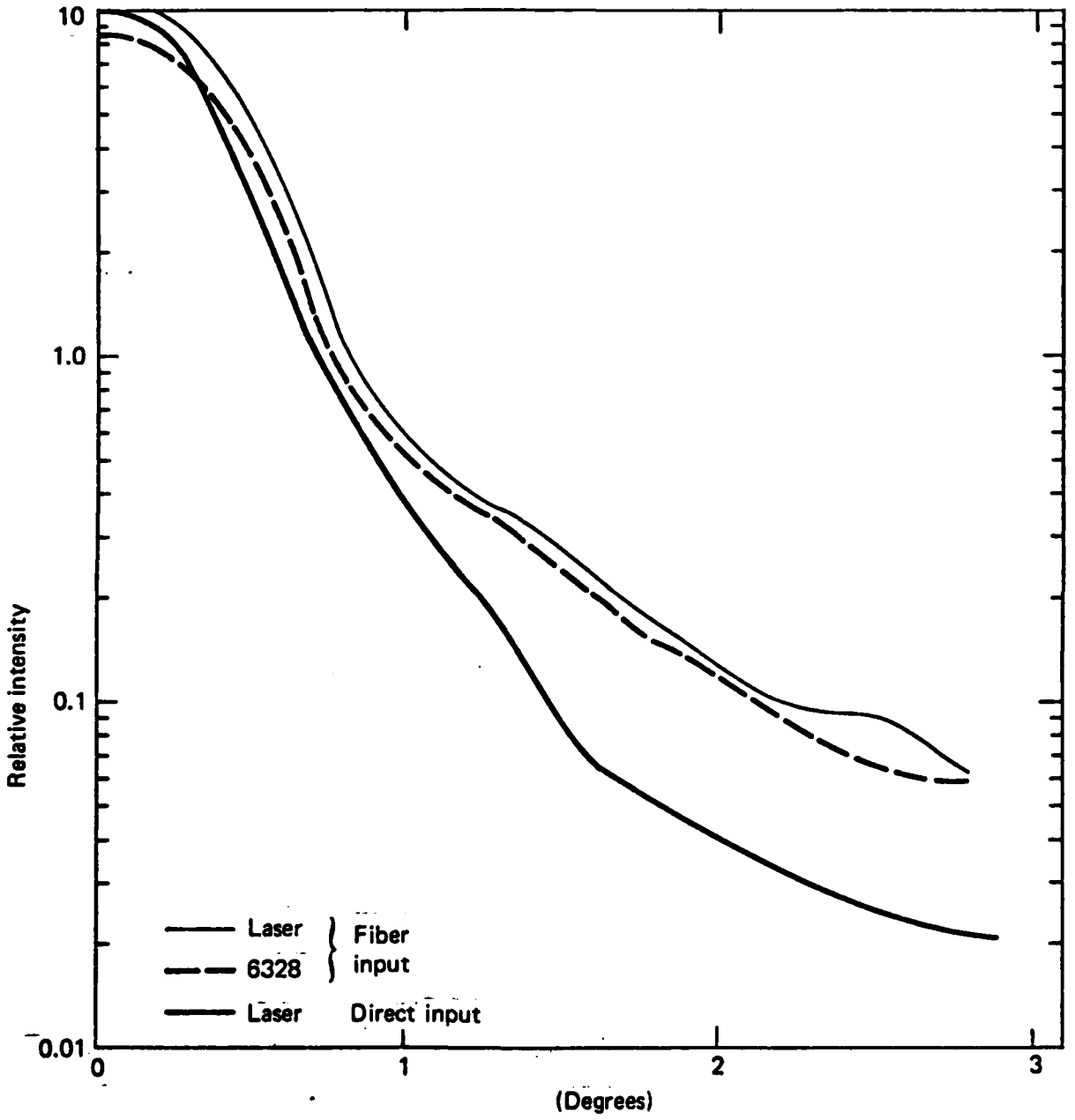
10
1.0
0.1
0.01
Relative intensity
0
1
2
3
(Degrees)
Laser
6328
Fiber input
Laser
Direct input

Fig. 6

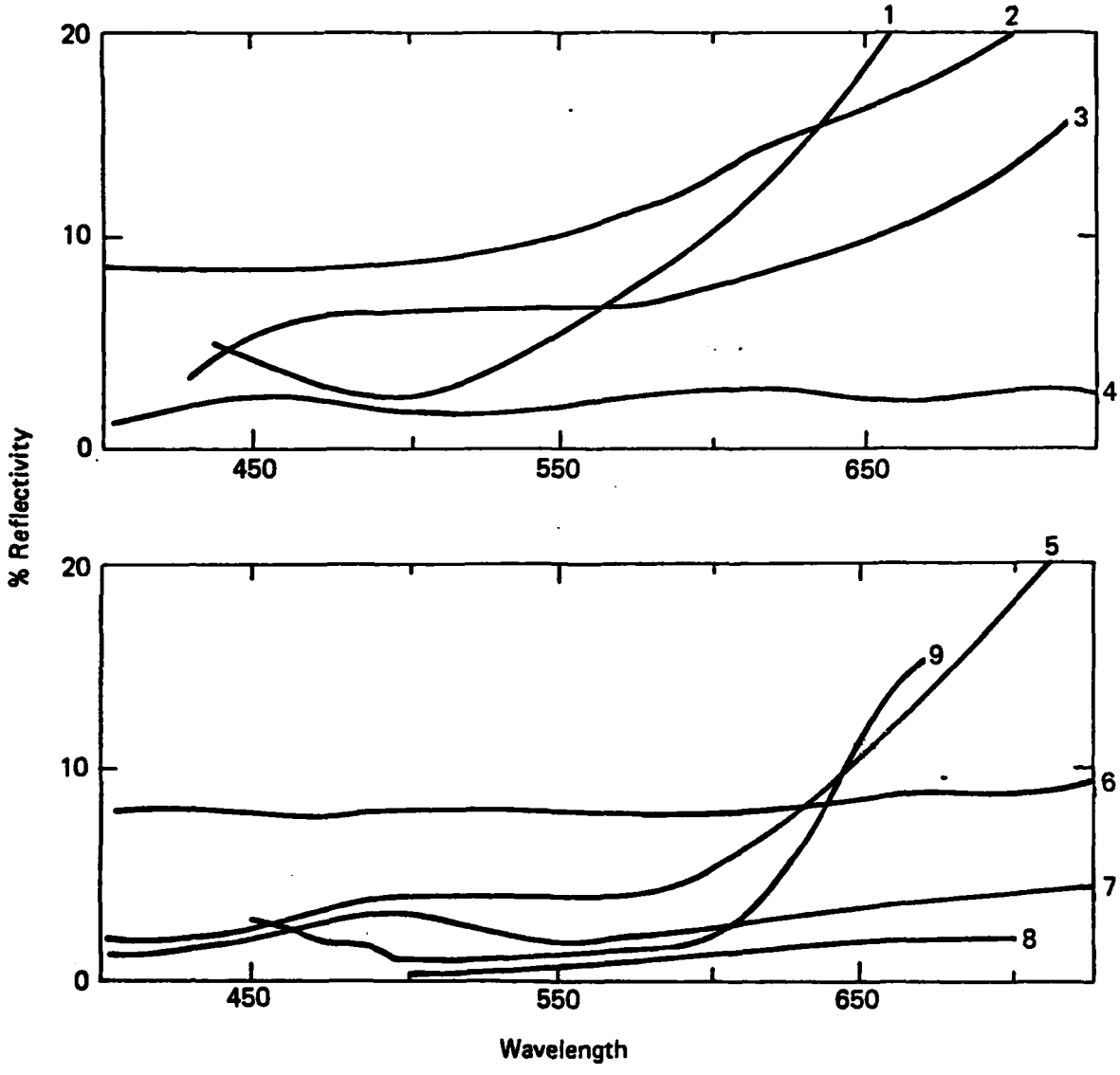

1. Vos (human)
2. Geeraets & Berry (human)
3. Hochheimer – present data (monkey)
4. Flower (monkey)
5. Flower (human-blond)
6. Geeraets & Berry (monkey)
7. Hochheimer (monkey)
8. Brindley & Willmer (human)
9. Alpern & Campbell (human)

Fig. 7

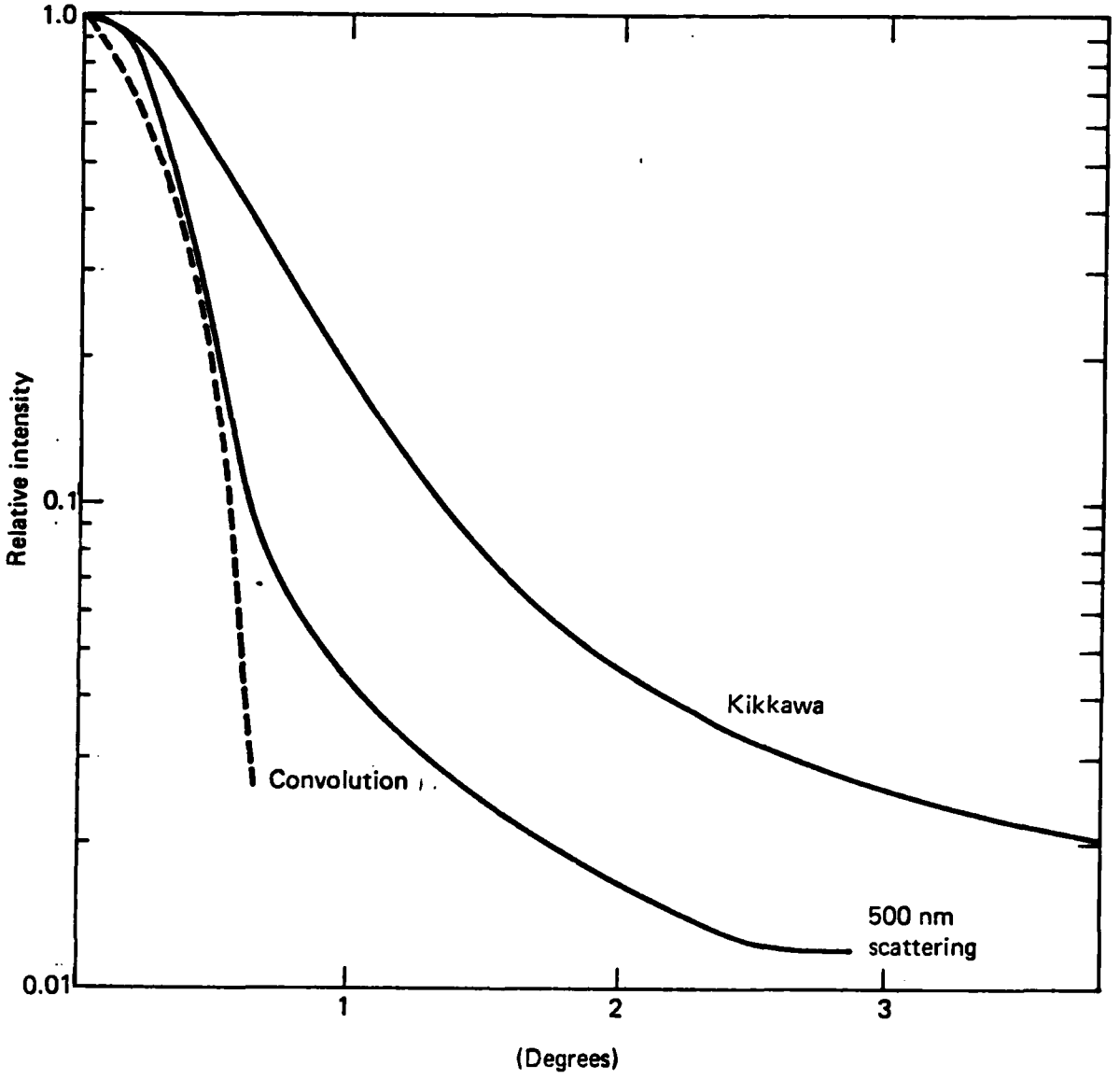
1.0
0.1
0.01
Relative intensity
Kikkawa
Convolution
500 nm
scattering
1
2
3
(Degrees)

Fig. 8

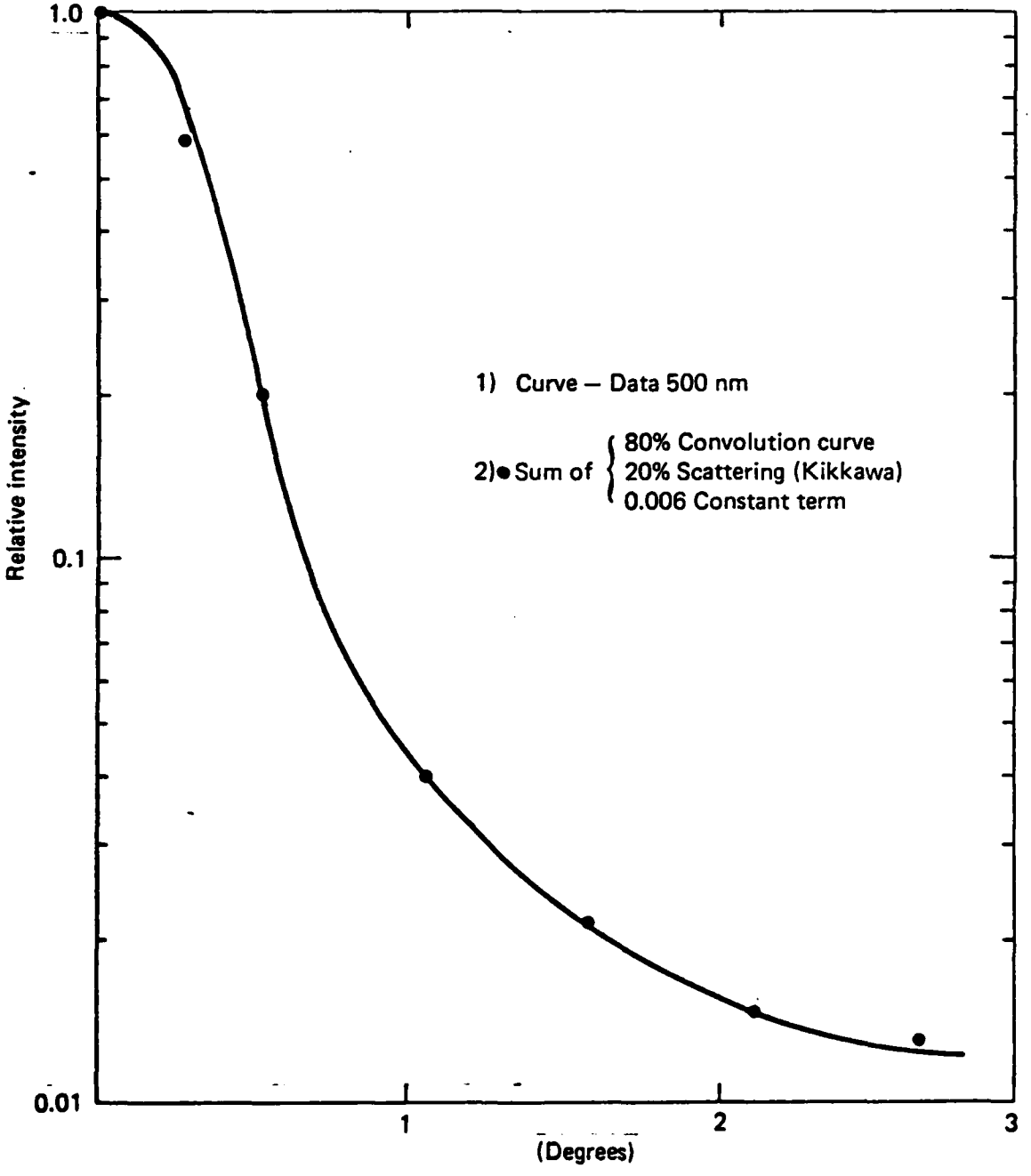
1.0
0.1
0.01
Relative intensity
1
2
3
(Degrees)
1) Curve – Data 500 nm
2) ● Sum of
80% Convolution curve
20% Scattering (Kikkawa)
0.006 Constant term

Fig. 9

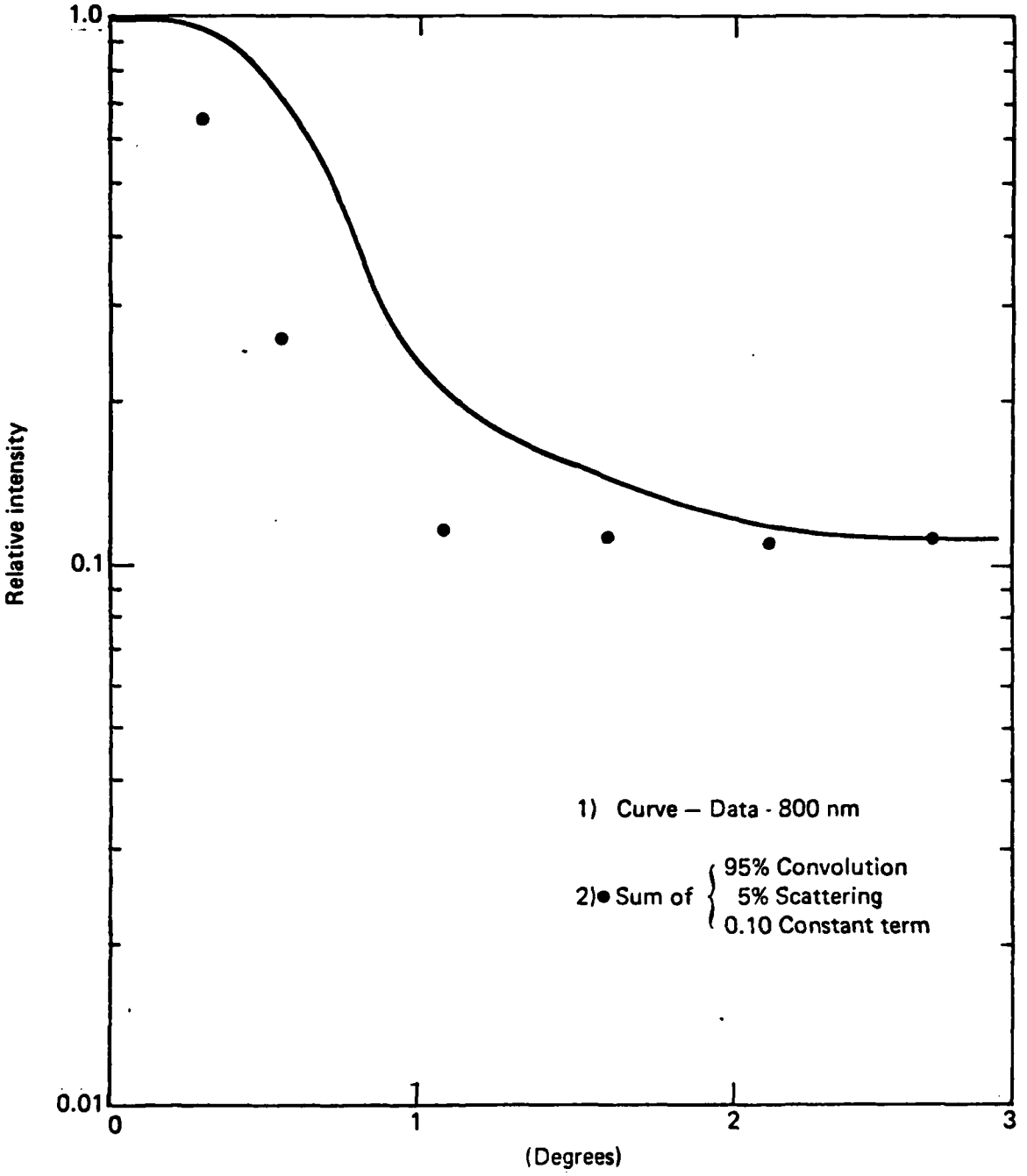
1.0
0.1
0.01
Relative intensity
0
1
2
3
(Degrees)
1) Curve – Data - 800 nm
2) ● Sum of { 95% Convolution
5% Scattering
0.10 Constant term

Fig. 10

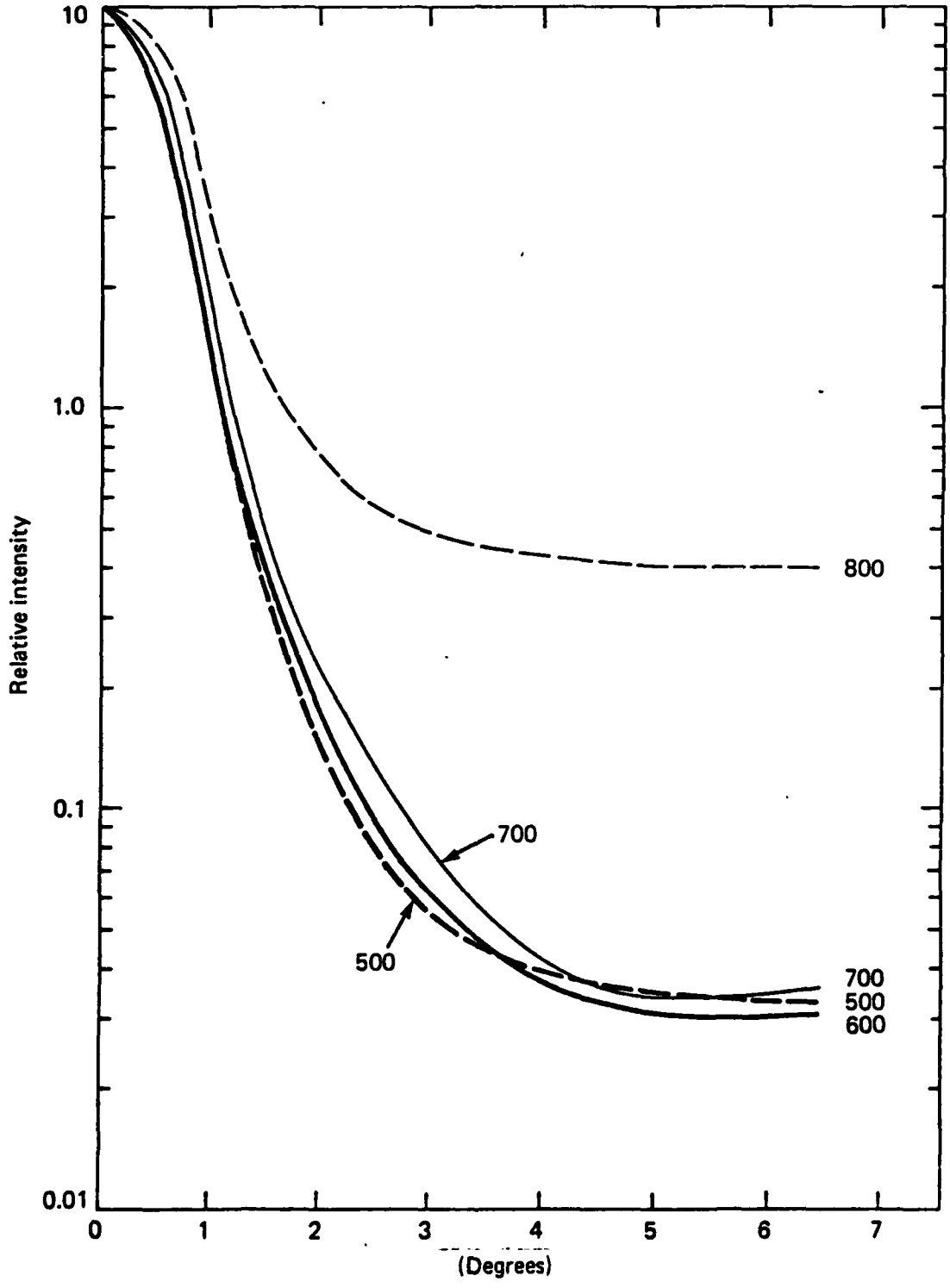
10
1.0
0.1
0.01
Relative intensity
0
1
2
3
4
5
6
7
(Degrees)
800
700
500
700
500
600

Fig. 11

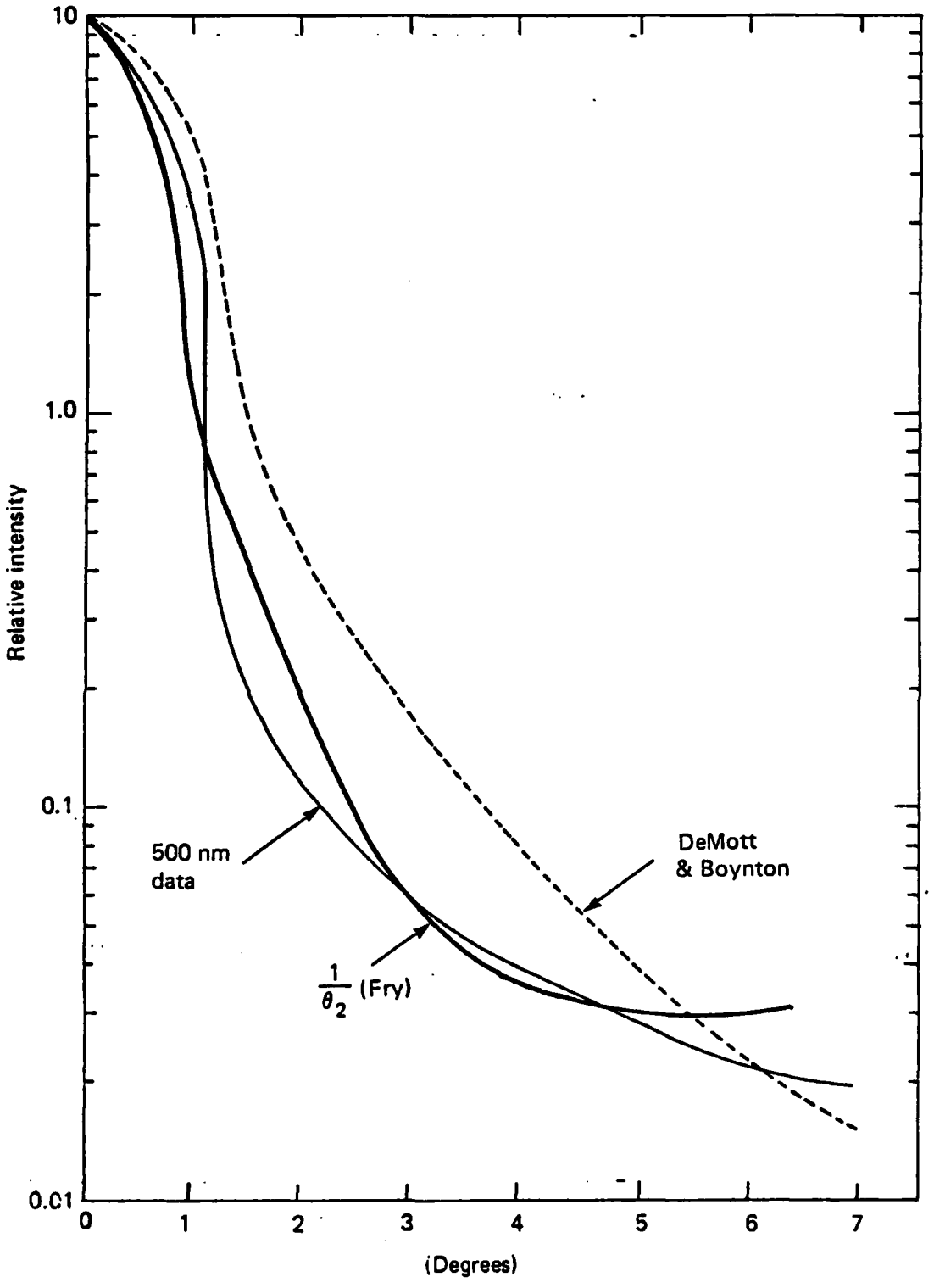
10
1.0
0.1
0.01
Relative intensity
0
1
2
3
4
5
6
7
(Degrees)
500 nm
data
DeMott
& Boynton
$\frac{1}{\theta_2}$ (Fry)

Fig. 12

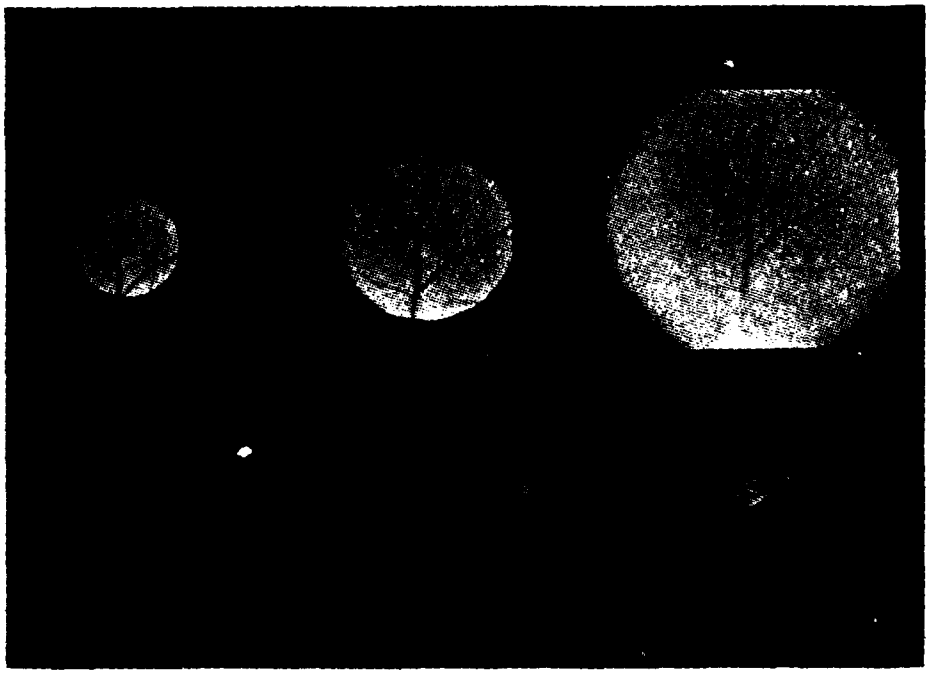

FIG. 13

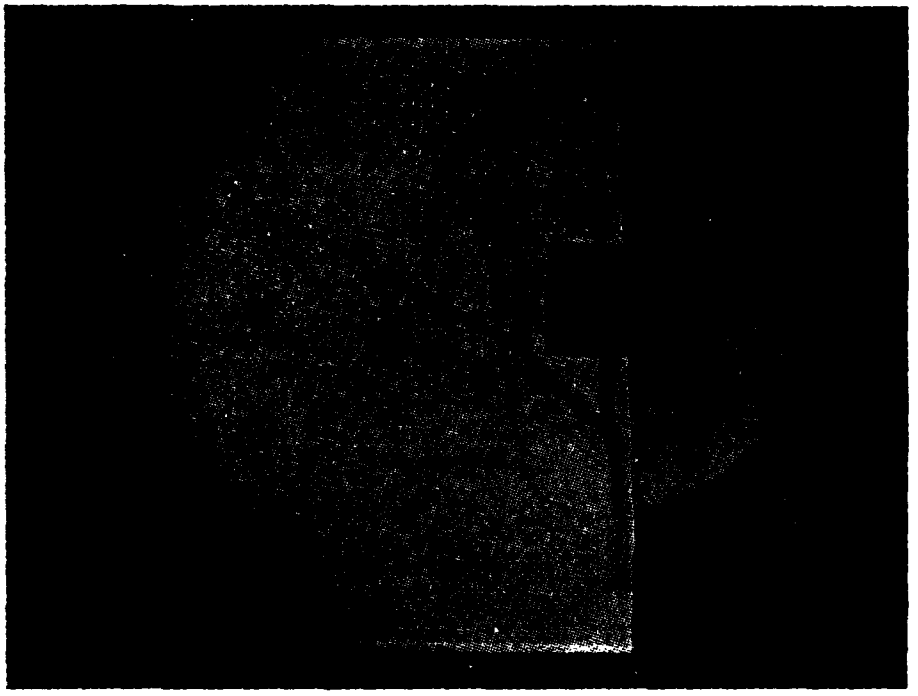

FIG. 14

Fluorescence Measurements

Introduction

Before 1960 the use of dyes in biology and medicine was confined to the study of histologic samples[1,2,3]. The ability of a dye to bind to a particular part of a cell was most important. The dye color, and sometimes fluorescence, emphasized specific areas of cells or membranes. In more recent times specific dye properties have been used to study cell cultures[3]. In particular the fluorescence properties of dyes, the excitation and fluorescence spectrum, the fluorescence polarizability, fluorescence decay time and fluorescence quantum efficiency, have been used to infer cell properties[4]. For these purposes the fluoresceins, rhodamines, acridines and various anilnonaphthalene sulfonic acids are often preferred[5,6,7].

Fluorescein angiography and angioscopy have been in use in ophthalmology since 1960[8]. These techniques give much spatial information, some blood dynamics[9], and useful data on the integrity of retinal membranes. Cunha-Vaz et al[10] have correlated the intensity of fluorescence of fluorescein in the vitreous with the degree of diabetic retinopathy. Aqueous dynamics have been studied with fluorescein by many investigators[8]. However, much information contained in the fluorescence of fluorescein is never utilized.

The fluorescence of any molecule can supply information on processes that take place in the molecule during the time between excitation and emission of light[11,12]. Although many types of fluorescent measurements can be made, the real problem in the use of fluorescent probes is the recognition and analysis of the primary photochemical processes that are involved. Fig. 1 indicates, in a very simplified way, some things that might happen when a molecule is excited by a photon. The dye molecule absorbs light whereby a molecular

electron is raised to an excited vibrational level. This energy may reappear as heat due to radiationless decay, it may be given up in normal fluorescence, or it may be transferred to a different electronic system. Excitation takes place in 10^{-15} seconds (all times are only approximate) and in 10^{-12} seconds the electrons undergo radiationless transitions to the lowest vibrational level of the first excited state. If the dye has a high fluorescence quantum efficiency the electrons will, in 10^{-8} seconds, most often return to the ground state, emitting a photon of light. Strongly fluorescent molecules have singlet ground states and higher level triplet states. Some excited state energy may, by inter-system crossing, be transferred to the triplet system in a reversible reaction. The triplet lowest state to singlet ground state transitions is partially forbidden, this shows up as a long decay time of 10^{-4} seconds.

If the dye molecule is in close proximity to another molecule, the excited state energy can be transferred from one molecule to another. This, in solution, is generally controlled by diffusion in which case a steady state is reached in 10^{-7} seconds. Some molecules, oxygen is of special importance in the eye, have triplet ground states and can, by energy transfer, deplete the dye molecule triplet state. Since the excited singlet state to triplet state transfer of energy ordinarily takes place in a reversible reaction in 10^{-8} seconds, the rapid depletion of the triplet state causes quenching of the primary fluorescence. Parker[13] gives a complete description of the processes that can take place in solutions while a molecule is in a state of electronic excitation.

As an example of a fluorescent dye that is influenced by its surroundings, consider fluorescein in the retina. Hodge and Clement[14] showed that the fluorescence spectra of fluorescein in blood depended on the degree of blood

oxygenation. A strong fluorescence peak at 615 nm in arterial blood suggest that there is an abnormally large triplet state interaction under these conditions. Haining and Lancaster[15] found that the peak excitation for blood samples withdrawn from patients varied with fluorescein concentration, blood hemoglobin and pH. Allen and Frazier[16] show twin excitation peaks, as did Haining and Lancaster, but a different fluorescent peak wavelength. Delori and Ben-Sira[18] recorded the excitation and emission spectra of fluorescein in the eye and show a wavelength shift in both, relative to the emission of fluorescein in water. All of these people were trying to find better filters to do fluorescein angiography and failed to take into account that the effects they were seeing may have been due to the binding of fluorescein dye molecules to constituents in the blood or in the retina itself.

The basic fluorescent quantities are the excitation and fluorescence spectra, the fluorescence quantum yield, the fluorescence polarizability and the fluorescence decay time. Measurement of these quantities can be used to infer the following conditions surrounding a fluorescent probe[19,20]:

1) Binding site polarity.

The separation between the excitation and emission spectra is very sensitive to local solvent polarity. This information is of importance in understanding membrane transport phenomena.

2) Environmental Constraints[21].

A viscous environment of the fluorescent molecule causes an increase in quantum yield and in polarizability. The polarizability can be used to infer the ratio of free to bound dye.

3) Distances Measurements[22].

Electronic energy can be transferred between separated molecular systems, the rate of transfer is proportional to the sixth power of the separation

distance. The distances betwen binding sites of fluorescent probes can often be inferred by fluorescence energy rate measurements.

4) Accessibility[13].

Fluorescence quenching can be caused by a number of molecules, oxygen is a particularly important and powerful quencher. By comparing the quantum yield of the free and bound fluorescent probe, the exposure to the quencher can be estimated. Local oxygen partial pressure can, with suitable probes, be monitored with fast time resolution.

5) Rotational Mobility[23,24,25].

Polarization measurements of bound fluorescent probes indicate the relative mobility of the binding site.

6) Local pH[26].

Most fluorescent probes have intensity and spectral changes with changes in pH. Fluorescein may not be the *most sensitive* but it does show widely different characteristics with changes in solvent pH.

7) Heterogeneous interaction[7,27,28].

Under favorable circumstances several fluorescent decay times can be resolved. This indicates binding sites with different environments.

Objective

Our objective in this project is to apply fluorescence techniques to aid in an understanding of cellular changes in the retina from disease or trauma. We will use the fluorescence methods devised by cell biologist in their assessment of cells and membranes as well as new methods perfected in our laboratory. We wish to be able to obtain all of the fluorescence data that is possible and analyze it for its usefulness in the determination of retinal problems. Comparisons will be made with in-vitro studies of dye solutions and dyes incorporated in live cell colonies. Methods and equipment

will be simplified so they can be used in a clinical setting with human subjects.

At the present time there is very little that can be ascertained at the cellular level of the changes that occur in the retina with age, disease or trauma except through histologic examination. The in-vivo tests that are availabe enable only the gross changes to be seen. If retinal damaging effects can be examined at the cellular level then we will have a better understanding of the mechanisms producing damage and improved prevention and treatment methods can be devised.

Program Goals

When this program was started a list of goals were out.lned. Although this list has been somewhat revised it has not drastically changed. Some of these goals have already been met, some are being worked on at present and others we hope to work on in the future. This is a long term project that could involve many dyes but for the present we are only using sodium fluorescein dye as it already is approved for human use.

Our list of goals is as follows:

1. Demonstrate that we can measure the excitation and fluorescence spectra, the polarizability, the dye decay time and the quantum efficiency.

The measurement of the first three of these has been done in animal models with no adverse effects to the retina. We can measure the relative fluorescence efficiency but not the absolute (or even relative) quantum efficiency.

2. Determine how to obtain instrument independent data.

We can now do this for all of our measurements either as the measurements are taken or by applying correction factors. This is absolutely necessary if data is to be compared between investigators.

3. Obtain all the data repeatedly after a single injection of fluorescein dye.

This can be done semi-automatically now under computer control with the exception of the decay time. An argon-ion laser has been recently obtained and we already have a light modulator and a high frequency, phase sensitive, lock-in amplifier. When these are incorporated in our system this goal will be met.

4. In-vitro determination of dye fluorescence properties in a wide variety of solvents.

Studies have been done in polar solvents, in aqueous solvents of variable pH, in aqueous solvents as a function of concentration and in glycerin and dextrose solution of variable viscosity. All of these measurements will be repeated under the same condition used in our animal studies, our initial measurements were not always corrected for instrumental effects.

5. In-vitro determination in blood-dye solutions[29,30,18].

This study will be done this year. The variables will be pO_2, pH concentration, and hematocrit.6. Measurement in normal and test animals[31].

This has already been started. In the progress sections are shown typical measurement on a normal monkey retina.

7. Freeze-dried histologic analysis of retinal sections obtained after a dye injection [32,33,34,35,36].

We need to know where the dye we are examining really is. For normal retinas the retinal vessels and the choroid contain most of the dye. There have been several previous studies on normal retinas that we can use as a starting point. However, nothing seem to have been done on diseased or damaged retinas. This analysis will also be started this year.

8. Comparison of animal and in-vitro data[29,30,37,38].

This will be started this year. Some limited comparisons are already available using our in-vitro solvent-dye data and data from the published literature.

9. Improvements are need in the following areas[39]:

a) Instrumentation simplicity

b) Accuracy, precision, sensitivity

c) Smaller and multiple retinal areas

d) Data presentation

This is a goal which we are always working on, it probably never will be finished.

10. Determination of membrane and cellular changes which result from retinal damage.

This goal, the most important one, lies somewhere in the future, hopefully the near future.

11. The use of dyes other than fluorescein[40,41,42,57].

Our equipment is capable of measurements of any fluorescent dye with a high fluorescence efficiency at wavelengths where the eye is transparent. As we have been studying the feasibility and characteristics of fluorescent dyes for a number of years this could be started at any time, however, at the present only fluorescein is being used.

12. Cell colony studies[43,25,44,45].

Most cell colony fluorescence studies have used dyes that were chosen for a particular biological characteristic. We are under the constraint that the dye must be non-toxic, water soluble, and compatible with live animals. For clinical purposes it must also be approved for human use, this is why fluorescein was chosen for our initial studies. There are several individual

cell studies now under way at Wilmer Institute, we will utilize this expertise that is already available. This study will not start until sometime in the future.

Progress

1) Instrumentation

The optical system is the same as that shown in the previous section on light scatter. Instead of the fiber optics source either a white light source or a monochromatic source is used. The white light source is used for the reflectivity, and fluorescence spectra and polarizability. A tungsten-iodide source and a small grating monochromater are used for the monochromatic light, the spectral bandwidth of the monochromater is approximately 17 nm. The white light source is a tungsten-iodide lamp.

The output of the photomultiplier tube that comes after the rotating interference monochromater is read with a 6-1/2 digit voltmeter. A second photomultiplier is used to detect the fluorescence energy when the excitation spectra is measured. A mirror can be inserted after the enlarging relay lens to direct the energy to this photomultiplier. Its output is amplified with a PAR 124A lock-in amplifier. The monochromatic excitation source is chopped and a phase signal is fed from the chopper to the lock-in amplifier.

A Schott OG 550 barrier filter (50% transmission at 550 nm, long pass filter) is used to eliminate short wavelength light for the excitation measurements. Ditric Optic 460 nm and 600 nm long-pass cut off filters are used together as an exciter filter for the fluorescence emission measurements. The 460 nm cuts off the long wavelengths (50% transmission at 460 nm) the 600 nm cut off filter eliminates a long wavelength transmission of the 460 filter. A 500 nm long pass Schott filter is used as a barrier filter for emission measurements to avoid overloading the photomultiplier. A neutral

density of 2 filter is used for the reflectivity measurements, again to prevent overloading of the photomultiplier. Rotating polarizers (Polaroid HN 32) can be inserted in both the input and output light paths.

2) Correction Factors

2A) Correction Factor for Polarizability

What we wish to measure is the polarizability P defined as

$$P = \frac{A-B}{A+B}$$

where A is the intensity with input and output polarizers parallel and B is the intensity with input and output polarizers crossed. What is measured is

$$P_1 = \frac{C_1 A - C_2 B}{C_1 A + C_2 B}$$

and

$$P_2 = \frac{C_3 A - C_4 B}{C_3 A + C_4 B}$$

where C_1 denotes input and output polarizer verticle, C_2 denotes the input polarizer vertical and the output horizontal, C_3 denotes the input and output polarizers horizontal, and C_4 denotes the input horizontal and the output verticle. With frontal illumination and collection of fluoresence P_1 should equal P_2; they differ because of partially polarizing elements in the optical paths. The maximum obtainable value, with this type of illumination, is 33%. C_1 is made up of two factors, K_1 for the input polarizer and K_2 for the output polarizer,

$$C_1 = K_1 K_2$$

In the same manner

$$C_2 = K_1K_3$$

$$C_3 = K_4K_3$$

$$C_4 = K_4K_2$$

so that

$$P_1 = \frac{K_1\,K_2A - K_1\,K_3B}{K_1\,K_2A + K_1\,K_3B} = \frac{\frac{K_2}{K_3}\,A - B}{\frac{K_2}{K_3}\,A + B} = \frac{N\,A-B}{N\,A+B}$$

and

$$P_2\,\frac{K_4\,K_3A - K_4\,K_2B}{K_4\,K_3A + K_4\,K_2B} = \frac{\frac{K_3}{K_2}\,A - B}{\frac{K_3}{K_2}\,A + B} = \frac{\frac{1}{N}\,A - B}{\frac{1}{N}\,A + B}$$

if P is expressed as

$$P = \frac{\frac{A}{B} - 1}{\frac{A}{B} + 1} = \frac{Q - 1}{Q + 1}$$

and P_1 as $$P_1 = \frac{N\,\frac{A}{B} - 1}{N\,\frac{A}{B} + 1} = \frac{NQ-1}{NQ+1}$$

and P_2 as $$P_2 = \frac{\frac{1}{N}\,\frac{A}{B} - 1}{\frac{1}{N}\,\frac{A}{B} + 1} = \frac{\frac{1}{N}\,Q - 1}{\frac{1}{N}\,Q + 1}$$

P_1 and P_2 now contain only two unknowns, one of which is needed to solve for P. Rearranging P_1

$$P_1 (NQ+1) = NQ-1$$

and solving for N

$$N = -\frac{(P_1+ 1)}{(P_1- 1)} \frac{1}{Q}$$

and for P_2

$$N = -Q \frac{(P_2- 1)}{(P_2+ 1)}$$

these two equations are equated, eliminating N

$$\frac{1}{Q} \frac{(P_1+ 1)}{(P_1- 1)} = Q \frac{(P_2- 1)}{(P_2+ 1)}$$

and solving for Q

$$Q = \frac{(P_1+ 1)\ (P_2+ 1)}{(P_1- 1)\ (P_2- 1)}^{1/2}$$

Q is inserted in the equation for P

$$P = \frac{Q - 1}{Q + 1}$$

P may have plus or minus values; the absolute value must be taken for the square root that determines Q. If P is positive, both P_1 and P_2 will be positive and if P is negative, both P_1 and P_2 will be negative. A check on the sign of P_1 will remove any ambiguity.

2B) Corrections for excitation spectra

The central stop, in the input light path that is just before the mirror with the central hole in our modified fundus camera, is a silicon diode detector. This detector measures a fraction of the input light energy. The only off axis component after the detector is the mirror. This mirror is coated to equally reflect the P and S polarization components to within a few percent. The diode detector wavelength sensitivity curve has been least squares fitted to a third order equation. The measured input light fraction, corrected for the detector wavelength sensitivity, is used to apply a correction factor to the excitation spectra and the excitation polarization.

2C) Corrections for emission spectra

The fluorescence emission spectra is measured by inputing white light through a short pass exciter filter and detecting the fluorescence energy with a photomultiplier after it has passed through the rotating interference monochromater. A standard lamp has its emission curve fitted to a third order equation. The lamp is placed at the front of the camera so that the filament image is centered on the exit aperture that just precedes the monochromater. The lamp output energy is measured as a function of wavelength and a transmission plus detector response function computed. This response function is used to correct the fluorescence emission data.

No correction factor is used at present for the polarized excitation energy used for the fluorescence emission polarization spectra. The light measuring diode cannot be used as it is overloaded with the excitation energy. We plan to insert a neutral density filter before this detector but this has not yet been done. The fluorescence emission polarization spectra is at present only a relative, not fully corrected value. The correction factor is very small, less than one measurement accuracy.

2D) Corrections for reflection spectra

The retinal reflection spectra measurements are divided by similar measurements on a 17% reflectivity artificial eye retina and then multiplied by 0.17. The artificial eye data can be taken any time before the dye injection; the data is stored on magnetic tape for future use.

2E) Wavelength calibration

The rotating interference monochromater is calibrated with a low pressure mercury penray lamp. The calibration is checked at frequent intervals with a set of narrow-band interference filters.

3) In-vitro solvent data

All of the measurements reported in this section are for frontal illuminated samples, similar to what is done with the retina. We did not make corrections for spectral changes in light output or for instrument transmission; however, these contribute only minor changes, mostly in absolute values, not in relative values.

The fluorescence characteristics of fluorescein have been measured in a variety of solutions. In water the pH and concentration were varied[26,46,47,51]. Fig. 2 shows the change in peak excitation wavelength as the pH is varied from three to eleven. The concentration was 10^{-5}. Above 6.6 the peak wavelength is constant, 492 nm. Fig. 3 shows the change in the intensity of the peak versus pH, this is peak intensity of the excitation curve when all of the fluorescence energy above 540 nm is collected. The variation in intensity is 30% for pH 6 to 8. We do not yet have the equivalent data for the fluorescence spectra.

Figs. 4 and 5 show the changes in peak excitation wavelength and peak emission wavelength with variations in concentration. Our initial data was taken using glass bottles of solutions, the bottles are approximately 5 cm in diameter. Since we did not expect this much variation in peak wavelength with changes in concentration, it was suspected that there was an inner filter effect giving these results. We next used 2 mm thick cuvettes and found only a slight difference from the previous results. Also measured were the relative integrated fluorescence intensities in the 2 mm cuvettes and the 5 cm bottles. Fig. 6 shows this data, the curves are normalized such that the peak recorded value was made equal to 100. There are no great differences between these curves.

The fluorescence polarizability was run in dextrose-water and glycerol-water solution[48,49,50]. See Fig. 7. The concentration was again one part in 10^{-5}. In the dextrose solutions the polarizability appears constant over a viscosity range of 1 to 8. In glycerol solutions, the polarizability follows a smooth curve as the viscosity is varied from 6.6 to over 1000. The peak wavelength of the excitation curve was also measured for the glycerol solution. This is shown in Fig. 8. I can think of no reason why the polarizability should be constant for the dextrose solutions or why the peak excitation wavelength should shift so much with viscosity.

Peak wavelengths for the excitation spectra and for the fluorescence spectra are shown as Figs. 9 and 10 for solvents of different polarity[52,53]. In Fig. 9 the points for 100% acetone, chloroform and ethylene glycol clearly fall rather far from the straight line through the remaining points. The reason for this is that fluorescein is not completely soluble in these solvents. These three solvents were not used for Fig. 10. Two points on this curve, DMSO and Dimethyl Formide, are at very long wavelenghts. the color of

these solutions is very orange compared to the others. It may be that the true curve should be much steeper than I have drawn it.

We have a limited amount of fluorescence data taken on solutions of fluorescein in whole blood[40]. This data was taken in 1974 on a study of fluorescent dyes. The fluorescence emission spectra, Fig. 11, the fluorescence excitation spectra, Fig. 12, and the intensity as a function of concentration, Fig. 13, were taken in 100μ thick cells, with frontal illumination.

4) Computer Program

All of our animal data collection, computations and data output are done using a Hewlett-Packard 9845 B computer. The polarizers and the interference monochromater are rotated by stepping motors. These motors are indexed by pulse output signals from the computer.

A program has been written that automatically records data and rotates the stepping motors. The program pauses, and alerts the operator, when filters, mirrors, or polarizers need to be changed. This data collection system is only semi-automatic but is quite adequate for our research purposes.

5) Animal Data

The next twelve figures (Figs. 14 thru 25) show part of a data run for a normal monkey. Fig. 14 is data retrieved from storage on the excitation spectra of fluorescein in water and the transmission correction factor. Fig. 15 is the stored data of the PMT output for the reflection spectra for the artificial eye. If this initial data is not satisfactory, it can be rerun before any animal data is taken.

Before the dye injection is given the animal is sedated with Ketamine and anesthsized with Halothane. A contact lens is placed over the eye to prevent drying. The animal is placed in front of the camera and properly positioned. The retinal reflection spectra is taken to be used as a referenece

spectra. See Fig. 16. Before the dye is injected the computer is instructed as to the number of data runs to be taken and the starting time for each run. As seen in Fig. 16 the starting time for the first data run was 7 minutes after injection. The starting time for the second data run was 22 minutes after injection. Data from the second data run will be shown in the next several figures. The first set of data taken after the injection of fluorescein is the retinal reflection spectra. This reflection data is compared with the pre-injection data and the integrated difference from 425 to 500 nm is computed. See Fig. 17.

The fluorescence emission spectra is then measured, Fig. 18. The integrated fluorescence intensity (510 to 650 nm) is computed and compared to the integrated absorption. This is labeled on the bottom of Fig. 17 as the Quantum Efficiency. It is not the quantum efficiency, it is only a relative measure of fluorescence efficiency. The decrease in reflected light before and after the dye injection is a measure of the light absorbed by the fluorescein and the integrated fluorescence emission is a measure of emitted intensity.

The excitation polarizability spectra and excitation fluorescence spectra are recorded next, Figs. 19 and 20. The average polarizability and the integrated excitation spectra are computed and recorded. The finish time shown in Fig. 20 as the third line down from the top is 0 days, 0 hours, 33 minutes and 54.9 seconds after injection, the starting time for this run was 22 minutes.

The difference in spectra between the excitation spectra of water and the excitation spectra from the animal retina is shown as the top graph in Fig. 21. The lower graph is the difference in the excitation spectra recorded in

the first and second run in this series. The top difference spectrum is between normalized data while the lower spectrum refers to the actual data difference. Difference spectra are powerful methods to detect changes.

After all the runs in a series are completed several sets of data are plotted as a function of finish time. This is shown in Figs. 22 through 25.

Fig. 22 - Top - Log of integrated excitation spectra.

Bottom - Rate of change of integrated excitation spectra. As can be seen, this graph is incorrectly done.

Fig. 23 - Top - Average Excitation Polarization. The time is not plotted under all spectra, all time scales are as indicated here.

Bottom - Integrated fluorescence intensity.

Fig. 24 - Top - Integrated absorption.

Bottom - Fluorescence polarization (average value).

Fig. 25 - Top - Fluorescence Efficiency.

Discussion of Results

1) Excitation Spectra[31]

The excitation spectra is influenced by the conditions imposed on the ground state of the molecule, usually pH and polarity are the most influential. In water, we find the peak excitation wavelength to be 503 nm, and in the monkey retina to be 492 nm, a shift of 9 nm. The shapes of these excitation curves are also quite different, the water solution spectra is much flatter. The shape difference is not difficult to understand since the absorption spectra of most retinal absorbers varies significantly in this spectral region. The peak wavelength is consistent with a local pH of 7 and a concentration of one part in 10^6.

2) Emission Spectra

The emission spectra is influenced by conditions imposed on the excited state of the molecule. It should be remembered that in the excited state the electronic configuration can be much different than in the ground state and it is not initially in an equilibrium configuration. The local polarity often determines the peak emission wavelength. Our animal data indicates a peak wavelength of 530 nm, the same as found for a blood-fluorescein solution and considerably longer than 488 nm which is usually given for a water fluorescein solution, see Fig. 26. If the local polarity is about 80, this would account for the wavelength shift. The shapes of the emission curve in water or in the retina appear similar. I would have expected a greater fluorescence near 640-650 nm if there was any significant triplet state population[54].

3) Fluorescence Intensity

The fluorescence intensity is controlled by polarity, pH and molecular binding sites. Since the pH is probably around 7, the maximum intensity might be expected. In blood the intensity is lower than in water by over a factor of 2. This would indicate a large binding site influence, expecially since a large fraction of the dye is not bound.

4) Quantum Yield

The quantum efficiency is determined not only by the intrinsic efficiency but also by any packing constraints or by changes in the geometry of the upper state during the period that the fluorescent molecule is excited. We do not measure quantum efficiency, we only measure the ratio of the integrated intensity to the integrated increase in absorption. Fig. 25 shows values of this ratio plotted at approximately 10, 25 and 40 minutes after injection. This curve might be interpreted by a change in the packing constraints with time. If the dye molecules come very close together, dye complexes, called dimers,

can be formed. These dimers have low quantum yields. This is the reason usually given for the fall off in fluorescence intensity when a dye is in a very concentrated state.

5) Overlap Integral

The overlap integral is the integral over the area where the excitation and emission spectra are not separated. This value is influenced by both the viscosity of the medium but more so by any intersystem crossing that occurs in the excited state. In water solution, see Fig. 26, the separation of the peak intensity of the excitation and fluorescence spectra is only 8 mm; this separation is closely related to the overlap integral. Our animal data shows a peak separation of 38 mm. This separation would indicate at least a moderate to large amount of intersystem crossing and hence a relatively large number of molecules being transferred to the triplet state. The lack of any triplet state emission spectra shows that the triplet state is being quenched, probably by oxygen.

6) Polarizability

The fluorescence polarizability is determined by viscosity. For bound dye molecules the size, shape and flexibility of the molecule that is attached to the dye determines the polarizability. We measure the fluorescence polarizability in a monkey retina to be 9.6 for excitation and 8.8 for emission, an average of about 9. This corresponds to a viscosity of 9.6.

Dandliker[21,55] has derived an equation relating the polarizability to the ratio of bound versus free dye.

$$\frac{c_b}{c_f} = \left(\frac{I_f}{I_b}\right)\left(\frac{p - p_f}{p_b - p}\right)$$

where c_b/c_f is the ratio of bound to free dye, I_f/I_b is the intensity ratio for free versus bound dye, p the measured polarizability, p_f the polarizability of free dye and p_b the polarizability of bound dye. p_f is approximately 0.02 and p_b probably 0.33, see Fig. 7. I_f/I_b is 2.2 as measured by Brubaker for dye bound to human plasma. Inserting these values we find that C_c/C_f is 0.64, that is 60% of the dye is free and 30% is bound. Our measured value of polarizability may be somewhat low due to light scatter but is probably not in error by more than 10%. It is usually accepted that a large fraction of fluorescein is bound in a blood solution, as much as 80 to 90%. If this same ratio held true in the retina, we would have measured a polarizability of 0.22. It seems very unlikely that we are in error by this amount; therefore, we must conclude that the amount of free dye in the retina is much higher than it is in a blood solution.

Brubaker[48] has measured the unbound fraction of dye in plasma as a function of dye concentration. His data is shown as Fig. 27. At a concentration of 10^{-4} the unbound fraction is over 50%. Our determination may not be too much in error.

7) Lifetime of the Excited State

The lifetime of the excited state, measured by the fluorescence decay time is determined by the intrinsic fluorescence lifetime and by any triplet state interactions, usually triplet state quenching reactions. Parker[13] has derived an expression for the quenching of fluorescence due to oxygen.

$$\text{Percent Quenching} = 100\left(1 - \frac{1}{(1+N)}\right)$$

where

$$N = K_Q \tau_0 S\ pO_2$$

K_Q is the rate constant for quenching of dye molecules by oxygen. K_Q is

usually about 5× the diffusion rate constant, K_c. S is the solubility and pO_2 the partial pressure of oxygen. τ_0 is the intrinsic dye decay time.

A change is quenching results from a change in pO_2 for systems with constant K_Q and S. In a water-fluorescein solution:

$K_Q = 2\times10^{10}$ liter mole^{-1} sec^{-1}

$S = 5\times10^{-3}$ mole liter^{-1} atm^{1}

$\tau = 10^{-8}$ sec

pO_2 can readily be determined if it lies in the range of 0 to 2 atm. S is likely to be much different in blood and the value of K_Q is not well known. Since we have no data as yet on decay times, we do not know if fluorescein will prove to be a useful dye for oxygen partial pressure measurements in the retina; however, other dyes such as pyrenes ($t_0 = 10^{-6}$) or eosin (τ_0, phosphoresence, $= 10^{-3}$) offer a wide range of possibilities.

8) Lifetime Dependent Measurements of Decay Time, Spectra and Polarizability

These quantities together with those mentioned above enable solutions to be found for the rate equations of energy transfer[56]. These solutions enable dye binding site separations and the separation of energy states to be calculated. These types of measurements and calculations are only in the early planning stages at the present time.

9) Polarizability Spectra

Changes in polarizability with wavelengths indicate overlapping electronic transitions and can indicate multiple binding sites. Our polarization excitation spectra for the retina show a significantly increased value at the longer wavelengths. We do not have sufficient data to interrupt this in any meaningful way.

References

1) Gurr, E.
Synthetic Dyes in Biology, Medicine and Chemistry,
Academic Press, New York, 1971.

2) Lillie, R.D.,
H.J. Conn's Biological Stains,
eighth edition, The Williams and Wilkins Co.,
Baltimore, 1969.

3) Melamed, M.R., Mullaney P.F., and Mendelsohn M.L.
Flow Cytometry and Sorting,
John Wiley and Sons, New York, 1979.

4) Thaer, A.A. and Sernetz, M.,
Fluorescence Techniques in Cell Biology
Springer-Verlag New York, (1973)

5) Nairn, R.C.,
Fluorescent Protein Tracing
E. & S. Livingstone Ltd London (1969)

6) Steiner, R.F., and Edelhoch, H.
"Fluorescent Protein Conjugates"
Nature 192, 873, (1961)

7) Brand, and Gohlke, R.,
"Fluorescence Probes for Structure",
Ann Rev Brochem 41, 843, (1972)

8) Wessing
Fluorescein Angiography of the Retina,
The C.V. Mosby Company, Saint Louis (1969)

9) Dollery, C.T., Hodge, J.V. and Engel,
"Studies of the Retinal Circulation with Fluorescein",
British Medical Journal Nov 10, 1962, page 1210

10) Cunha-Vaz, J., De Abrew, F., Campos, A.J, and Figo, G.M.
"Early Breakdown of the Blood-Retinal Barrier in Diabetes",
B.J.O. 59, 649, 1975.

11) Guilbault, G.C.
Practical Fluorescence
Marcel Dekker, Inc., New York (1973)

12) Wehry, E.L.,
Modern Fluorescence Spectroscopy, Vol. 2
Plenum Press, New York (1976)

13) Parker, C.A.,
Photoluminescence of Solutions
Elsevier Publishing Company, New York, (1968)

14) Hodge, J.V., and Clemett, R.S.,
"Improved Method for Fluorescence Angiography of the Retina".
AJO, 61, 1400, (1960)

15) Haining, M., and Lancaster, C.,
"Advanced Techniques for Fluorescein Angiography",
Arch Ophthal 79, 10, (1968)

16) Allen, L. and Frazier, O.,
"Evidence Favoring Wide Band Filters for Fluorescein Angiography"
Proc int Symp Fluorescein Angiography, Albi Fr, 1969

18) Delori, F.C., Castany, M.A. and Webb, R.H.,
"Fluorescence Characteristics of Sodium Fluorescein in Plasma and Whole Blood",
Exp. Eye Res., 27, 417, (1978)

19) Chen, F. and Edelhoch,
Biochemical Fluorescence: Concepts Vol 1
Marcel Dekker, Inc., New York (1975)

20) Leach, J.,
Physical Principles and Techniques of Protein Chemistry
Academic Press, New York (1969)

21) Burns, V.W.,
"Measurement of Viscosity in Living Cells By a Fluorescence Method",
Biochem and Biophys Res Comm.
37, 1008 (1969)

22) Stryer, L and Haugland, R.P.
"Energy Transfer: A Spectroscopic Ruler",
Proc. Nat. Acad. Sci., 58, 719, (1967).

23) Weber
"Rotational Brownian Motion and Polarization of the Fluorescence of Solutions".
Fluorescence and Phosphoresence Analysis
Edited by D. Hercules, Interscience, New York, (1966)

24) Weber and Anderson, R.,
"The Effects of Energy Transfer and Rotational Diffusion upon the Fluorescence Polarization of Macro-molecules,
Biochemistry 8, 362, (1969)

25) Udkoff, R. and Norman, A.
"Polarization of Fluorescein Fluorescence in Single Cells",
J. of Histochemistry and Cytochemistry, 27, 49 (1979).

26) Visser, J.W.M., Jongeling, A.A.M. and Tanke, H.J.,
"Intracellular pH-Determination by Fluorescence Measurements",
J. of Histochemistry and Cytochemistry, 27, 32, (1979).

27) Ainsworth, S. and Flanagan, M.T.,
"The Effects that the Environment Exerts on the Spectroscopic Properties of Certain Dyes that are Bound by Bovine Serum Albumin",
Biochimica et Biophysica Acta, 194, 213 (1969)

28) Chance, B, Lee, C. and Blasie, J.K.
Probes of Structure and Function of Macromolecules and Membranes, Vol. 1
Academic Press, New York (1971)

29) Lund-Anderson, H. and Krogsaa, B.
"Fluorescein in Human Plasma in Vitro".
Acta Ophthal 60, 701, (1982)

30) Lund-Anderson, H., Krogsaa, and Jensen
"Fluorescein in Human Plasma in Vivo",
Acta Ophthal 60, 709, (1982)

31) Delori, C. and Ben-Sira,
"Excitation and Emission spectra of Fluorescein Dye in the Human Ocular Fundus,
Invest Ophthal 14, 487, (1975)

32) Grayson, M.C. and Laties, A.M.,
"Ocular Localization of Sodium Fluorescein",
Arch. Ophthal., 85, 600, (1971)

33) Grayson, M. Tsukahara, S. and Laties, A.M.,
"Tissue Localization in Rabbit and Monkey Eye of Intravenously-Administered Fluorescein",
Fluorescein Angiography, p. 235 (1974)

34) Tsukahara, I. and Ota, M.,
"Angiographic-Histologic Study on the Location of Sodium Fluorescein in the Fundus",
Fluorescein Angiography, p. 230 (1974)

35) Mizuno K., Sasaki, K and Ohtsuki, K.,
"Histochemical Identification of Fluorescein in Ocular Tissue",
Fluorescein Angiography, 221, (1974).

36) McMahon, R. T., Tso, M.O.M. and McLean, I.W.,
"Histologic Localization of Sodium Fluorescein in Human Ocular Tissues",
Am. J. of Ophthalmol., 80, 1058, (1975).

37) Ben-Sira, I. and Riva, C.E.,
"Fluorescein Diffusion in the Human Optic Disc",
Invest. Ophthal. 14, 205, (1975).

38) Flower, R.W. and Hochheimer, B.F.,
"Quantification of Indicator Dye Concentration in Ocular Blood Vessels",
Exp. Eye Res. 25, 103, (1977)

39) Gupta, R.K., Salzber, B.M., Grinvald, A., Cohen, L.B., Kamino, K., Lesher, S., Boyle, M.B., Waggoner, A.S., and Wang, C.H.,
"Improvements in Optical Methods for Measuring Rapid Changes in Membrane Potential",
J. Membrane Biol. 58, 123 (1981)

40) Hochheimer, B.F. et al Final Progress Report October 1, 1976, NEI Contract EY-3-2139,
"Evaluation of Indicator Substances for Use in the Study of the Retinal and Choroidal Circulations".

41) Hochheimer, B.F. and D'Anna, S.A.,
"Angiography with New Dyes",
Exp. Eye Res. 27, 1, (1978).

42) Grimes, A. Stone, A., Laties, M. and Li,
"Carboxyfluorescein-a Probe of the Blood-Ocular Barriers with Lower Membrane Permeability than Fluorescein",
Arch. Ophthalmol., 100, 635 (1982)

43) Tasaki, L. Carnay, I. and Watanabe, A.,
"Transient Changes in Extrinsic Fluorescence of Nerve Produced by Electric Stimulation",
Proc. Nat. Acad. Sci. 64, 1362, (1969)

44) Waggoner, A.S.,
"Dye Indicators of Membrane Potential",
Ann. Rev. Biophys. Bioeng. 8, 47 (1979)

45) Laurence, D.J.R.,
"A Study of the Adsorption of Dyes on Bovine Serum Albumin by the Method of Polarization of Fluorescence",
Biochem J. 51, 168 (1952)

46) Lavorel, J.,
"Influence of Concentration on the Absorption Spectrum and the Action Spectrum of Fluorescence of Dye Solutions",
Z Electrochem., 61, 1600 (1957).

47) Pitet, P., Amalric, P and Hygounenc, O.,
"Etude analytique de la fluorescence des solutions de fluoresceinate de sodium",
C.R. Symp. Int. Angiographic Fluoresceinique (1969).
Karger, Basel, (1971).

48) Brubaker, F., Penniston, T., Grotte, A. and Nagataki,
"Measurement of Fluorescein Binding in Human Plasma Using Fluorescence Polarization",
Arch Ophthal 100, 625, (1982)

49) Jovin, M.,
"Fluorescence Polarization and Energy Transfer: Theory and Application",
Flow Cytometry and Sorting
John Wiley and Sons, New York (1979)

50) Weber, G.,
"Polarization of the Fluorescence of Macromolecules",
Biochem J, 51, 145, (1952)

51) Winkler, H.,
"Fluorescence Depolarization - A Study of the Influence of Varying Excitation Wavelength and Solution Concentration"
Biochemica et Biophysica Acta, 102, 459, (1965)

52) Kosower, E.M.
"The Effect of Solvent on Spectra I: A New Empirical Measure of Solvent Polarity: Z-Values"
J. Am Chem Soc 80, 3253, 1958.

53) Kosower, E.M.
"The Effect of Solvent on Spectra II: Correlation of Spectral Absorption Data with Z-Values"
J Am Chem Soc 80, 3261, 1958.

54) Dougherty, J.,
"Activated Dyes as Antitumor Agents",
J. of the National Cancer Institute,
52, 1333 (1974).

55) Dandliker, W.B., Kelly, R.J., Dandliker, J., Farquhar, J. and Levin, J.
"Fluorescence Polarization Immunoassay. Theory and Experimental Method",
Immunochemistry, 10, 219, (1973)

56) Turro, J.,
Modern Molecular Photochemistry
The Benjamin/Cummings Publishing Co., Inc.
Menlo Park, California (1978)

57) Lopatin, E. and Voss, W.,
"Fluorescein. Hapten, an Antibody Active-Site Probe".
Biochemistry 10, 208, (1971)

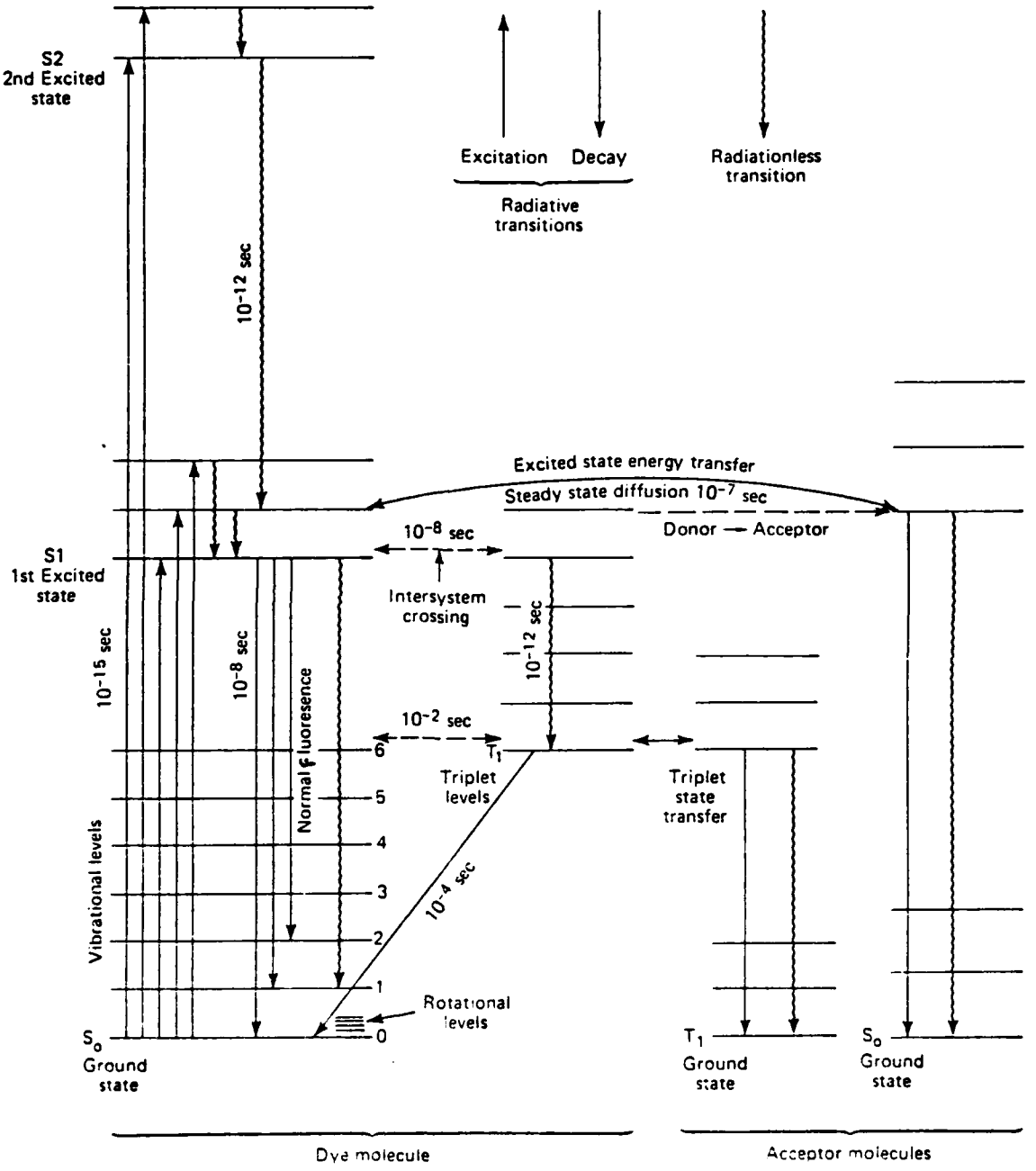
S2
2nd Excited state
Excitation
Decay
Radiationless transition
Radiative transitions
10^{-12} sec
Excited state energy transfer
Steady state diffusion 10^{-7} sec
Donor — Acceptor
10^{-8} sec
S1
1st Excited state
Intersystem crossing
10^{-12} sec
10^{-15} sec
10^{-8} sec
Normal fluorescence
10^{-2} sec
T_1
Triplet levels
Triplet state transfer
Vibrational levels
6
5
4
3
2
1
0
10^{-4} sec
Rotational levels
S_o
Ground state
T_1
Ground state
S_o
Ground state
Dye molecule
Acceptor molecules

Fig. 1.

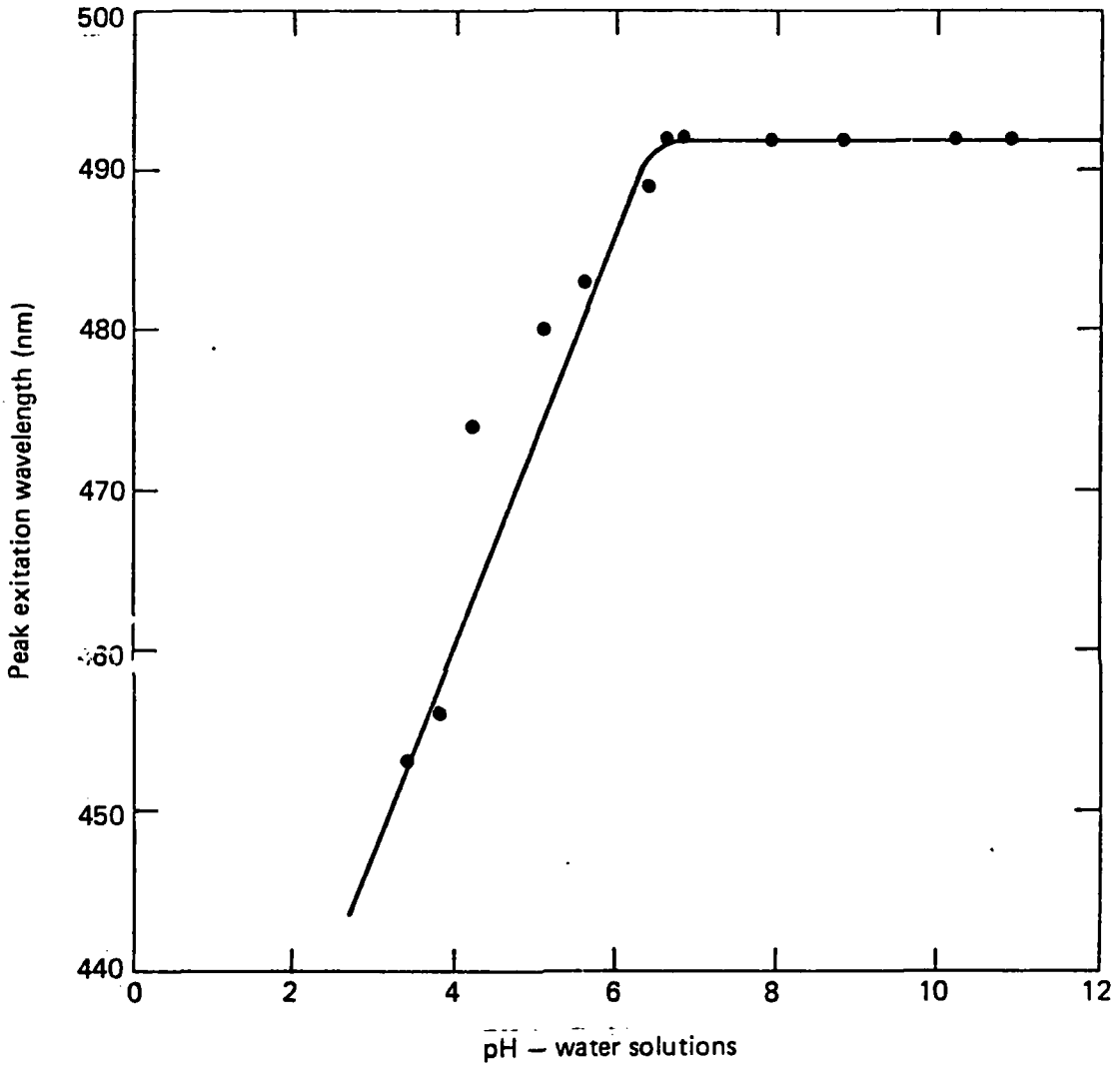
500
490
480
470
460
450
440
Peak exitation wavelength (nm)
0
2
4
6
8
10
12
pH – water solutions

Fig. 2

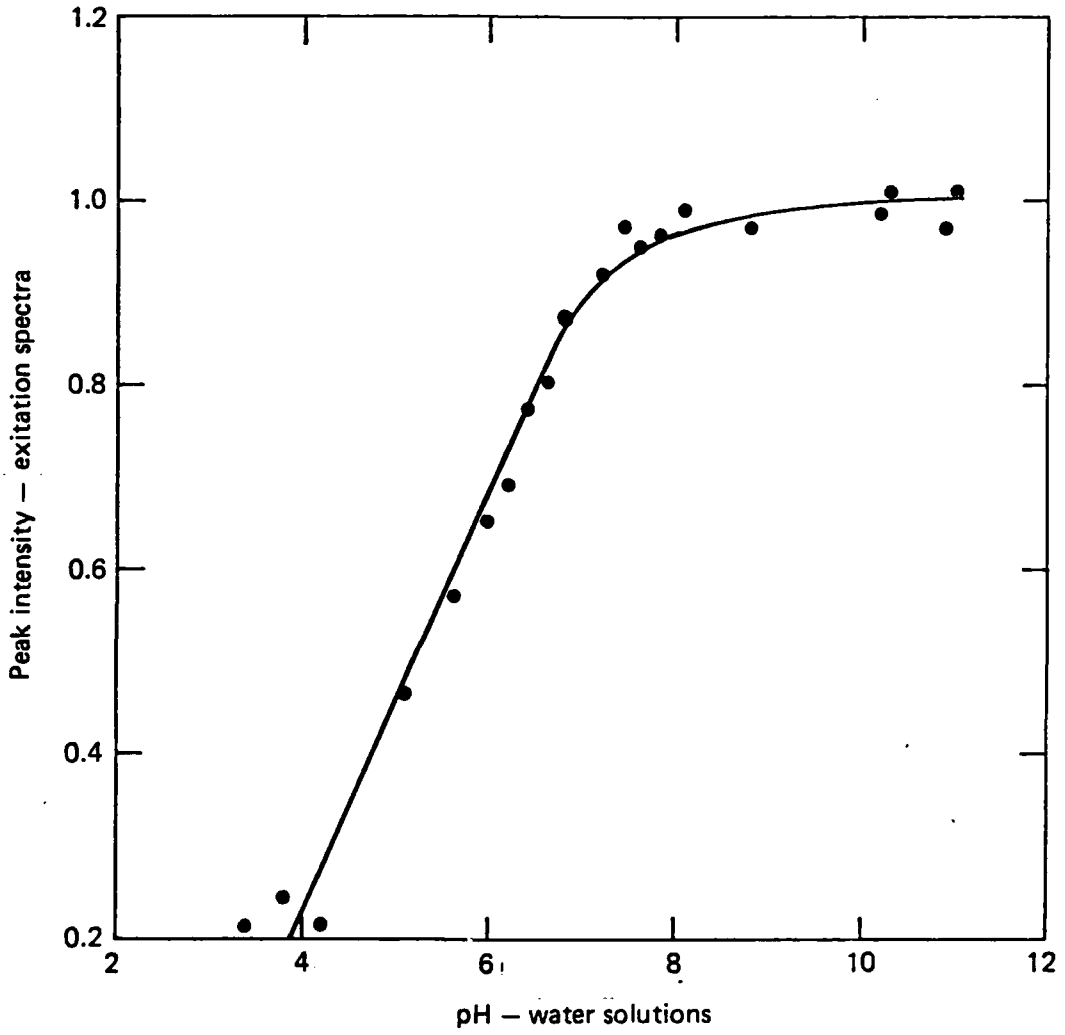
1.2
1.0
0.8
0.6
0.4
0.2
Peak intensity — exitation spectra
2
4
6
8
10
12
pH — water solutions

Fig. 3

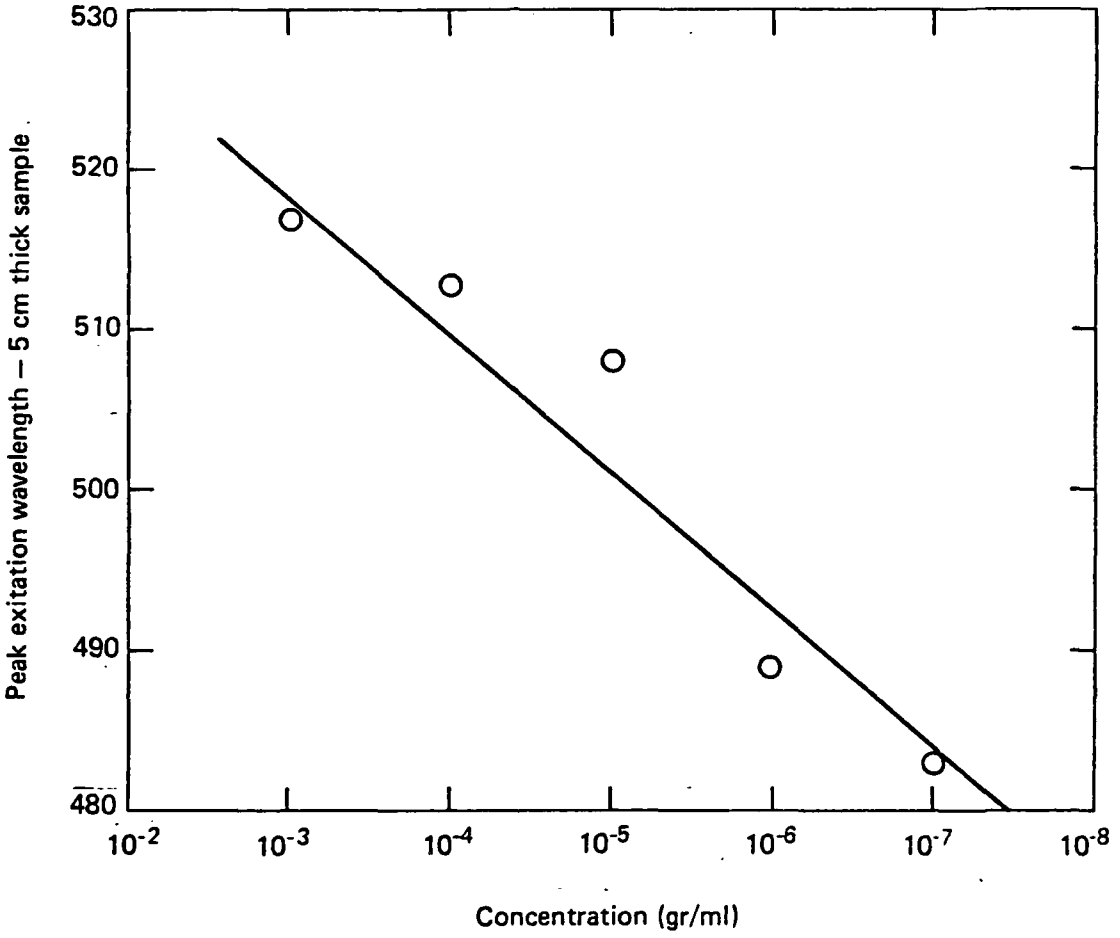
530
520
510
500
490
480
Peak exitation wavelength – 5 cm thick sample
10^{-2}
10^{-3}
10^{-4}
10^{-5}
10^{-6}
10^{-7}
10^{-8}
Concentration (gr/ml)

Fig. 4

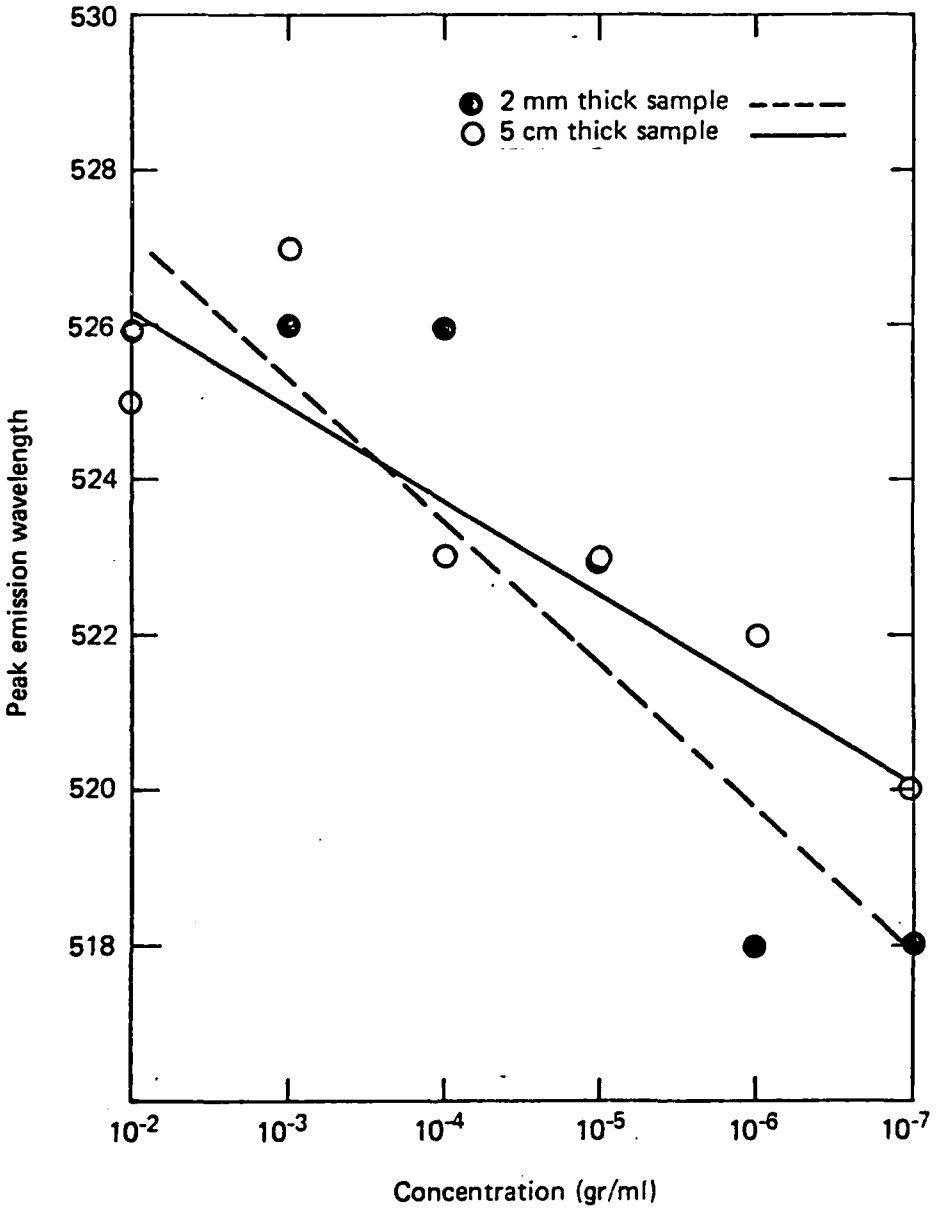
530
528
526
524
522
520
518
Peak emission wavelength
2 mm thick sample
5 cm thick sample
10^{-2}
10^{-3}
10^{-4}
10^{-5}
10^{-6}
10^{-7}
Concentration (gr/ml)

Fig. 5

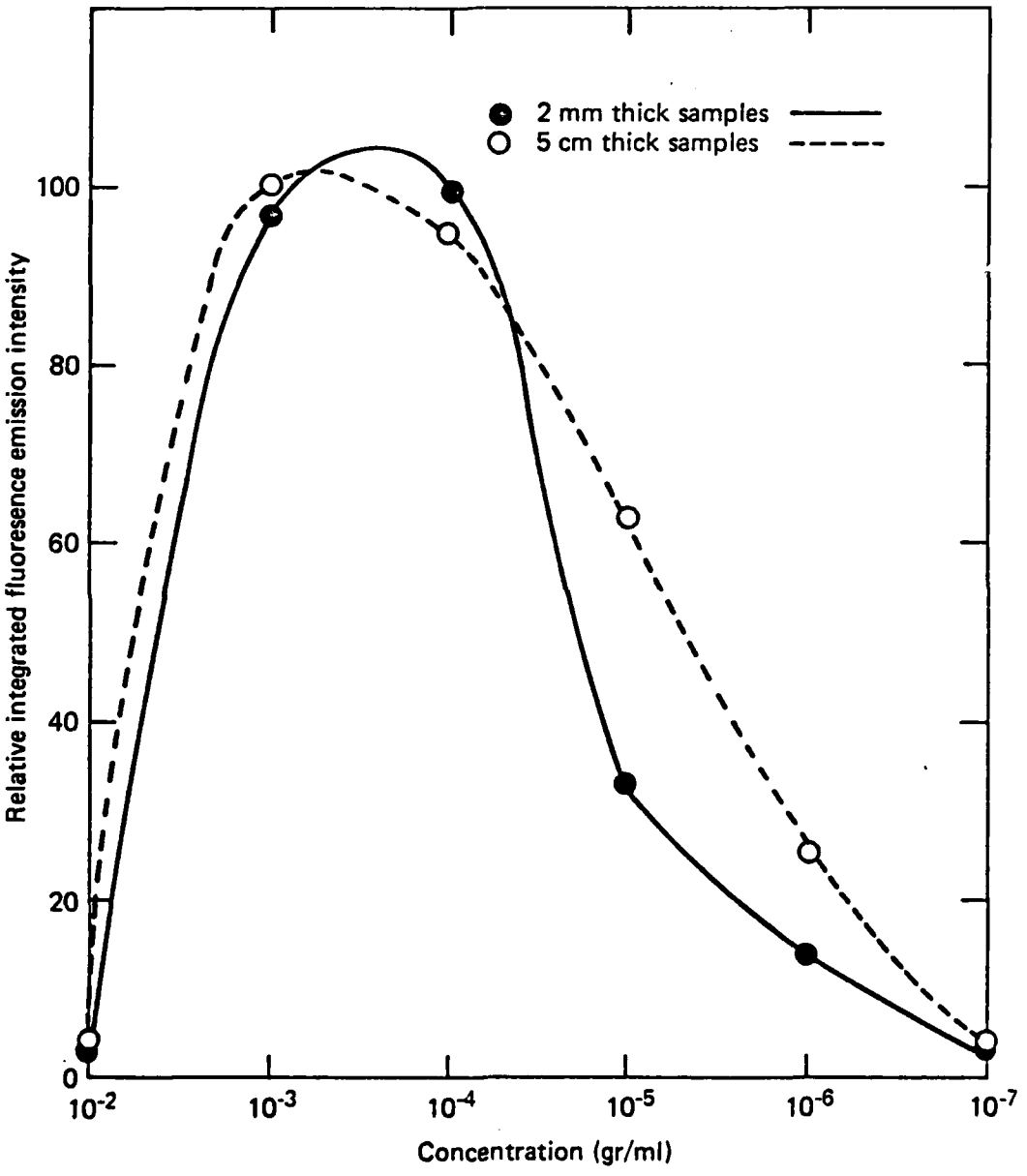
2 mm thick samples
5 cm thick samples
Relative integrated fluoresence emission intensity
0
20
40
60
80
100
10^{-2}
10^{-3}
10^{-4}
10^{-5}
10^{-6}
10^{-7}
Concentration (gr/ml)

Fig. 6

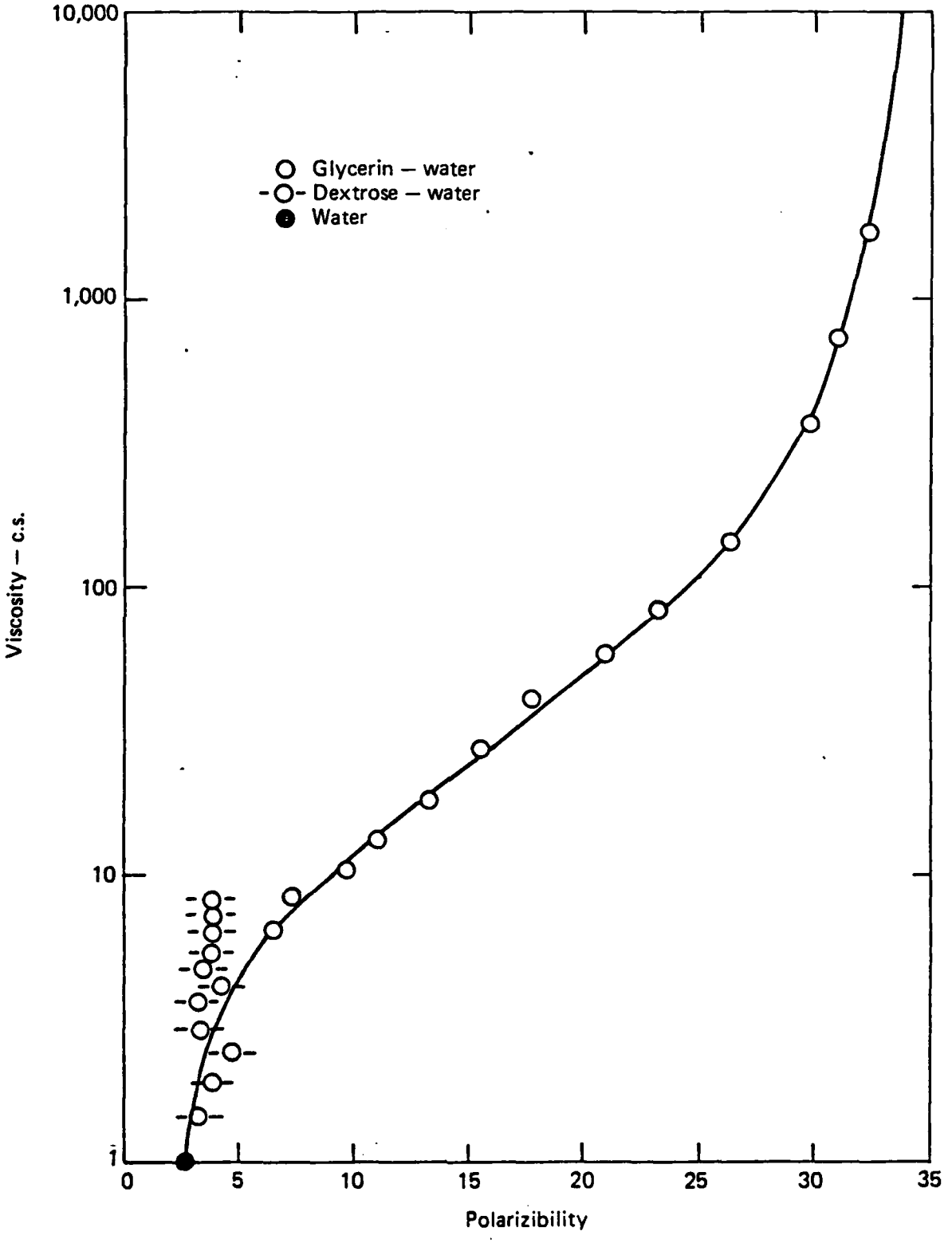
10,000
1,000
100
10
1
Viscosity — c.s.
Glycerin — water
Dextrose — water
Water
0
5
10
15
20
25
30
35
Polarizibility

Fig. 7

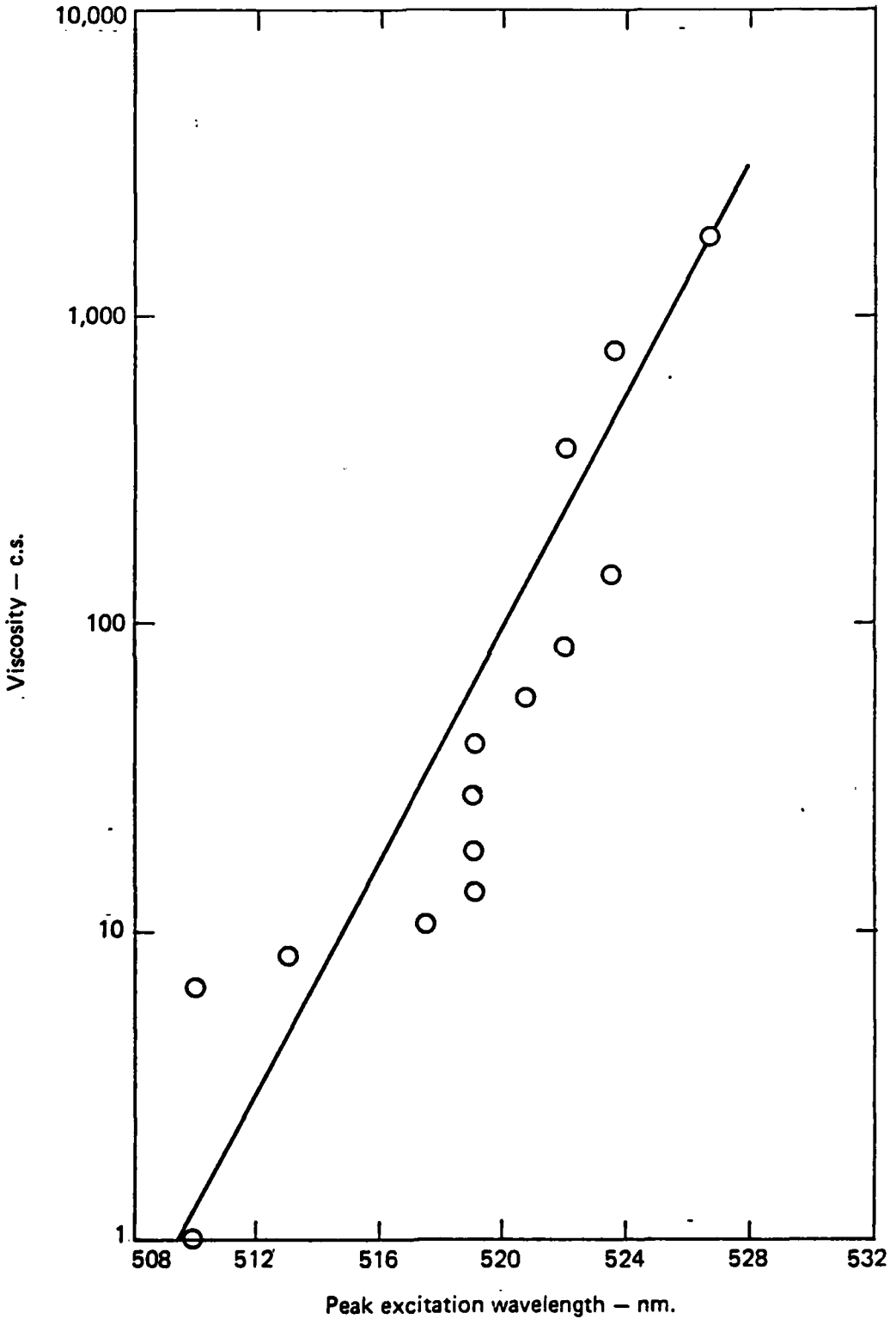
10,000
1,000
100
10
1
Viscosity — c.s.
508
512
516
520
524
528
532
Peak excitation wavelength — nm.

Fig. 8

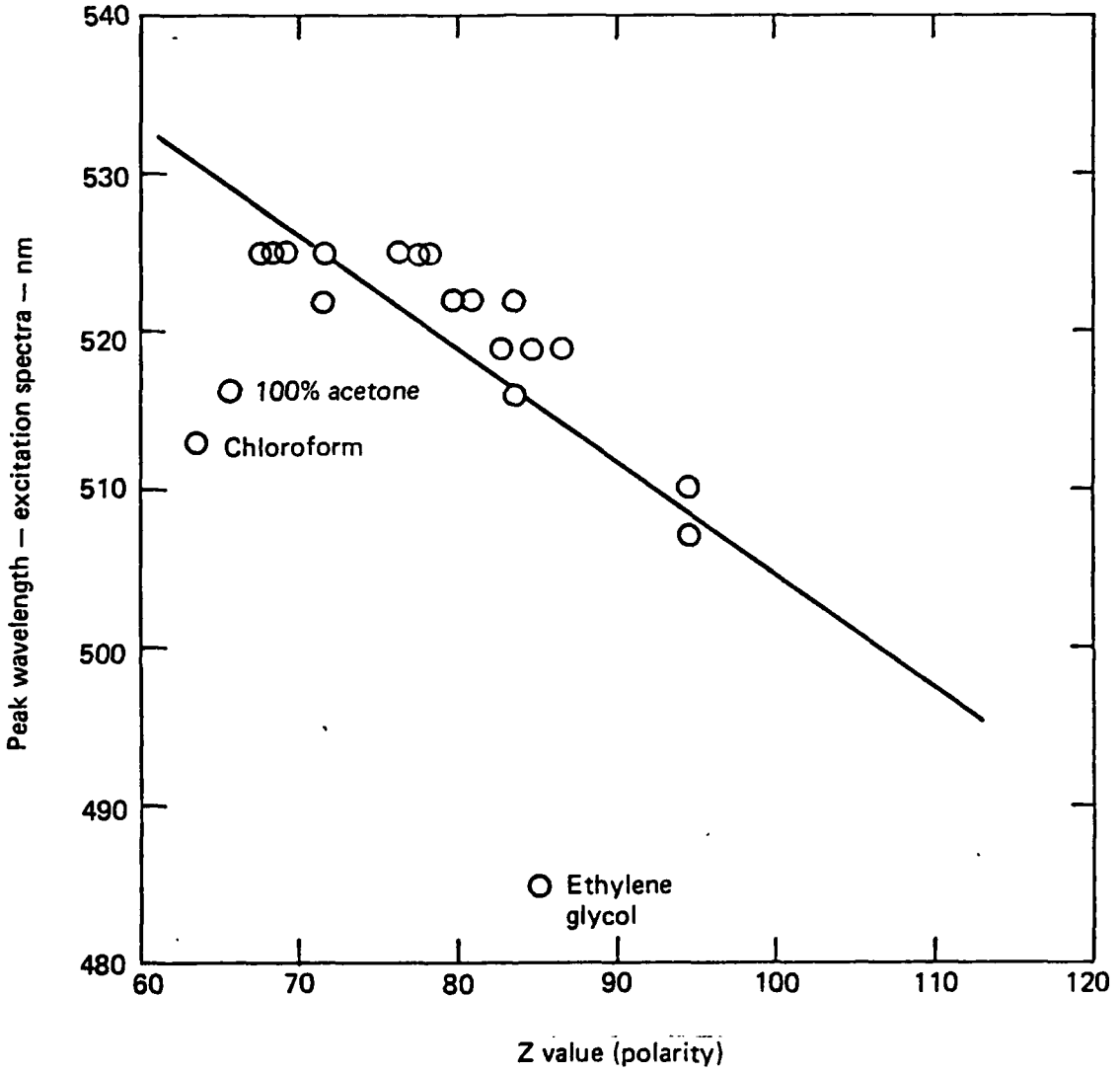
Peak wavelength – excitation spectra – nm
540
530
520
510
500
490
480
60
70
80
90
100
110
120
Z value (polarity)
100% acetone
Chloroform
Ethylene glycol

Fig. 9

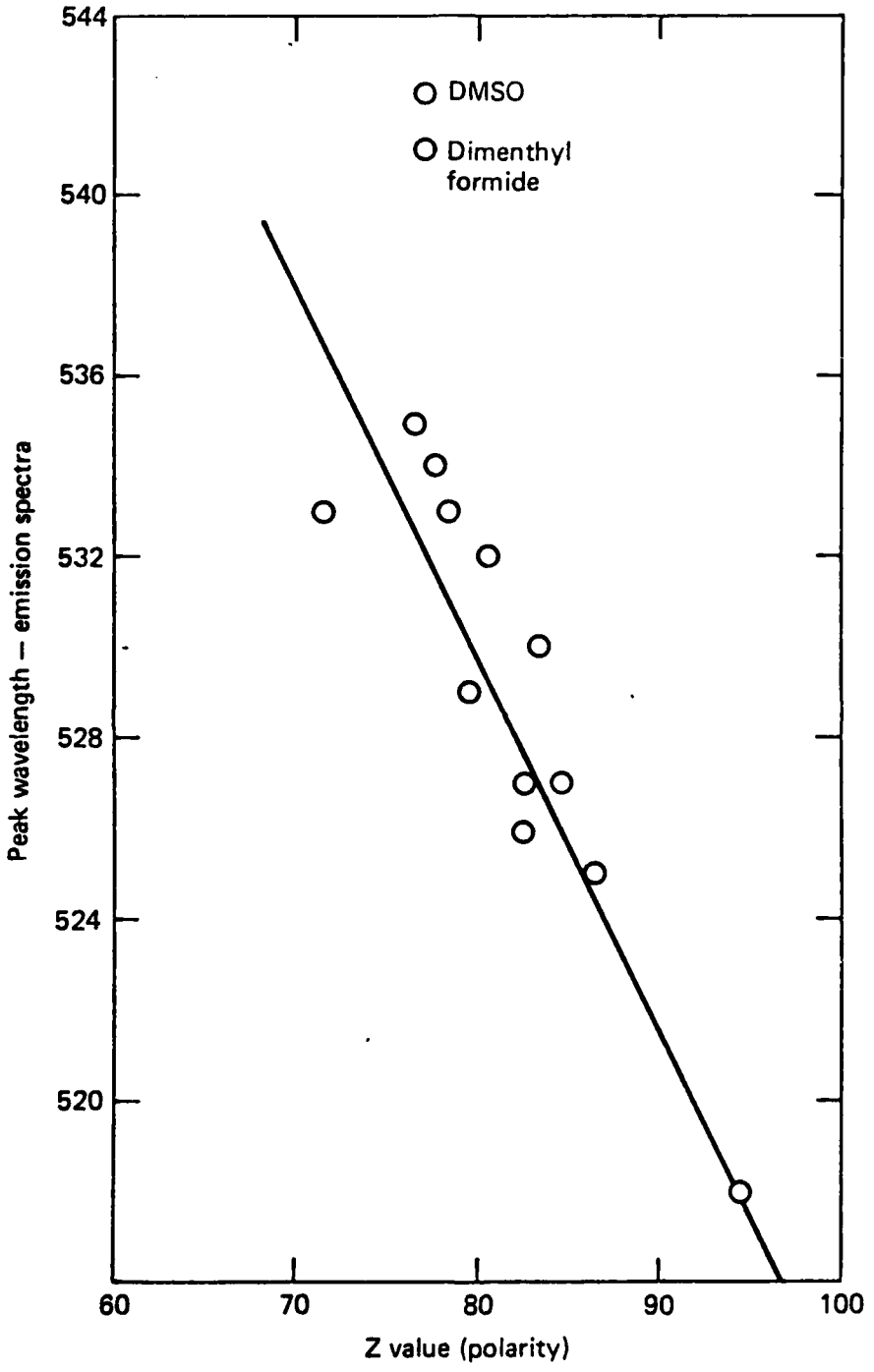
544
540
536
532
528
524
520
DMSO
Dimenthyl formide
Peak wavelength – emission spectra
60
70
80
90
100
Z value (polarity)

Fig. 10

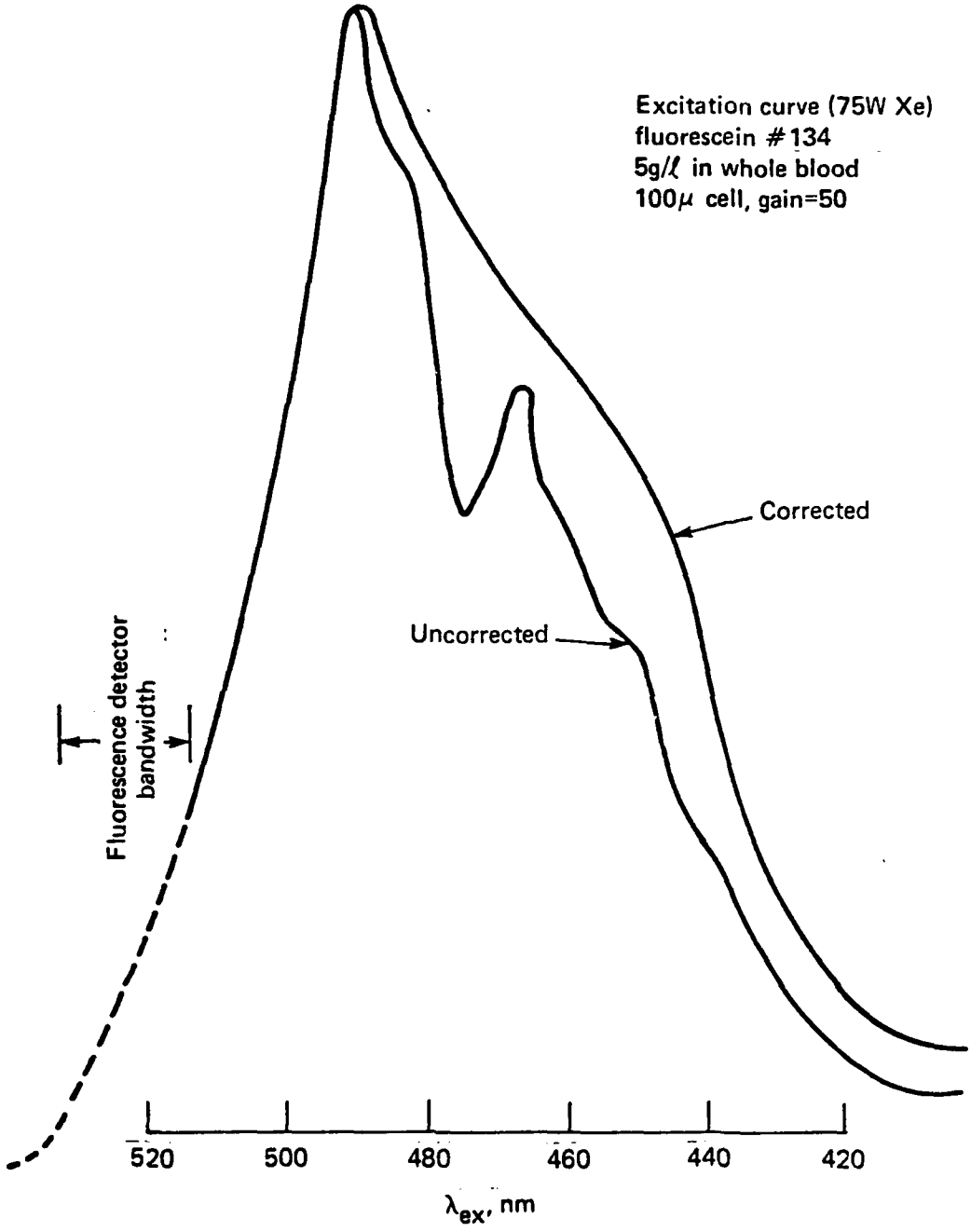
Excitation curve (75W Xe)
fluorescein #134
5g/ℓ in whole blood
100μ cell, gain=50
Corrected
Uncorrected
Fluorescence detector bandwidth
520
500
480
460
440
420
λex, nm

Fig. 11

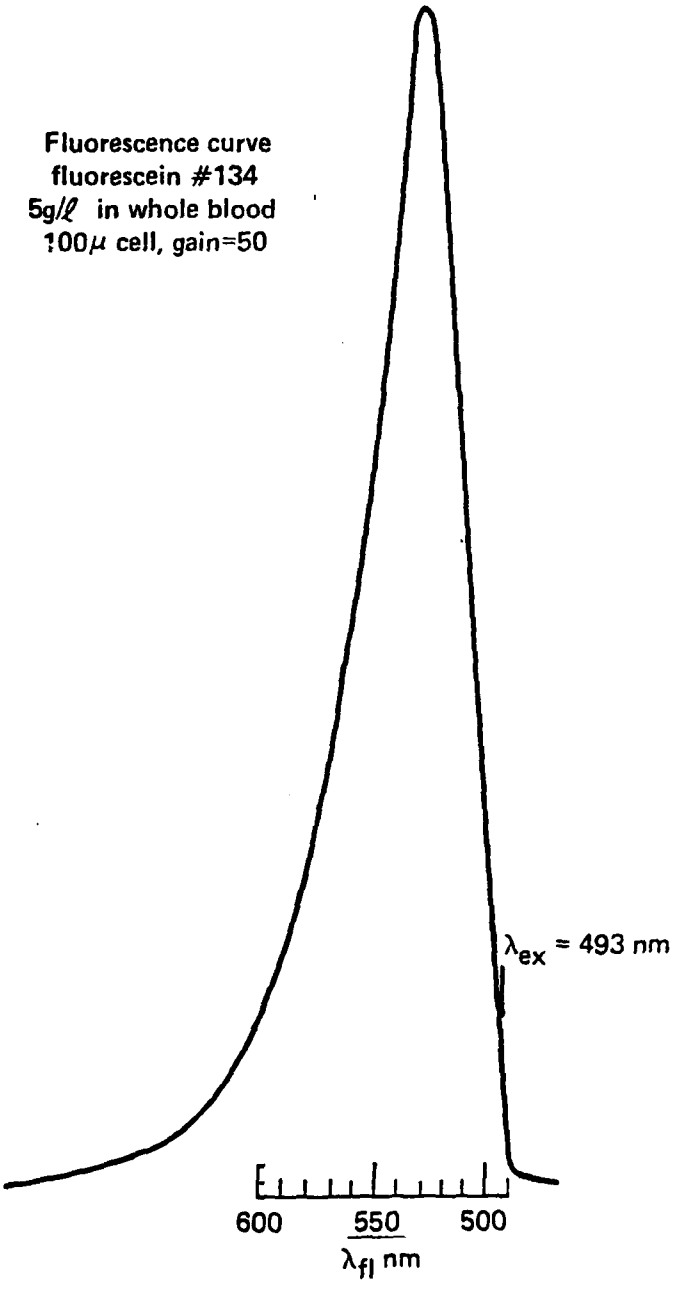
Fluorescence curve
fluorescein #134
5g/ℓ in whole blood
100μ cell, gain=50
λex = 493 nm
600
550
500
λfl nm

Fig. 12

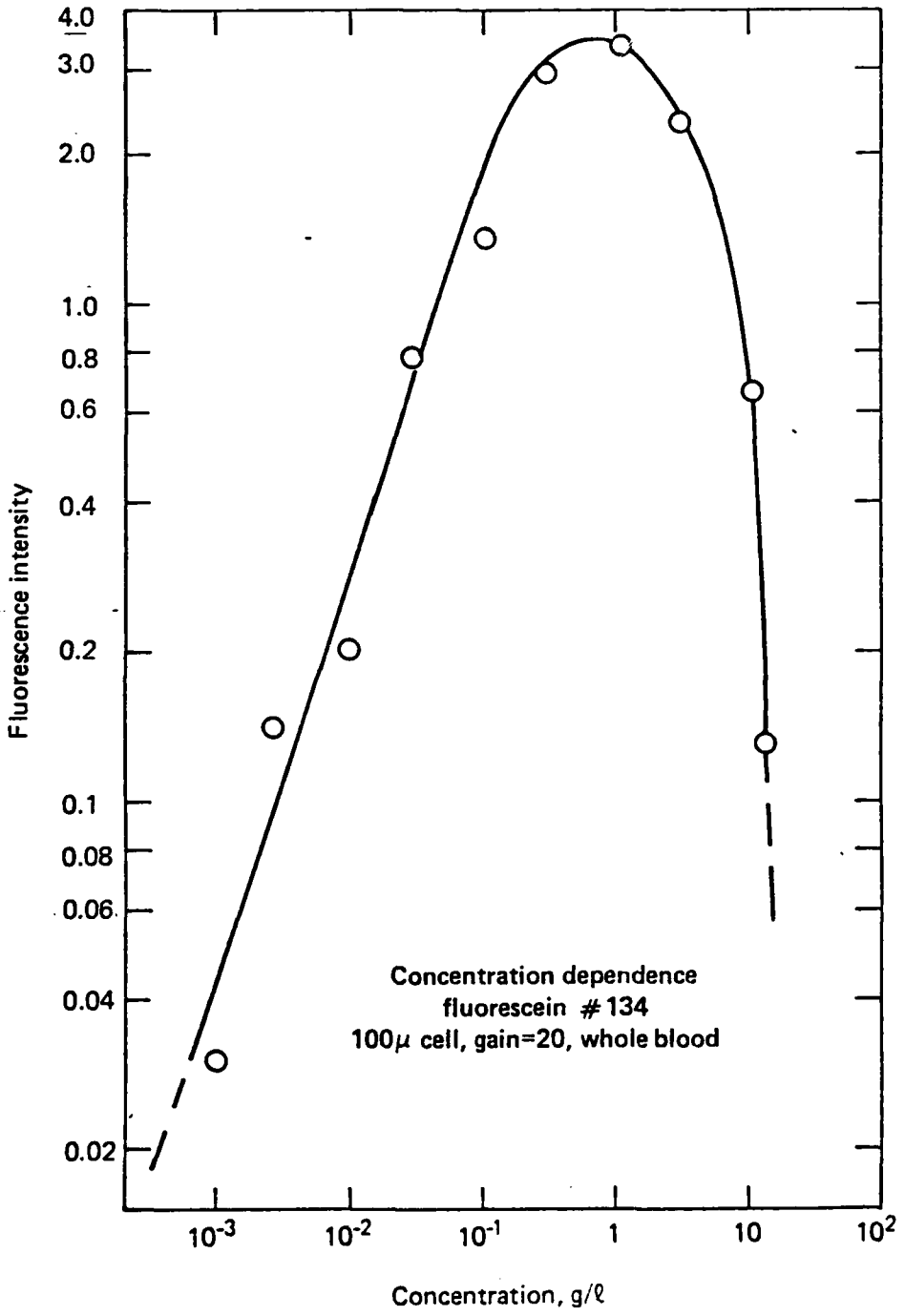
4.0
3.0
2.0
1.0
0.8
0.6
0.4
0.2
0.1
0.08
0.06
0.04
0.02
Fluorescence intensity
Concentration dependence
fluorescein #134
100μ cell, gain=20, whole blood
10^{-3}
10^{-2}
10^{-1}
1
10
10^{2}
Concentration, g/ℓ

Fig. 13

DATE IS 1/12/83
H2O-FLUORESCEIN EXITATION STORED DATA

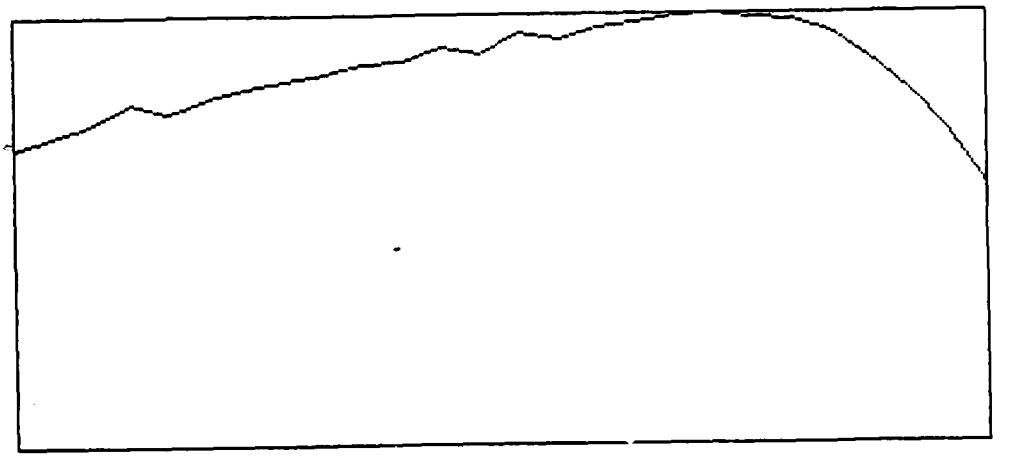

WAVELENGTH 450 TO 525nm

CORRECTION FACTOR FOR TRANSMISSION

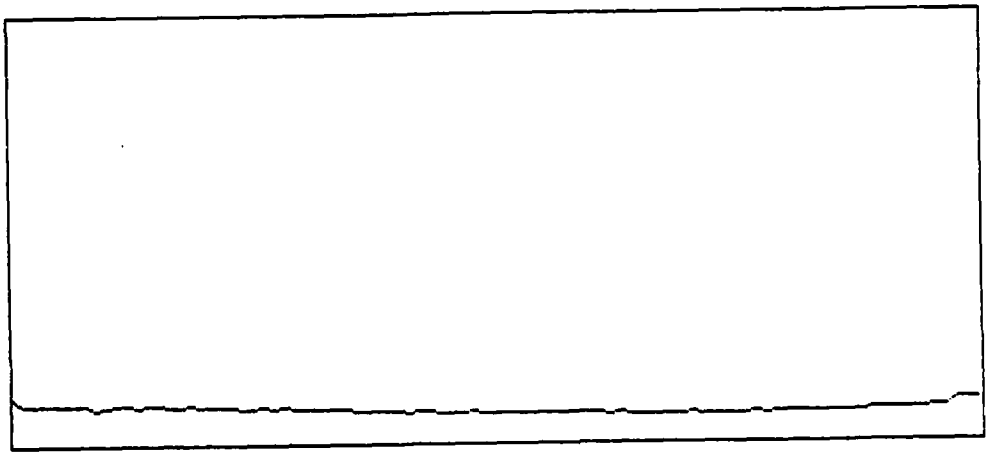

WAVELENGTH--400 TO 725nm

Fig. 14

AD-A127 340 A STUDY OF LOW LEVEL LASER RETINAL DAMAGE(U) JOHNS HOPKINS UNIV LAUREL MD APPLIED PHYSICS LAB B F HOCHHEIMER 15 MAR 83 N00024-83-C-5301 2/2

UNCLASSIFIED F/G 20/5 NL

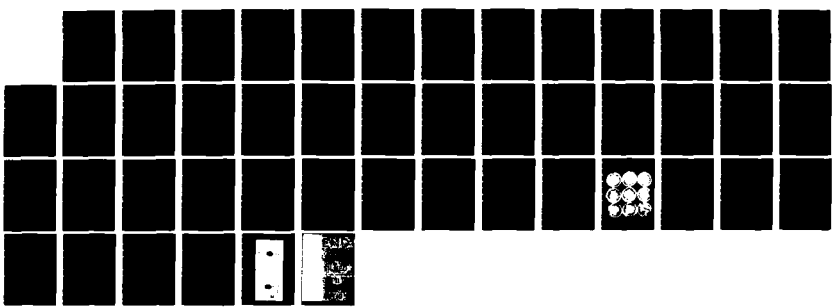

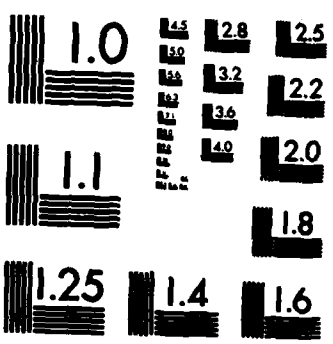

STORED REFLECTIVITY OF ARTIFICIAL EYE

90

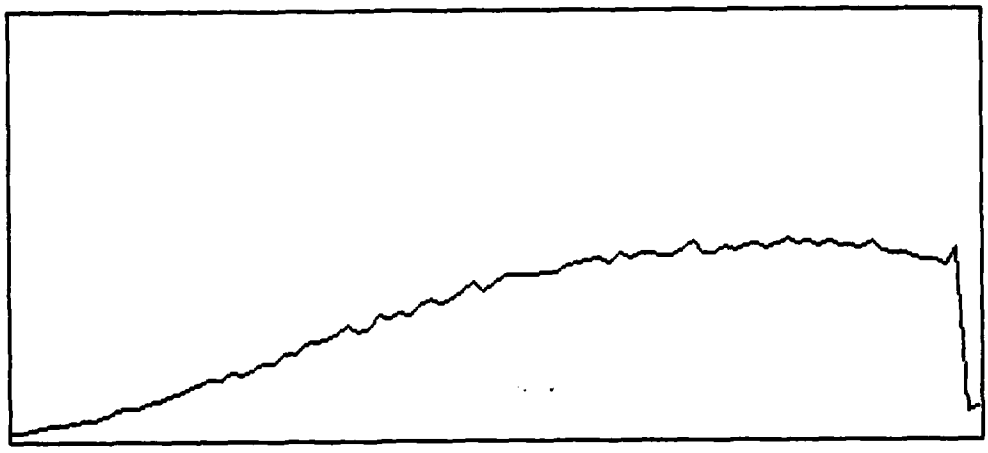

WAVELENGTH 400 TO 725nm

Fig. 15

NORMAL REFLECTIVITY

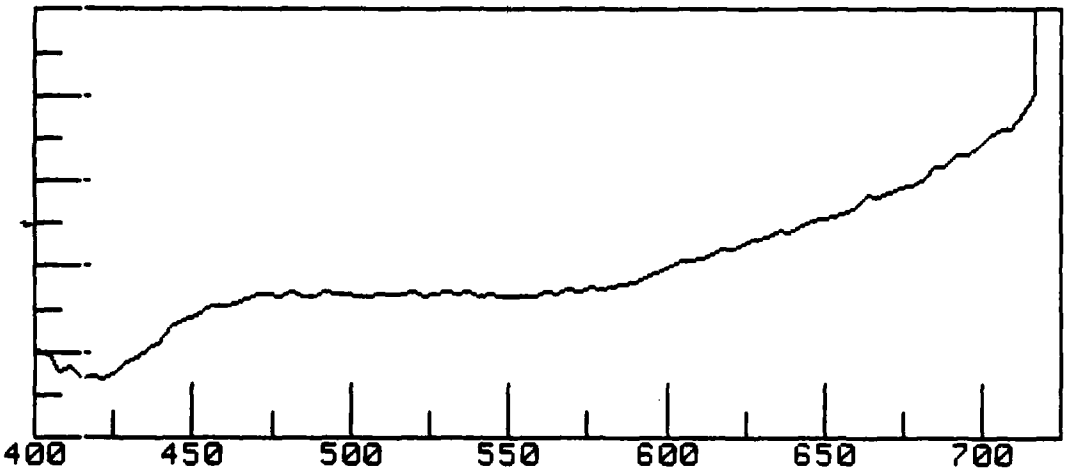

START TIME, REFLECTION DATA ? 0
Int_ab_refl .170581333433
INTEGRATED ABSORPTION IS .2988

Fig. 16

FLUORECEIN REFLECTIVITY RUN NO 2

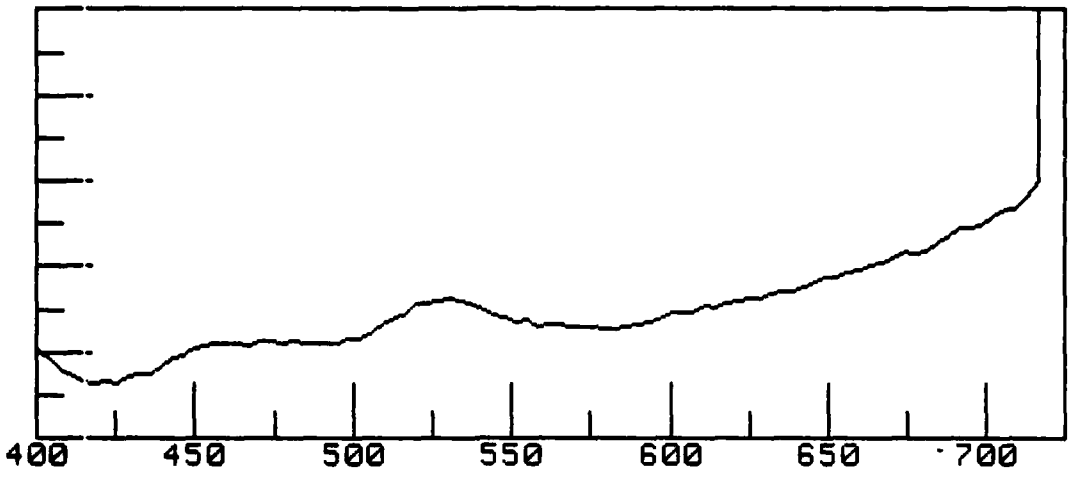

DIFFERENCE SPECTRA

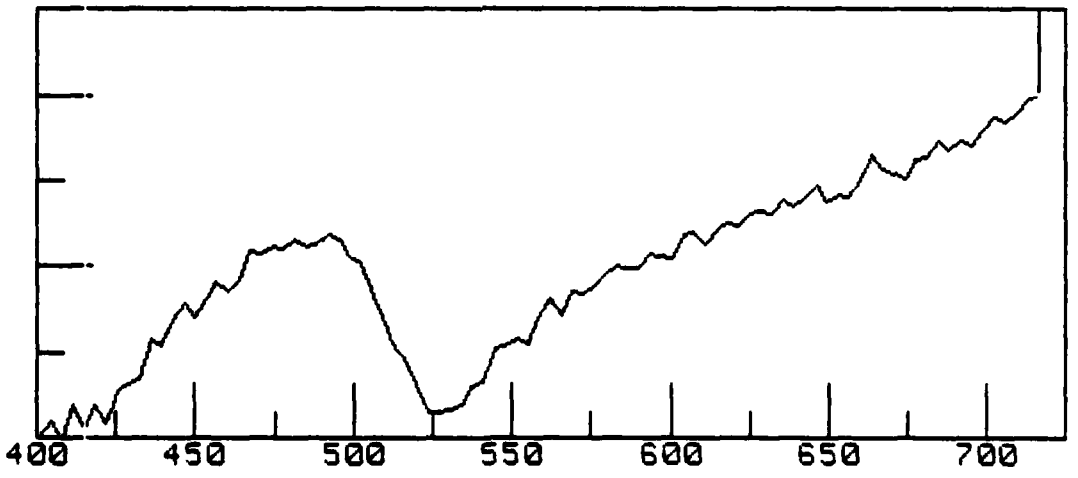

FINISH TIME, REFLECTION DATA 23 51.5
FLUORESENCE DATA COLLECTION FINISHED AT 25 17.3
Time_fl 1517.3
Int_int_fl 3.60536744423
INTEGRATED FLUORESENCE INTENSITY (510 TO 650nm) IS 3.605
---QUANTUM EFFICIENCY---- 3.169

PEAK LAMBDA IS 530.35
PEAK J VALUE IS 46
PEAK VOLTAGE VALUE IS .119961644145

Fig. 17

FLUORESCEIN FLUORESENCE SPECTRA

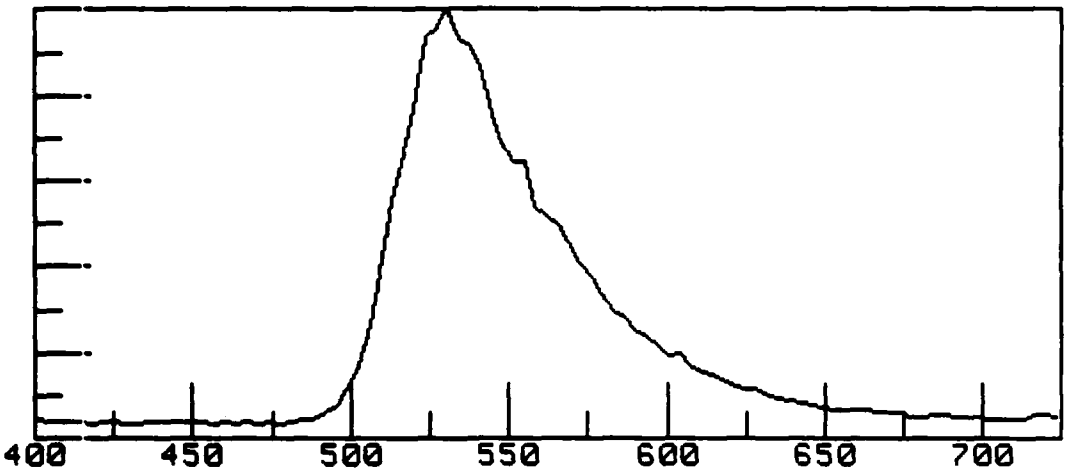

START TIME, FLUORESENCE POLARIZATION SPECTRA 25 39
FINISH TIME, FLORESENCE POLARIZATION SPECTRA 29 12.1
Ave_pol_f1 4.46246251591E-02

AVERAGE EMISSION FLUORESENCE POLARIZABILITY IS .04462

FLUORESENCE POLARIZABILITY SPECTRA

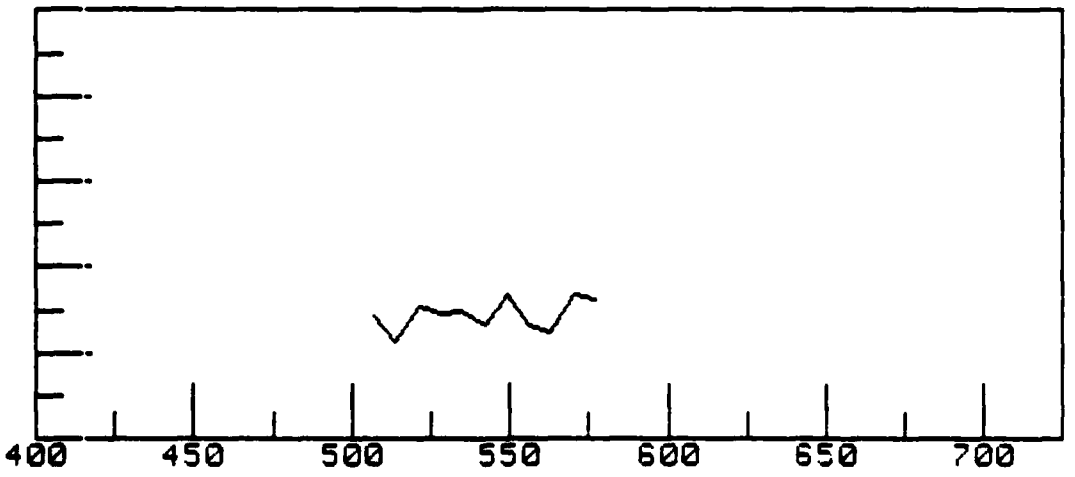

Fig. 18

TIME AT END OF RUN NUMBER 2 IS 33.9 MINUTES

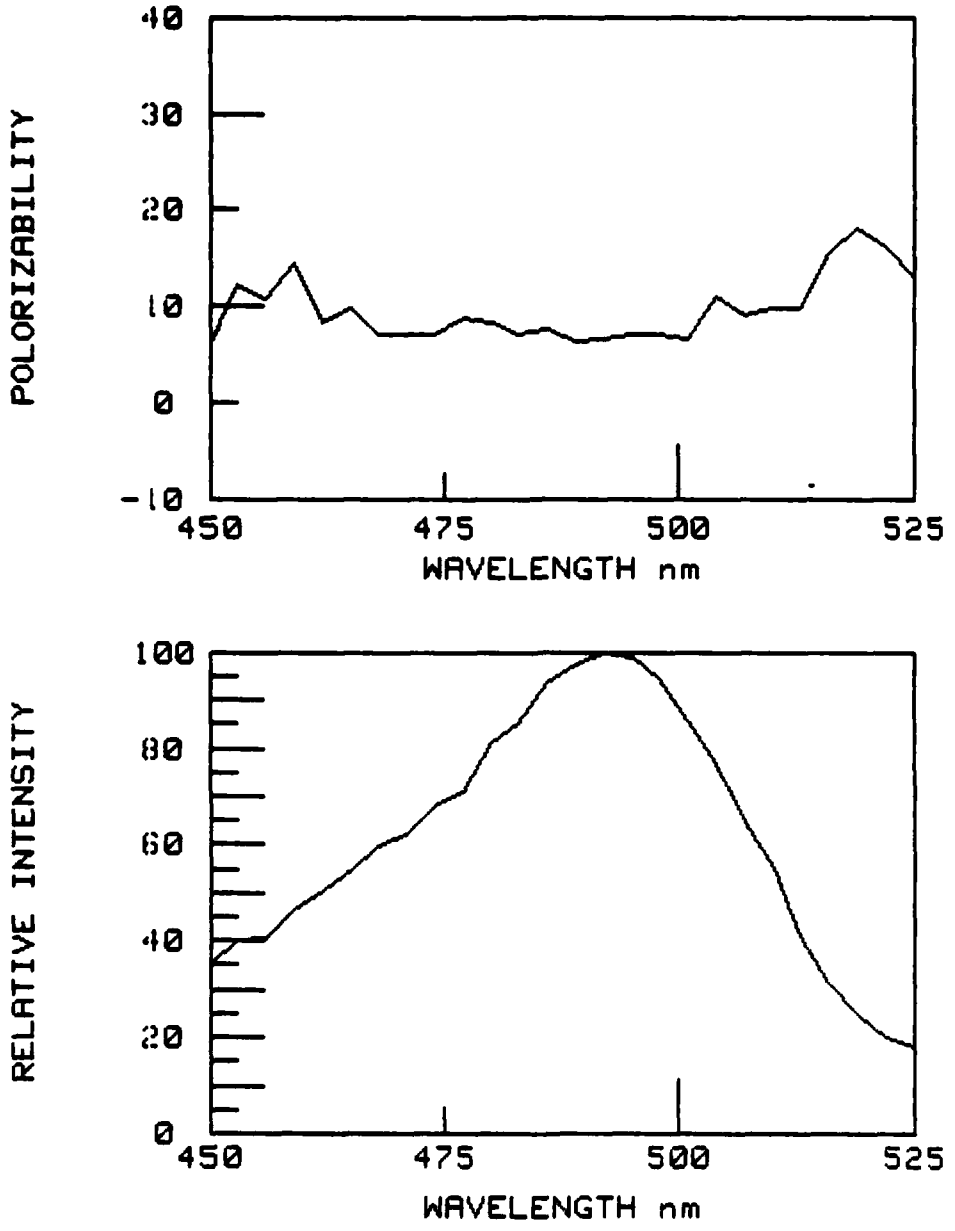

Fig. 19

```
Nn 26                I 2
NO ERRORS DETECTED DURING DATA COLLECTION

 0                   0                   33                  54.9

NO. OF AVERAGING POINTS IS  26
AVERAGE EXITATION POLORIZABILITY IS EQUAL TO 9.68E-02

INTEGRATED EXITATION INTENSITY FOR RUN 2.00E+00 IS 1.22E+02
```

Fig. 20

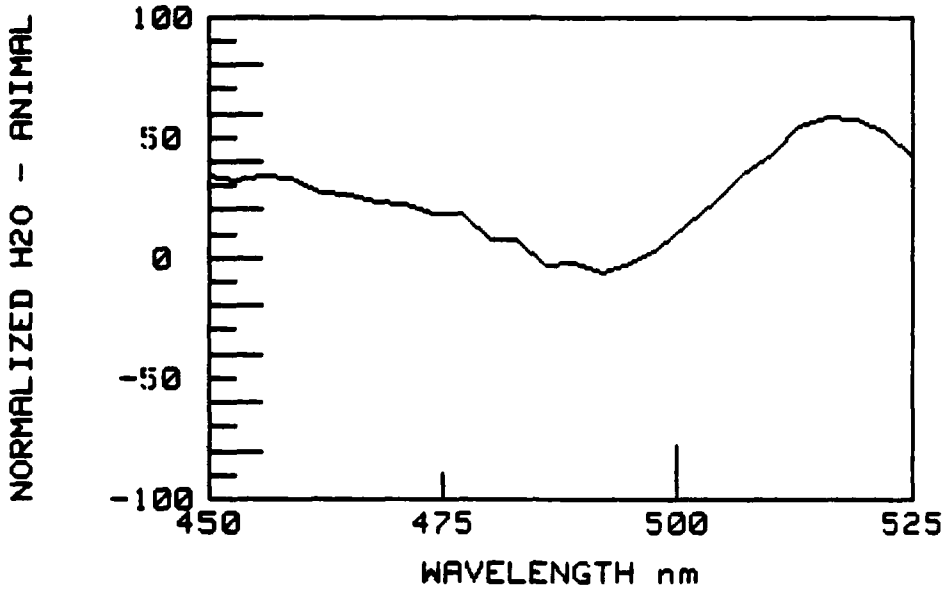

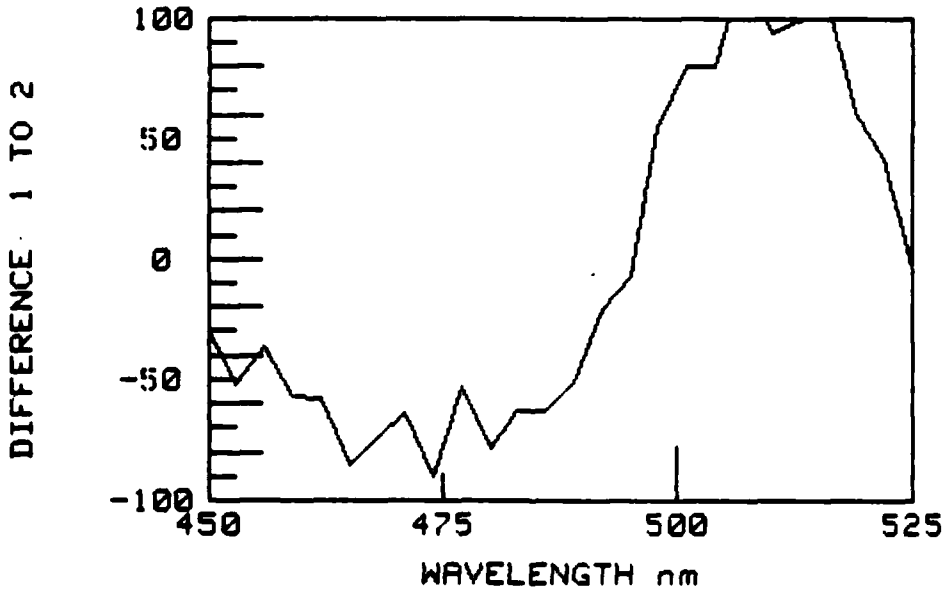


```
Run 3
J                       2
Int_int_ex              121.5237
Ave_pol_ex              9.68412269231E-02
Time_ex                 2034.9
START TIME, REFLECTION DATA  39          0
Int_ab_refl             .929624555505
INTEGRATED ABSORPTION IS  1.629
```

Fig. 21

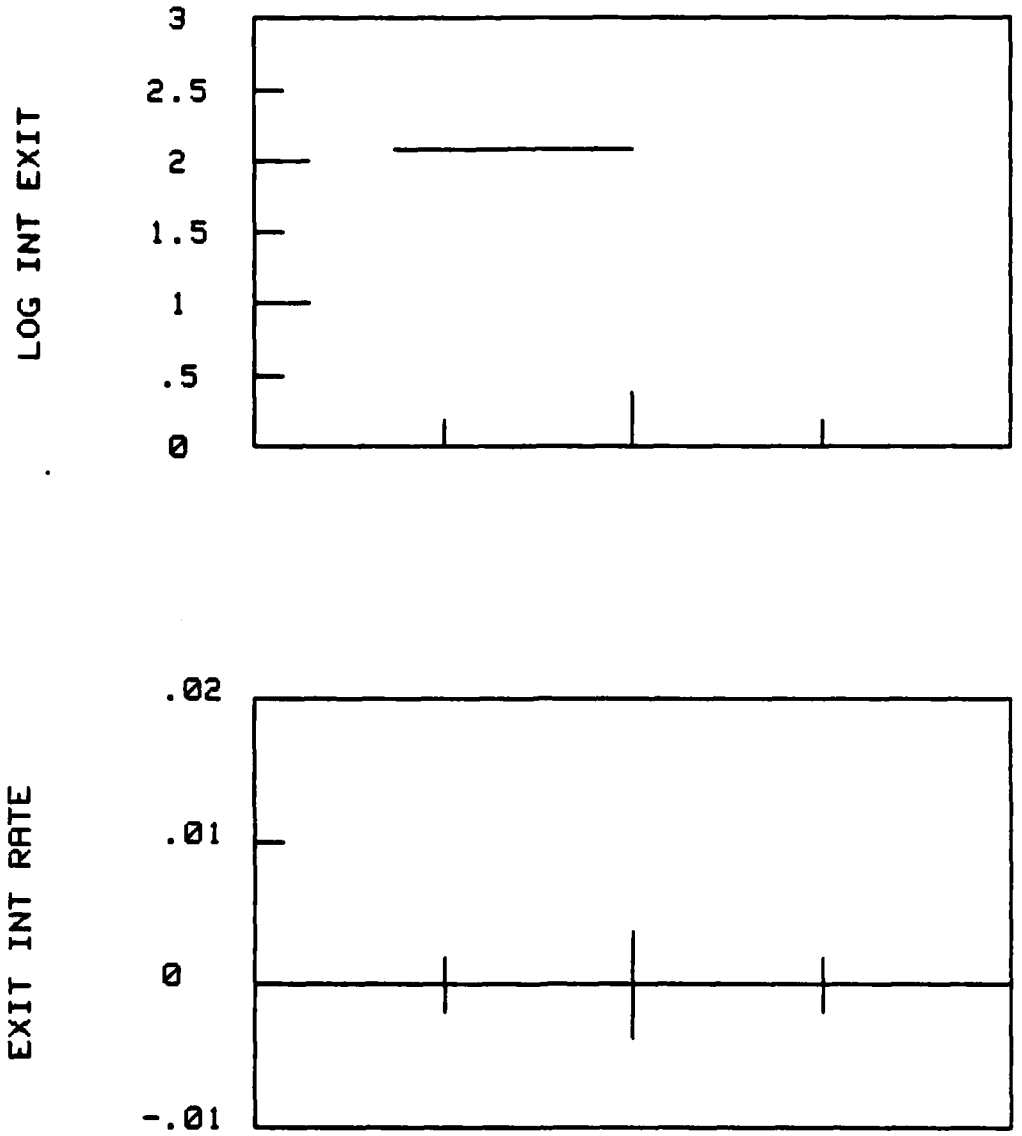

Fig. 22

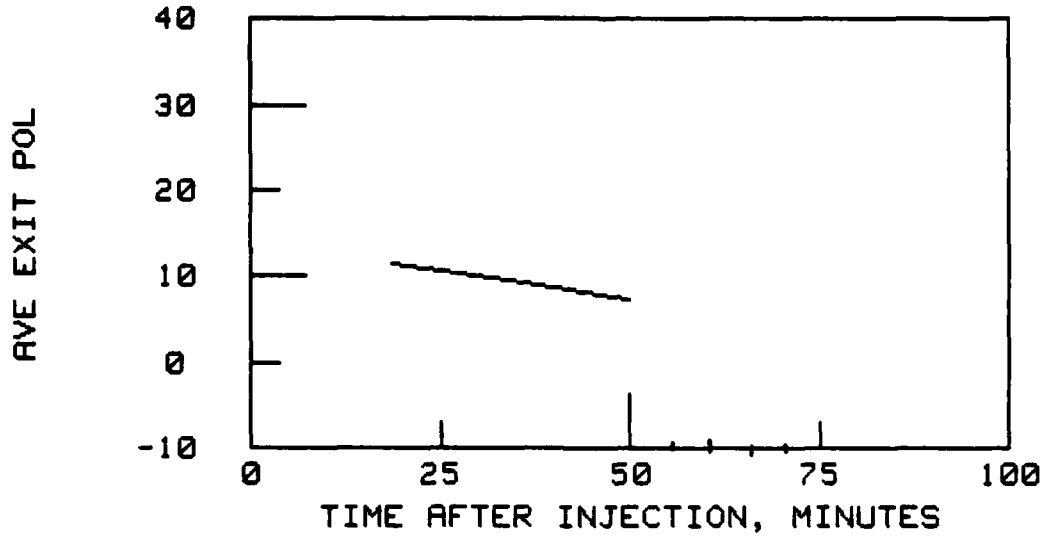
AVE EXIT POL
40
30
20
10
0
-10
0
25
50
75
100
TIME AFTER INJECTION, MINUTES

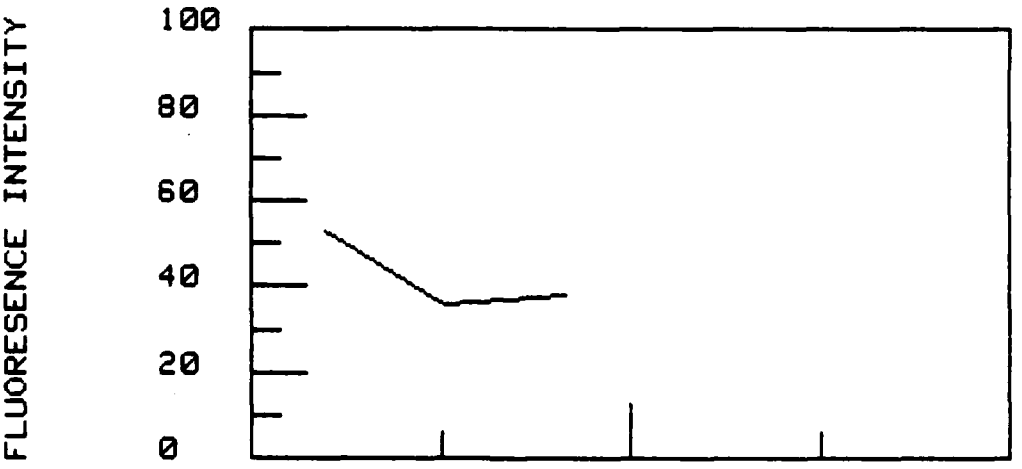
FLUORESENCE INTENSITY
100
80
60
40
20
0

Fig. 23

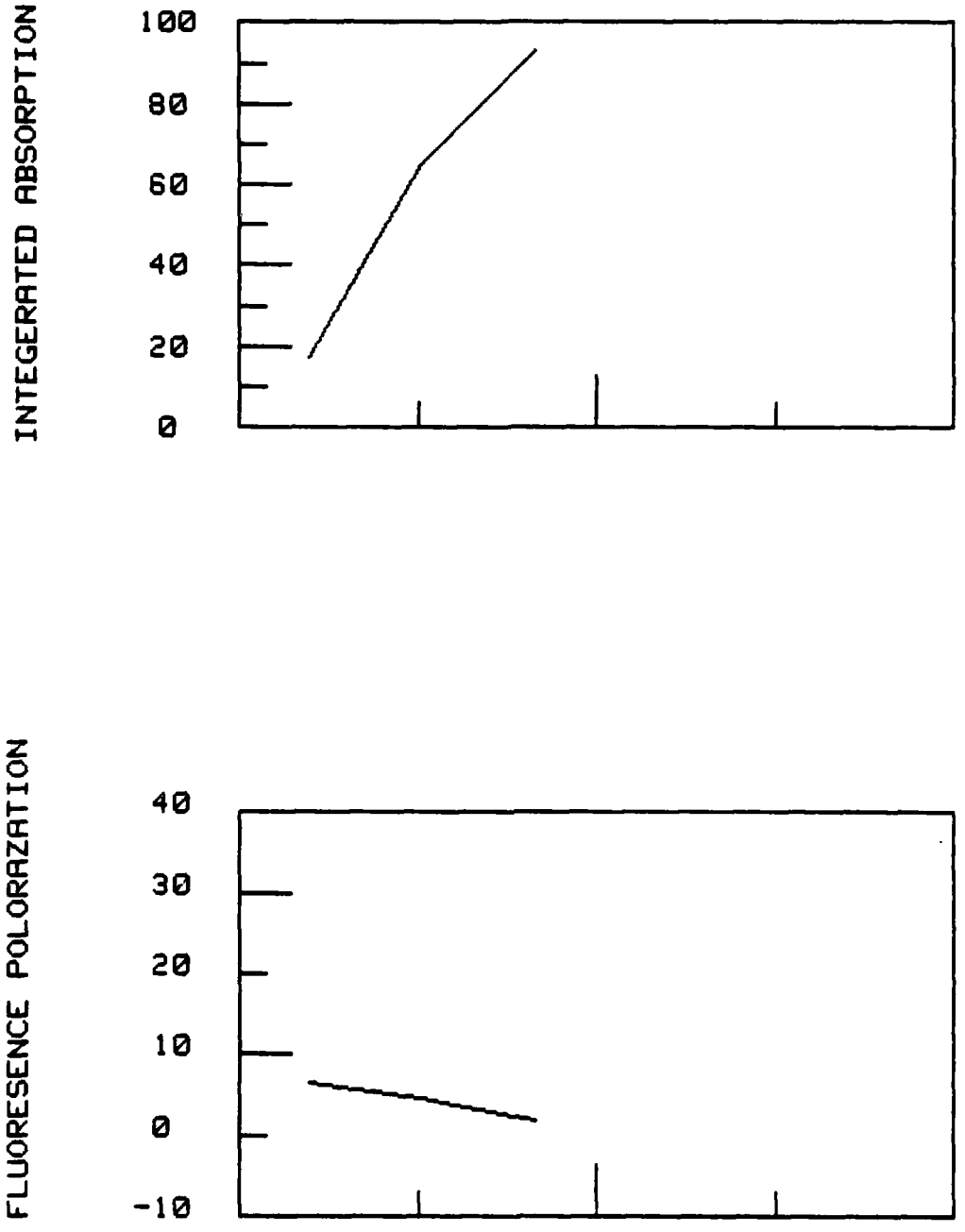
INTEGERATED ABSORPTION
100
80
60
40
20
0
FLUORESENCE POLORRAZATION
40
30
20
10
0
-10

Fig. 24

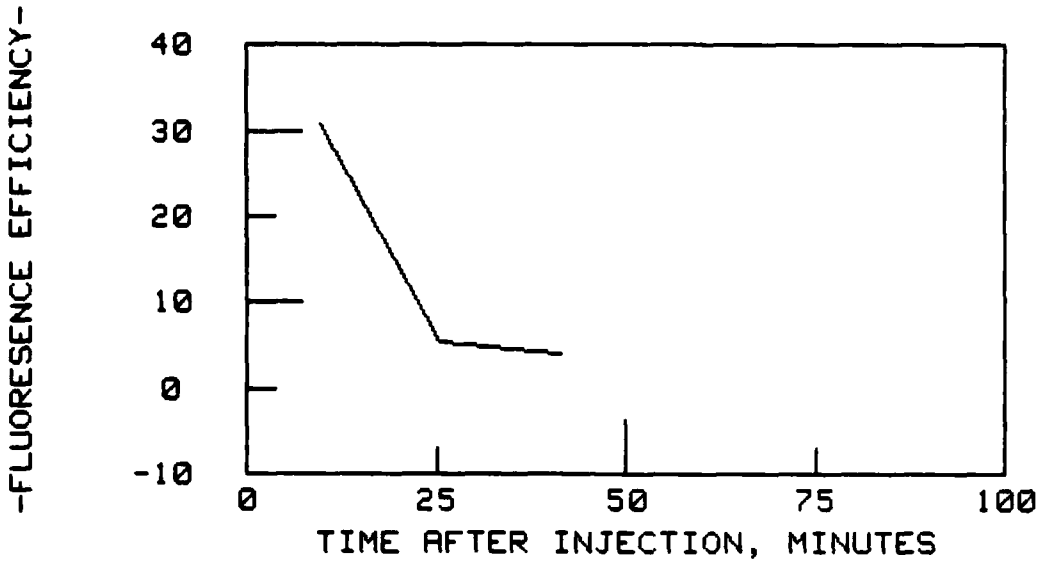

FINISHED

Fig. 25

$C_{20}H_{10}Na_2O_5$

Mol. Wt. 376.27

Concentration 10 ppm in Water

Recorded on an Aminco-Bowman SPF Spectrophotofluorometer

	EXCITATION SPECTRUM	EMISSION SPECTRUM
Excitation Monochromator		280 nm
Emission Monochromator	516 nm	
Emission Entrance Slit	2.0 mm	0.2 mm
Emission Exit Slit	2.0 mm	0.5 mm
Excitation Exit Slit	0.1 mm	5.0 mm
% Full Scale	30	3
Sensitivity	42	76
MAXIMA	281 nm, 320 nm, 464 nm, 480 nm, 488 nm	514 nm

Source of chemical: Arthur H. Thomas Company

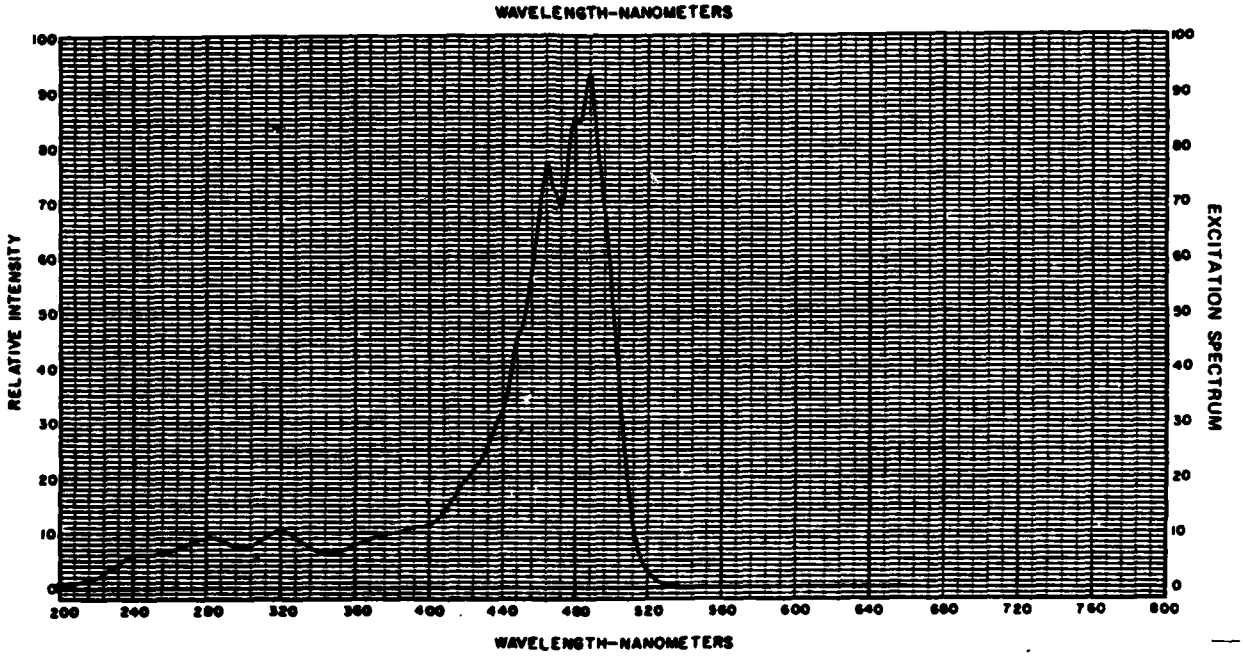

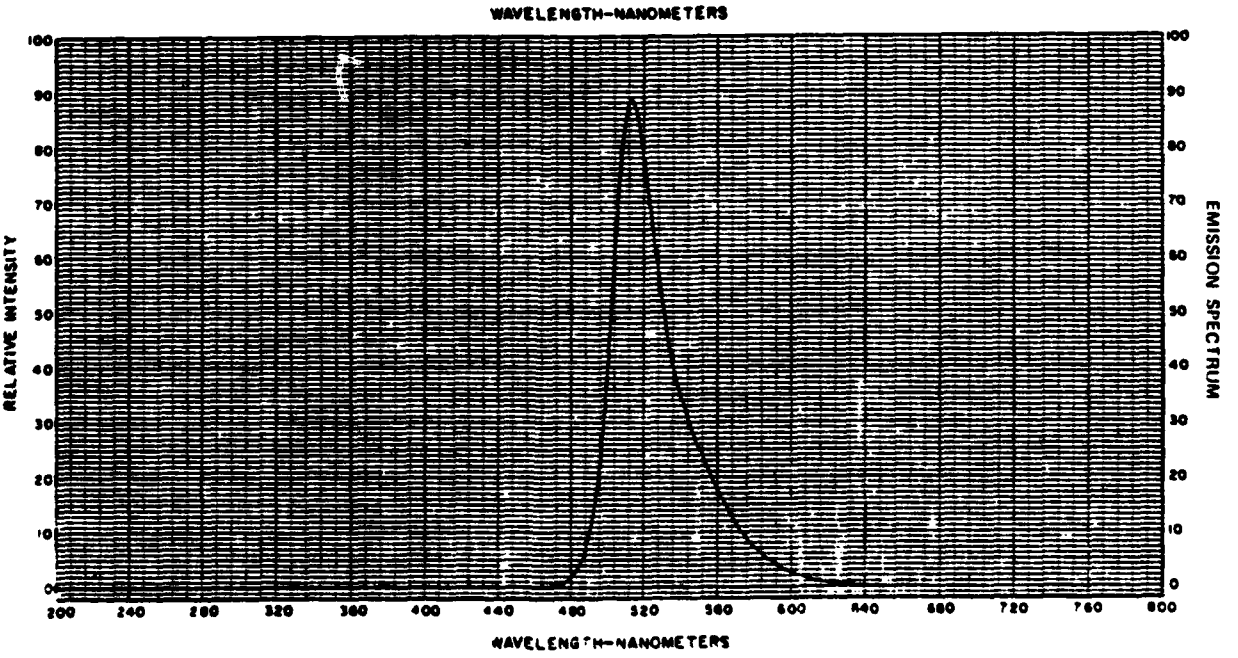

Fig. 26

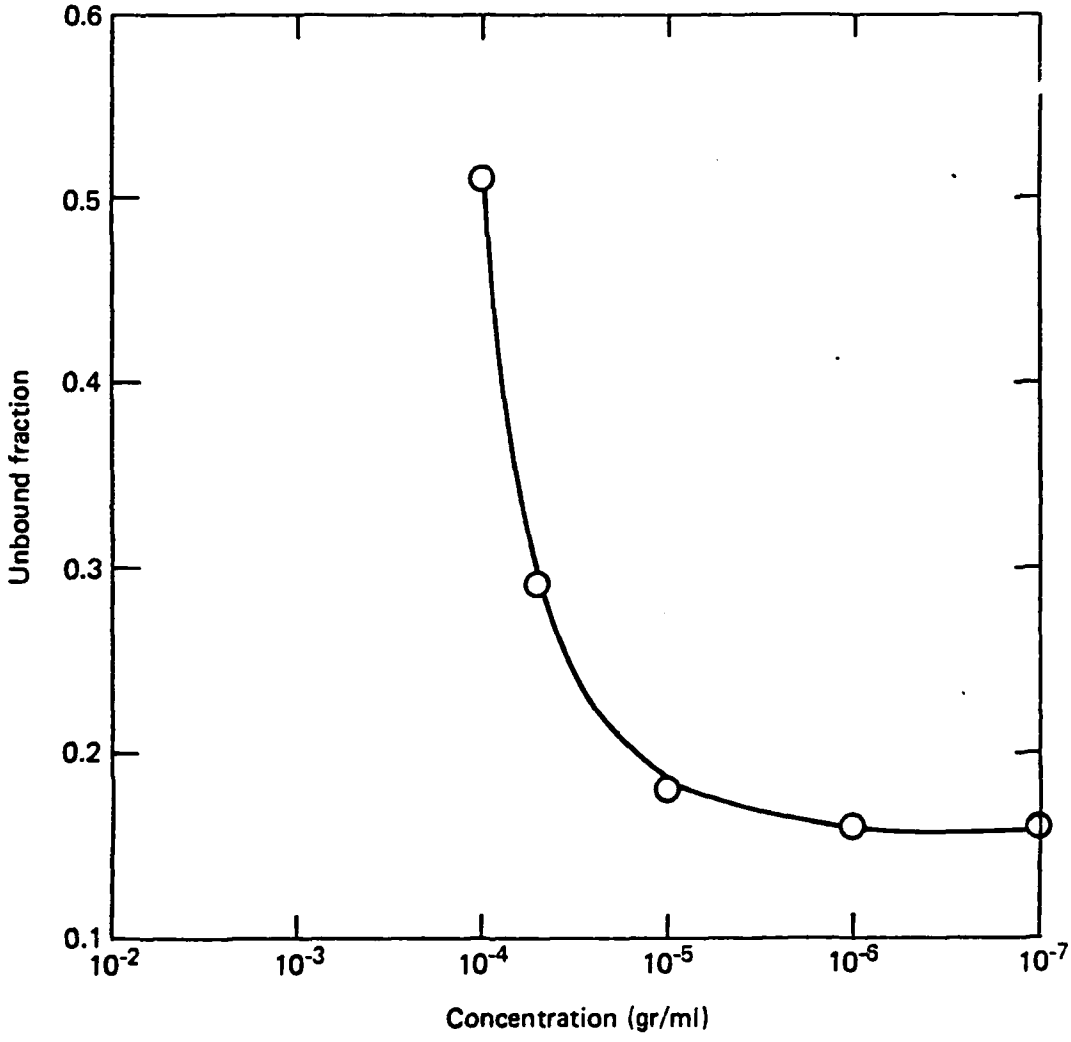
0.6
0.5
0.4
0.3
0.2
0.1
Unbound fraction
10^{-2}
10^{-3}
10^{-4}
10^{-5}
10^{-6}
10^{-7}
Concentration (gr/ml)

Fig. 27

Retinal Reflectivity

Objective

The objectives of this project are to document the progression of laser induced retinal damage, to determine the optimum wavelength for the detection by photographic methods of laser retinal damage and to aid in the determination of the mechanisms of laser induced retinal changes.

D.J. Lund[1] has shown that the visibility of infra-red laser retinal burns changes dramatically as the post irradiation time is increased from immediately after the laser irradiation to one year later. At short times after the irradiation the laser burns are most easily seen in photographs taken with monochromatic light photographs using wavelengths in the blue or green spectrum. As time progresses the burns are more readily seen at longer wavelengths. After the burns are one year old they are invisible in blue or green monochromatic photographs, can barely be seen with red light photographs but are easily seen in photographs taken in the near infrared around 800 to 850 nm.

Kornup[2], Behrendt[3, 4] and Delori[5] have advocated the use of variable wavelength examination of the retina with monochromatic light. Different retinal layers are most easily seen at a specific wavelength. The wavelengths they have used have extended from 400 to 700 nm. Monkey retinas have been photographed to longer wavelengths, beyond 900 nm by Hochheimer.[6] As the wavelength increases deeper layers of the retina become visible because retinal pigments and blood become more transparent.

It should be possible to determine what retinal layers are initially damaged and the changes in damage that occur with time if the changes in spectral reflectivity of the damaged retinal area is precisely known as a function of time after the damage occurs. Changes in retinal reflectivity

during and immediately after the time when the laser beam irradiates the retina will provide some knowledge of what is occuring in the retina when it is being damaged by a laser.

We also wish to objectively document, and if possible determine the origin of the retinal "clouding" effect reported by Beatrice and Lund[7] that is seen when the retina is irradiated with an infra-red laser at low levels.

Background

Accurate measurement of retinal reflectivity is not easily accomplished. In the section of this report on scattered light, the published data for several investigators is given. These published results vary over wide ranges, they are highly dependent on the method chosen as well as the animal species used. Our first measurements[5] are probably as bad as anyone elses.

In addition to the problems associated with scattered light our first reflectance measurements were made using photographic techniques. The photographic process, under the very best conditions, is not well adapted to accurate measurements of light intensity. The photographic process is non-linear and has only a low dynamic range. Very minor changes in processing can induce large variations in the results. If the spatial information that is available with retinal photography is not important than photometric techniques are much superior for the determinates of retinal reflectivity.

For documentation of retinal changes during irradiation we first used 16 mm photography. The resolution was poor and the intermittent spacing of the photographs combined with the intermittent retinal exposures to the pulsed YAG laser caused innumerable interpretational difficulties. 16 mm photography could not be used in the near infrared because of low film sensitivity.

A silicon diode television camera was used to record near infrared retinal pictures, the results were unacceptable because of poor resolution and low dynamic range. 35 mm film recording was used, again the results were disappointing. Time exposures were necessary to record data during laser exposure and resolution was poor due to saccadic eye movements. An analysis indicated that photometric measurements, similar to that useful for measurements of retinal reflectivity, should be a big improvement over photography for documentation during the exposure of the retina to the laser beam.

Our first attempt at the use of white light, a monochrometer and a photomultiplier to measure retinal reflectivity was also unsuccessful. We realized that if scattered light was to be minimized that only a small area of the retina should be illuminated. Apertures were inserted at appropriate retinal conjugates in our fundus camera to limit the illuminated retinal area. This area was reimaged by the fundus camera to a small aperture that was reimaged onto the slits of a small grating monochrometer and photomultiplier. The photomultiplier signal was amplified with a d.c. amplifier. The monochrometer was activated by a computer which recorded, analyzed and outputed the data.

The light input optics on the Zeiss fundus camera were designed to flood a 30° field of the retina uniformly with light. Our aperture size was less than 100 microns (referred to the retina) and exhibited a large amount of color fringing due to chromatic aberration. The lateral chromatic aberration was estimated to be in excess of 50 microns.

The grating monochrometer was very slow, a spectrum took almost five minutes to record. The resolution, approximately 10 nm was more than adequate.

The retinal image was apertured to accept energy from the illuminated area, it was only slightly larger than this area. It was presumed to be centered over the illuminating area by moving the input light aperture until a signal maximum was obtained. We did not know the exact location of the retinal image aperture.

The d c amplifier had some drift that caused inaccuracies at the lower signal levels. The A/D converter was an 8 bit converter and while this was perfectly adequate at high signal levels, it did lack the necessary dynamic range.

Even with all of these limitations we did show that it is possible to obtain photometricly useful, if not particularly accurate, spectral reflectivities for small retinal areas. This initial configuration also defined what improvements were necessary to obtain the desired accuracy.

Equipment Modifications

The light input system optics in a Zeiss camera consists of three groups of lenses. We removed entirely the flash lamp condensing system since this is not needed for our application. The next two lens groups were replaced with high quality photographic objectives, each lens is separately aberration corrected. A small area of the retina can now be illuminated with the only remaining detectable aberrations being those of the eye itself. For the visible spectral region this should be less than a few microns.

We can illiminate an area of the retina as small as fifty microns. This reduces internal light scatter in the eye to a small value if only a small retinal area is measured. Suitable baffels and stray light stops were incorporated both in the input light system and in the collection light system to eliminate any external optical system stray light. (See the section on

scattered light in the eye).

The retinal area to be measured can be examined by a low power microscope that views the retinal image. We are now absolutely certain as to the retinal area being measured.

The grating monochrometer was replaced with a rotating interference monochrometer. This is a continuously variable interference filter arranged as a circular annulus on a glass plate backing. This variable interference filter is arranged in two halves. One half circle transmits from 400 at one radius to 700 at the opposite radius. The other half circle goes from 700 to 1300 nm. This monochrometer is driven by a stepper motor (400 steps per revolution) at speeds up to ten revolutions per second. A complete spectrum can be obtained at speeds only limited by the time constants necessary to obtain a suitable signal to noise ratio in the output. The stepper motor can be either allowed to free run under with own power supply or else it is controlled by a computer.

When this system was first tried we used a Princeton Applied Research signal averager to record the spectral output from the retina and from a grey artificial eye retina. The ratio of these two spectra supplies the retinal reflectivity, the ratio is automatically computed by the signal averager. The signal averager output is to an X-Y recorder, this recording takes almost two minute and limits the time between spectral runs. The signal averager has a digital output that is in a 20 bit parallel, word serial format. This is not compatible with our computer input.

We now have a 6 1/2 digit voltmeter that has acquisition rates orders of magnitude greater than we utilize. It is directly linked to the computer via a 488 bus line. The voltmeter can be configured by the computer, it will internally store up to 100 data points that can be sent to the computer in a few milliseconds. Voltage readings are triggered by the computer. With 6 1/2 digits available both large and small signal levels are conveniently handled without even using the automatic ranging capabilities of the voltmeter.

Initial Data

In September 1982, a cynomolgus monkey retina was irradiated with a YAG laser and an easily visible lesion formed. The spectral reflectivity of this area was measured one hour after irriadiation and again in October and November. These curves, along with those from a non-irradiated area adjacent to the burned area, are shown as Fig. 1. This data was taken using the signal averager, each curve is the average of 20 individual sets of data. Each set took less than one second and after an average of 4 data sets there was no detectable change in the averaged signal.

This data was taken before our digital voltmeter was acquired. Since then, retinal reflectivity curves have been taken utilizing the computer and voltmeter. Examples of these are given in the fluorescence section of this report.

We now have the necessary system to record accurate retinal spectral reflectivity curves over defined (and known) retinal areas. Scattered light and optical aberrations have been reduced to a level well below our recording accuracy at least for the 400 to 700 nm spectral region. We can record

to 850 nm, this is limited by the photomultiplier long wavelength response. The long wavelength accuracy will be limited by chromatic aberration and scattering to a value that is presently indeterminate.

Future Tests

Monkeys will have their retinas irradiated with a pulsed YAG laser. Spectral reflectivity curves will be recorded during and after exposure. At weekly intervals for several months, then at monthly intervals, data will also be recorded. A program for this series of tests has been given in our proposal for 1983/84.

References

1) Lund, D.J. and Beatrice E.S.
"Spectral Photography of Retinal Lesions"
Supp Invest Ophthal and Vis Sci., April 1979, p.51

2) Kornerup, T.,
"An Investigation, in Successively Variable Monochromatic Light, of Vessels of the Human Eye in Diseased Conditions"
Acta Ophthal 4, 5, (1947)

3) Behrendt, T. and Wilson, L.A.,
"Spectral Reflectance Photography of the Retina"
Am. J. Ophthal., 59, 1079, (1965)

4) Behrendt, T. and Duane, T.D.,
"Investigation of Fundus Oculi with Spectral Reflectance Photography" Arch. Ophthal., 75, 375, (1966)

5) Delori, F.C., Gragondas E.S.,
"Examination of the Ocular Fundus with Monochromatic Light"
Ann Ophthal, 8, 703, (1976)

6) Delori, F.C., Gragondas E.S., Francisco,
"Monochromatic Ophthalmoscopy and Fundus Photography: The Normal Fundus"
Arch Ophthal 95, 861, (1977)

7) Ducrez, N.M., Delori, F.C. and Gragondas, E.S.
"Monochromatic Ophthalmoscopy and Fundus Photography: The Pathologic Fundus"
Arch Ophthal 97, 288, (1979)

8) Hochheimer, B.F.
"Light Reflected from Small Areas of a Monkey Retina"
J. Bio. Photo 45, 146, (1977)

9) Beatrice, E.S., Lund, D.J., Carter M and Talsma, D.M.
"Retinal Alterations Produced by Low Level Gallium Arsenide Laser Exposure"
LAIR Report #38, Feb., 1977

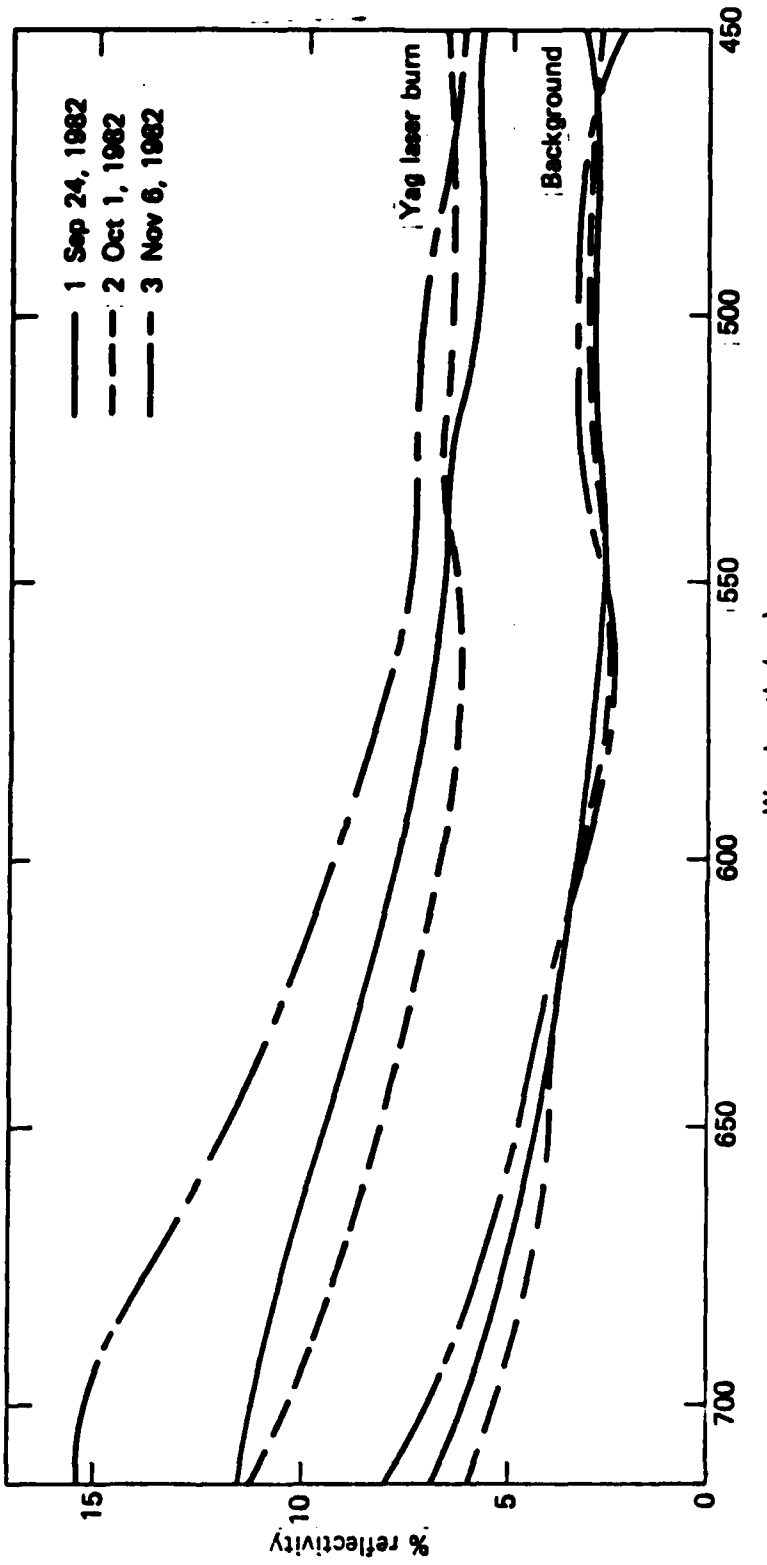
1 Sep 24, 1982
2 Oct 1, 1982
3 Nov 6, 1982
Yag laser burn
Background
% reflectivity
15
10
5
0
450
500
550
600
650
700
Wavelength (nm)

Fig. 1

Hematoporphyrin Dye Studies

Introduction

The work of Ham[1], Sperling[2] and Lawuill[3] show that there can be non-thermal light induced retinal eye damage. This usually termed photochemical damage although there is known damage mechanism[4]. Since there is reported evidence for second harmonic generation of light in the eye[5,6] and specifically in the cornea[7] we measured the efficiency in the rabbit cornea[8] and found a conversion value too low to be of any concern for damage to the retina. Another possibility for a mechanism for photochemical retinal light damage is the generation of singlet oxygen or peroxide radicals[9].

Oxygen absorption bands occur at the YAG and gallium arsenide laser wavelength[10] and Lund's[11] data on retinal damage thresholds in the red and near infrared show a reduced value near the 2-0 oxygen absorption band.

It is possible to raise oxygen to the excited singlet state by laser irradiation without the use of any dye. The 1-0 vibrational absorption band in oxygen is quite broad with a peak value nearly coincident with the 1.06 micron YAG laser emission line (10). Oxygen irradiation with the YAG laser has already been shown to produce significant quantities of singlet oxygen 0^2 $(^1\Delta g)$[12]. Parker[13] has used YAG laser irradiation to reduce coliform count in water and Frank[14] has reported the successful treatment of bladder tumors with the YAG laser. In order to test for the possibility of singlet oxygen production by light in the retina we have tried several indirect approaches. Glutathione is a known singlet oxygen quencher and is normally present at low levels in the retina[15]. We subjected a monkey retina to low levels of white light for periods of 20, 10, 5 and 2-1/2 minutes. The 20 minute exposure showed extensive retinal involvement while the 5 and 2-1/2

minute exposure showed no visible indication of change by either visible examination or by fluorescein angiography. The monkey was then given massive doses of glutathione, 1 gram per kilogram of body weight, every day for five consectuve days and then we irradiated the other retina in the same manner as the first one. There was no change in the appearance of damage, the 20 and 10 minute exposures produced damage and the 5 and 2-1/2 minute exposures did not. We do not know if the retinal levels of glutathione were increased so that this experiment was inconclusive.

Dougherty[16,17] has shown that when hematoporphyrin dihydrochloride is intravenously injected it will preferentially accumulate in tumor cells. If the tumors are irradiated with red light the tumor is killed. Experiments were performed that indicated that the interaction of light and hematoporphyrin produced singlet oxygen and that the singlet oxygen destroyed the tumor cells. Although the hematoporphyrin is preferentially absorbed by tumor cells it also accumulates in all body tissues[16]. If the interaction of light and hematoporphyrin does indeed produce singlet oxygen this reaction should mimic light induced retinal photochemical damage of the photochemical damage is due to singlet oxygen. Several experiments were carried out to test this hypothesis.

It is interesting to note that Dougherty's[18] early experiments were carried out using fluorescein dye. While not as efficient as hematoporphyrin the same results were found, tumors were killed by the interaction of light with fluorescein dye.

Rabbit Experiments

V_2 rabbit carcinoma[19] was implanted in rabbit corneas and allowed to grow and become vascularized. The rabbit was given an intravenous injection of hematoporphyrin dye and the next day the cornea was irradiated with a helium

neon (632.8 nm) laser. The entire eye suffered massive damage, including gross retinal detachment. The tumors however were not completely destroyed, only partially so.

Another rabbit had one retina exposed to a HeNe laser in order to find the level needed to produce an easily visible lesion. At one half the level needed to produce this lesion no visible lesions were formed. The lesion size on the retina was very small, certainly less than 50 microns. The rabbit was then injected with hematoporphyrin dye and after one hour the other retina was irradiated with the HeNe laser at a dose one tenth of that needed to produce a visible lesion in the first retina. The hematoporphyrin-laser energy combination produced lesions in the rabbit retina more than ten times the diameter of the lesion produced by the laser without the hematoporphyrin.

Another rabbit was given an injection of hematoporphyrin and its retina irradiated ten times with a HeNe laser. For each of these irradiations the product of laser power and irradiation time was kept constant. The time was varied from 10 to 2400 seconds. Visible lesions were produced only at the intermediate times. The short, less than 40 sec, and long, greater than 600 sec, exposures produced no visible damage.

These rabbit experiments were reported last year, they are briefly reported here for a better understanding of our cell culture studies.

Cell Culture Experiments

Confluent cultures of rabbit Greene melanoma cells 20 were grown in 3.5 cm^2 dishes in RPMI 1640 with 10% fetal calf serum, 200 μ/ml Penicillin G and 200 μg/ml Streptomycin Sulfate. 150 g of hematoporphyrin derivative was added per ml of media. After one hour of incubation in the dark at 37°C with 5% CO_2, the media was removed, the monolayers washed two times with basic salt solution and then fresh RPMI 1640 was added. The cultures were kept in the

dark through the entire experiment. After one hour incubation in fresh media the cultures were irradiated with a 10 mm diameter beam, 20 mW power, from a Helium-Neon laser. The irradiation times were as follows: 1) 15 sec.; 2) 30 sec.; 3) 1 min.; 4) 3 min.; 5) 5 min.; 6) 7.5 min.; 7) 10 min.; 8) 15 min.; 9) 20 min.

After irradiation the cultures were incubated for one hour, then fixed in gluteraldehyde paraformaldehyde overnight. The cells were then dehydrated in methanol and stained with Wright's-Giemsa.

Fig. 1 is a photograph of the 3.5 cm^2 dishes after irradiation. Note that there is an ever increasing diameter of killed cells. The dead cell area in the 3 min. exposure is one cm in diameter, the irradiated area. Although it cannot be fully appreciated in these pictures there is a rather clear ring area surrounding the irradiated area and in this area the cell kill is 100% while inside the ring the cell kill is usually less than 100%. This ring diameter increases with increasing radiation time until at 20 minutes it is almost 1.5 cm diameter.

Discussion

Thorne[2] et al have suggested that tumors are destroyed by the dye-irradiation technique by oxygen starvation (anoxia) and not by singlet oxygen damage. His argument is based on the assumption that each photon absorbed by the dye will remove one molecule of oxygen from the tissue. If oxygen input to tissue is at a rate of 2.8×10^{-9} moles/sec for each gram of tissue and if 600 nm photons are used at a rate necessary to consume this amount of oxygen, then the power required is only 0.55 mW/gram of tissue. These assumptions are overly simplified. All the input energy is not absorbed by the dye, not every absorbed photon produces one singlet oxygen molecule, and some singlet oxygen molecules will decay to normal oxygen rather than be lost in a reaction. On

the other hand, complete loss of all oxygen is not necessary for cell death, it is only necessary to remove sufficient oxygen so that cells are asphyxiated.

Zemel and Hoffman[22] have investigated triplet energy transfers in hematoporphyrin and they conclude that, in a closed porphyrin - O_2 system, all of the O_2 can be consumed by singlet oxygen production and then the subsequent reaction of singlet oxygen and porphyrin. They point out that this is the reason for the destruction of porphyrin not stored in the dark. Porphyrin stored under anaerobic condition, O_2 replaced by N_2 in the solution, does not decay even under fairly intense illumination.

Consider some of the possible reactions that might occur as a result of the interaction of a dye molecule and light. (Table I). Equation 1 and 2 are the normal dye excitation and fluorescence. Equation 3 is the triplet excitation of the dye molecule. Singlet oxygen is produced by interaction of the dye molecule in the triplet state and a ground state oxygen molecule, Equation 4. The dye molecule itself can interact with oxygen, Equation 8 and 9, to consume oxygen. These are the usual dye decomposition steps. The addition of an oxygen quencher can remove oxygen by Equation 5 to prevent the quenching of singlet oxygen with the oxygen bound to the quencher and Equation 7 is the quenching with the release of free oxygen. There are other possible reactions and also possible intermediate steps that are ignored in this discussion. They may, however, be very important in any real reaction situation.

Steps 5, 6, 8 and 9 all remove oxygen from the system. Step 6 is the singlet oxygen interaction which is presumed to cause tissue destruction. A quencher can stop the formation of singlet oxygen by using up some of the

available oxygen, Step 5, or it can combine with singlet oxygen, Step 6, to prevent singlet oxygen damage to tissue.

All of these reactions are determined by rate equations with often widely varying rate constants. These rate constants can be affected by the amount of reaction materials present or can be affected by non-reacting catalytic molecules. In most cases, it is impossible to solve the reaction equations exactly.

It should be possible to determine if tumor destruction is due to anoxia or singlet oxygen. If due to singlet oxygen, irradiation, at a constant product of time and intensity, should always produce the same cell death, independent of intensity. If the destruction is due to oxygen deprivation, then there should be some low intensity value below which cells will not die no matter what the irradiation period is.

Weishaupt et al[23] have used a known oxygen quencher (1, 3 - diphenylisobenzofuran) along with hematoporphyrin and reported that the quencher, when present in amounts above 1.5×10^{-3} M intracellurlarly, protected cells from indirect light damage. Their conclusion was that it is indeed singlet O_2 that is killing cells. It may be that the quencher quenched the hematoporphyrin triplets or caused the singlet O_2 to return to the ground state. According to Matheson and Lee,[24] the reaction returning O_2 to the ground state is competitive with the consumption of O_2.

In the retina it may make little difference if the singlet O_2 or anoxia kills the tumor if lack of oxygen is detrimental to tissue adjacent to the tumor. If this is the case, although a constant intensity-time product is needed to produce singlet O_2, a very low intensity may save the rest of the retina.

Retinal destruction by anoxia should be a diffusion controlled reaction. If oxygen is being consumed by a dye-light quencher reaction then the amount of oxygen available for sustaining retinal cells is determined by the rate of oxygen consumption. With short irradiation times and small irradiation areas tissue death from anoxia would not be expected as cells can exist for some short period without oxygen. For very long irradiation times with very low light levels, tissue death from anoxia would not be expected to occur because enough oxygen can diffuse in to overcome the small amount used up.

For the rabbit experiment where the retina was irradiated at a constant intensity x time product the irradiation levels and times are given in Table II. This table also gives average diffusion distances assuming a diffusion rate for O_2 of 10^{-10} cm^2/sec. This rate is consistent with diffusion rates with most liquid with a viscosity greater than water.

The distance between capillaries in a rabbit choroid is approximately ten microns, so that for times shorter than ten seconds, diffusion can have only a negligible contribution. At times greater than 1000 seconds, oxygen can diffuse into tissue at the same rate it is consumed. Since the average lifetime of $^1\Delta g$ O_2 is approximately 10^{-5} seconds, diffusion of this species can play no part in damage as seen in the rabbit retina.

From our rabbit experiments it seems as if anoxia may be the cause of retinal tissue destruction with irradiation and hemataporphyrin and not singlet oxygen.

Our cell culture studies are not as easily interrupted. The increase in diameter of destruction with increase in irradiation time could be attributed to oxygen starvation and controlled by the rate of oxygen diffusion. The increase cell death in a ring at the edge of the destroyed cells and the lack of complete kill in the center seems more likely to be caused by singlet

oxygen production. This also could be controlled by the rate of diffusion of oxygen. As oxygen diffuses into the irradiated area it is converted quickly to singlet oxygen to kill cells at the edge of the irradiated area. In the center of this area all of the oxygen has been used up by conversion to singlet oxygen and there is not a sufficient amount to kill all of the cells.

Lund, Adams and Carver[25] have reported on the effects produced in the retina by irradiation with a gallium arsenide laser. The predicted retinal spot configuration was that of an elongated rectangle 20 by 170 microns. The retinal burns in all cases were circular in nature, approximately 160μ in diameter at the ED_{50} level. The early visible lesions were circular and well-circumscribed, they were doughnut shaped, central punched-out area surrounded by a peripheral ring. Exposures of 2X the ED_{50} power level produced lesions closely resembling the lower power level lesions except that they were larger in size, approximately 280 microns in diameter. The wavelengths used for these experiments was 860 nm.

Our rabbit experiments and especially our cell culture experiment produces results that very closely resemble the gallium arsenide laser burn experiments of Lund et al. This resemblance would suggest that anoxia might play some part in the retinal damage produced by the gallium arsenide laser as well as the possibility of some singlet oxygen effects.

Future Experiments

Several cell culture experiments are planned for the near future, hopefully this year.

1. Cell cultures of various cell types are being successfully grown at Wilmer Institute. These include endothelial rod outer segments, and pigment epithelial types. Although in most cases the cultured cells only have a resemblance to the cells grown in the eye itself. They are truly the desired

cell types. Hematoporphyrin will be incorported in these cells, they will then be irradiated with light at discrete wavelenghts with variable times and intensities. We hope to find the action spectrum for these time and intensities for the various cell types. A comparison can then be made with light induced non-thermal retinal damage.

2. The Green melanomas we used were grown in a medium that contained known singlet oxygen and oxygen radical quenchers including glutathione. Cells will be grown and transferred to a medium that does not contain these quenching agents.

In addition to these cell cultures we can add known quenching agents. Carotenoids[26] and ascorbic acid[27] are known quencher of singlet oxygen. It may be possible to choose a quenching agent with affinity for only certain cell types.

A variety of cell types will be grown with and without quenchers and hematoporphyrin. There can be irradiated with light of different spectral composition, times and intensities to study the interactions.

3. We have tried injected glutathione to protect the retina from photochemical damage. Other quenchers such as carotenoids or ascorbic acid could also be used in a similar manner. The uptake of these substances in the retina would be measured only if some effect due to their injection occurs.

Another possibility is to take advantage of an endogeneous quencher for singlet oxygen, trans-retinol[28]. If the retina is photobleached retinol is converted from the cis to the trans creating a large pool of endogeneous quencher.

Animal experiments, as suggested, will only be done if suitable additional funding is obtained.

References

1) Ham W.T., Mueller H.A. and Ruffolo J.J.
"Retinal Effects of Blue Light Exposure:
SPIE 229, 46, (1980)

2) Harwerth R.S. and Sperling H.G.
"Effects of Intense Visible Radiation on the Increment-Threshold Spectral Sensitivity of the Rhesus Monkey Eye"
Vis. Res. 15, 1193, (1975)

3) Law will, T., Crockett, S. and Currier G.
"Functional and Histological Measures of Retinal Damage in Chronic Light Exposure"
Doc. Ophthal 15, 285, (1977)

4) Sliney D. and Wolbarsht M.
Safety with Lasers and Other Optical Sources
Plenim Press, N.Y., 1980

5) Sliney D.H. Wangemann R.T., Franks J.K. and Wolbarsht, M.L.
"Visual Sensitivity of the Eye to Infrared Laser Radiation"
JOSA 66, 339, (1976)

6) Vasclenko L.S., Chebataev V.P. and Troitskii, Yiu, V.
"Visual Observation of Infrared Laser Emission"
Sov Phys JETP 21, 513, (1965)

7) Fine, S. and Hansen, W.P.
"Optical Second Harmonic Generation in Biological Systems"
Appl Opt 10, 2350, (1971)

8) Hochheimer, B.F.
"Second Harmonic Light Generation in the Rabbit Cornea"
App. Opt 21, 1516, (1982)

9) Lanum J.
"The Damaging Effects of Light on the Retina, Emperical Findings, Theoretical and Practical Implications"
Survey Ophthal 22, 221, (1978)

10) Cho C.W, Allen E.J. and Walsh H.L.
"Structure of the Infrared Atmospheric Bands in Liquid Oxygen"
J. Chem Phys 25, 371, (1956)

11) Lund D.J., Stuck B.E. and Beatrice E.S.
"Biological Research in Support of Project Miles"
Annual Rept. May 1981
Division of Biorheology, LAIR

D.J. Lind (private communication) has given me some of his preliminary data on ED50 data from a dye laser. There is a large reduction in the ED50 values for wavelengths around 850 to 900mm compared with those at 700 and 1060 mn.

12) Shields, J.
Survey of Ophthal 21, 443, (1977)

13) Parker, J.
"Laser Radiation Reduces Coliform Counts in Water"
Water and Sewage Works May (1976)

14) Frank (as quoted by Dougherty, T.)
Focus on the News p.12, Dec. 1979

15) McCay, P.B., Gibson D.D, Fong KL and Hornbrook, KR
"Effect of Glutathione Peroxidase Activity on Lipid Peroxidation in Biological Membranes"
Biochemica et Biophysica Acta 431, 459, (1976)

16) Dougherty, T.J., Kaufman, J.E., Goldfarb A. et al
"Photoradiation Therapy for the Treatment of Malignant Tumors"
Cancer Res 38, 2628, (1978)

17) Dougherty T.J., Gomer C.J., and Weishaupt K.R.
"Energetics and Efficiency of Photoinactivation of Murine Tumor Cells Containing Hematoporphrin"
Cancer Res 36, 2330, (1976)

18) Dougherty, T.S.
"Activated Dyes as Antitumor Agents"
J. Nat Cancer Inst., 52, 1333, (1974)

19) Folkman J. and Cotran R.
Int. Rev. Exp. Path. 16, 207, (1976)

20) Greene H. and Harvey E.
Cancer Res 26, 706, (1966)

21) Thorne, J.M., Kellis D.S. and Jones R.W.
"Tumor Growth Retardation with Photoactivated Dyes and Ar Laser Radiation"
Int'l. Conf. on Lasers, Orland Fl., Dec. 17, (1979)

22) Zemel H. and Hoffman B.M.
"Long-Range Triplet-Triplet Energy Transfer within Metal-Substituted Hemoglobins"
Am. Chem. Soc. 103, 1192, (1981)

23) Weishaupt K.R., Gomer C.J. and Dougherty T.J.
"Identification of Singlet Oxygen as the Cytotoxic Agent in Photo-inactivation of a Murine Tumor"
Cancer Res. 36, 2326, (1976)

24) Matheson, I.B.C. and Lee J.
"Reaction of Chemical Acceptors with Singlet Oxygen Produced by Direct Laser Excitation"
Chem Phy Lett. 7, 475, (1970)

25) Lund, D.J., Adams D.O. and Carver C.
"Ocular Hazards of the Gallium Arsenide Laser"
LAIR Report #30, October 1976

26) Foote C.S., Chang Y.C., and Denny R.W.
"Chemistry of Singlet Oxygen"
J. Am. Chem. Soc. 92, 5216, (1970)

27) Spikes J.D. and Livingston R.
"The Molecular Biology of Photodynamic Action: Sensitized Photoautoxidations in Biological Systems"
Adv. Rad. Bio. 3, 29, (1969)

28) Delmelle M.
"Retinal Sensitized Photodynamic Damage to Liposomes"
Photochem & Photobio. 28, 357, (1978)

TABLE I

S dye molecule, ground state

S^x dye molecule, excited state

T dye molecule, triplet state

0_2 oxygen molecule, ground state

$^1\Delta_g 0_2$ oxygen molecule, excited singlet state

Q_x quenching molecule

hv photon energy

1	$S + hv \rightarrow S^x$	dye excitation
2	$S^x \rightarrow S + hv$	fluorescence
3	$S^x \rightarrow T$	intersystem crossing
4	$T + 0_2 \rightarrow {}^1\Delta_g 0_2$	singlet 0_2 production
5	$Q_1 + 0_2 \rightarrow Q_1 0_2$	quenching of oxygen
6	$Q_2 + {}^1\Delta_g 0_2 \rightarrow Q_2 0_2$	quenching of singlet oxygen, oxidation
7	$Q_3 + {}^1\Delta_g 0_2 \rightarrow Q_3 + 0_2$	quenching of singlet oxygen
8	$S + {}^1\Delta_g 0_2 \rightarrow SO_2$	quenching by oxidation of dye molecule
9	$S^x + 0_2 \rightarrow SO_2$	quenching by oxidation of dye molecule

TABLE II

Laser Power Level (watts)	Irradiation Time (sec)	Damage Spot Size (microns)
6.1×10^{-3}	10	-
3.0	20	-
1.5	40	-
0.75	80	350
0.75	160*	400
0.40	160	250
0.20	300	200
0.10	600	-
0.05	1200	-
0.02	2400	-

* an extra spot was inserted at 2 IT for identification purposes.

Time (seconds)	Average Diffusion Distance
1	0.15 μ
10	0.4 μ
100	1.5 μ
1000	4.0 μ
10000	15 μ

0_2 diffusion rate (D) assumed to be 10^{-10} cm^2/sec, either 0_2 or $^1\Delta_g 0_2$

Average diffusion distance $x = \sqrt{2Dt}$

Lifetime $^1\Delta_g 0_2$ approximately 10^{-5} seconds.

Fig. 1

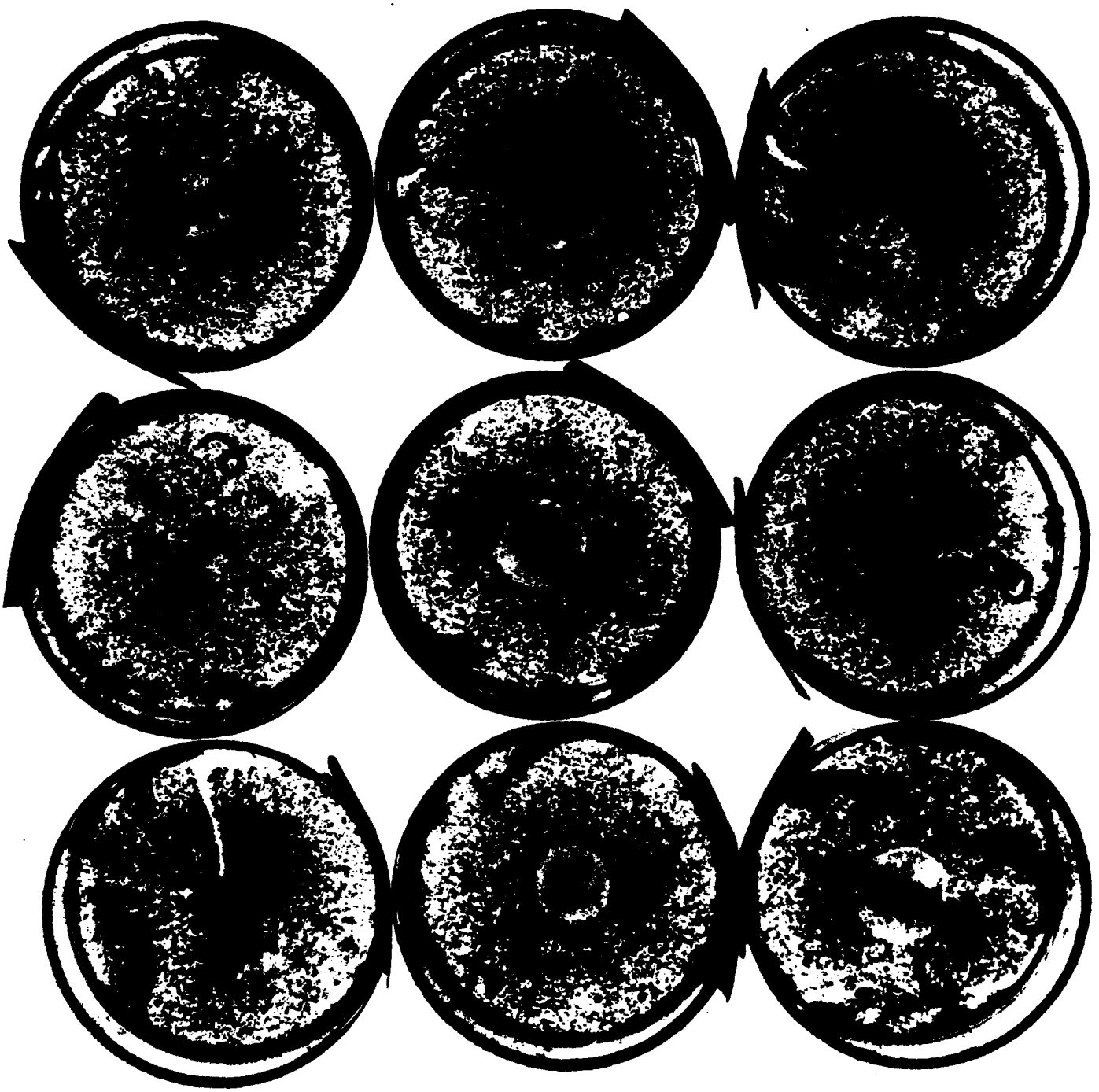

Dyed Tear Films for Laser Eye Protection

Introduction

Protection for soldiers in the field from the effects of laser radiation is desirable even if the protection is temporary and limited. Since the eye is the most vulnerable area for visible or near infrared lasers and eye damage can render militasry personnel incapable of performing vitally necessary tasks, protection of the eye from laser radiation is important.

Dyed artifical tear films may provide a ten fold increase in the damage threshold level from 532 nm irradiation, the frequency doubled YAG wavelength. A dye used in tear films must be water soluble, non-toxic, have a high coefficient of absorption at 532 nm and be highly transparent at all other wavelengths.

There are several good compilations of available dyes:

1. Sadtler Research Laboratories
   3316 Spring Garden Street, Philadelphia, Pa.
   Commercial spectra of ultraviolet and visible dyes is a listing of almost 600 spectral dye absorption curves.

2. Edward Gurr's Synthetic Dyes in Biology, Medicine and Chemistry,
   Academic Press, N.Y., 1971
   The composition, solubility and spectra of almost all of the availabe dyes used in biology is tabulated.

3. B. F. Hochheimer
   Third Year Progress Report, NIH Contract #NO1-EY-3-2139
   "Evaluation of Indicator Substances for use in the study of the Retinal and Choroidal Circulations," July 1, 1976
   Over 700 dyes were tested for solubility, toxicity and spectral characteristics for use in angiography.

These three sources plus several minor compilations were searched for useful substances. The only suitable dyes seem to be the fluorescein derivatives, Phloxine B, Erythrosine B and Eosin Y.

Dye Characteristic

These three dyes have intense absorption bands near 532 nm. The absorption spectra are shown as Figs. 1,2, and 3 for saline and Hypotears solutions. Hypotears are lubricating eye drops produced by Coopervision Pharmaceuticals Inc., San German, Puerto Rico, USA. It is polymer solution used to treat dry eye conditions and is similar to several other products used for the same purpose.

One important thing to notice in the absorption spectra is the wavelength shift that occurs with a change in solvent. Our first tests indicated that Phloxine B would be almost ideal, the spectra were run in saline solutions. Eosin Y would be a much better choice of Hypotears solutions are used since the peak absorption is shifted very close to 532 nm.

The absorbance of these dyes in water solution is:

1) Phloxine B - 1.0
2) Erythrosine B - 0.8
3) Eosin Y - 0.8

These values are almost the maximum obtainable with any dyes. These dyes have significant absorption from 500 to 550 nm and are almost transparent at other wavelengths.

Caution Notes

These dyes are all fluorescein derivatives, they have been widely used for biological stains, a plaque stain for teeth, cosmetic use and red inks. All are highly fluorescent dyes. All of the fluorone dyes have some triplet state reactions, eosin and erythrosine have the highest values. The long term toxicity of these reactions are not completely understood in biological systems. The short term toxicity is quite low.

Dyed Contact Lenses

Soft contact lenses can be easily dyed a variety of colors. The requirements for dyes for this purpose is very different than for tear film solutions. The dyes must be insoluble in water but soluble in either DMSO or Di-methylformide so that they can be diffused into the lenses and not be dissolved with tears. Several dyes are presently used, these are produced by Basf-Dye Corp., 100 Cherry Hill Road, Parsippany, New Jersey under the trade name Neo-Zapan dyes.

The Neo-Zapan dyes have fairly broad absorption bands and may not be useful for our purposes. Several cyanine dyes may have the necessary properties that are needed. These are NK 1149 and NK 1518 produced by the Nippon Kankoh-Shikiso Kenkyusho Corp., of Okayama, Japan. Cyanine dyes have very strong absorption bands but can be toxic. The toxicity of these dyes is relatively high when administered intraperitoneally but this may not interfere with their use in contact lenses if the water solubility is low enough.

It is also feasible to dye plastic with rhodamine dyes that have absorption characteristics similar to the fluorones. These could be used as protective eyeglasses or hard contact lenses.

Future Plans

The only frequency doubled YAG laser we have is a Q switched General Photonics System. When used in the Q switched mode it radiates an electromagnetic signal that interferes with all of our electronic measurement systems. We are constructing a new system for retinal irradiation with a variety of incoherent and coherent light sources. This system will incorporate shielding for pickup of stray electronic noise. When this system is finished we will test drops for protection of laser radiation using pigmented rabbits. The degree of protection as a function of time after the drops are instilled will be determined.

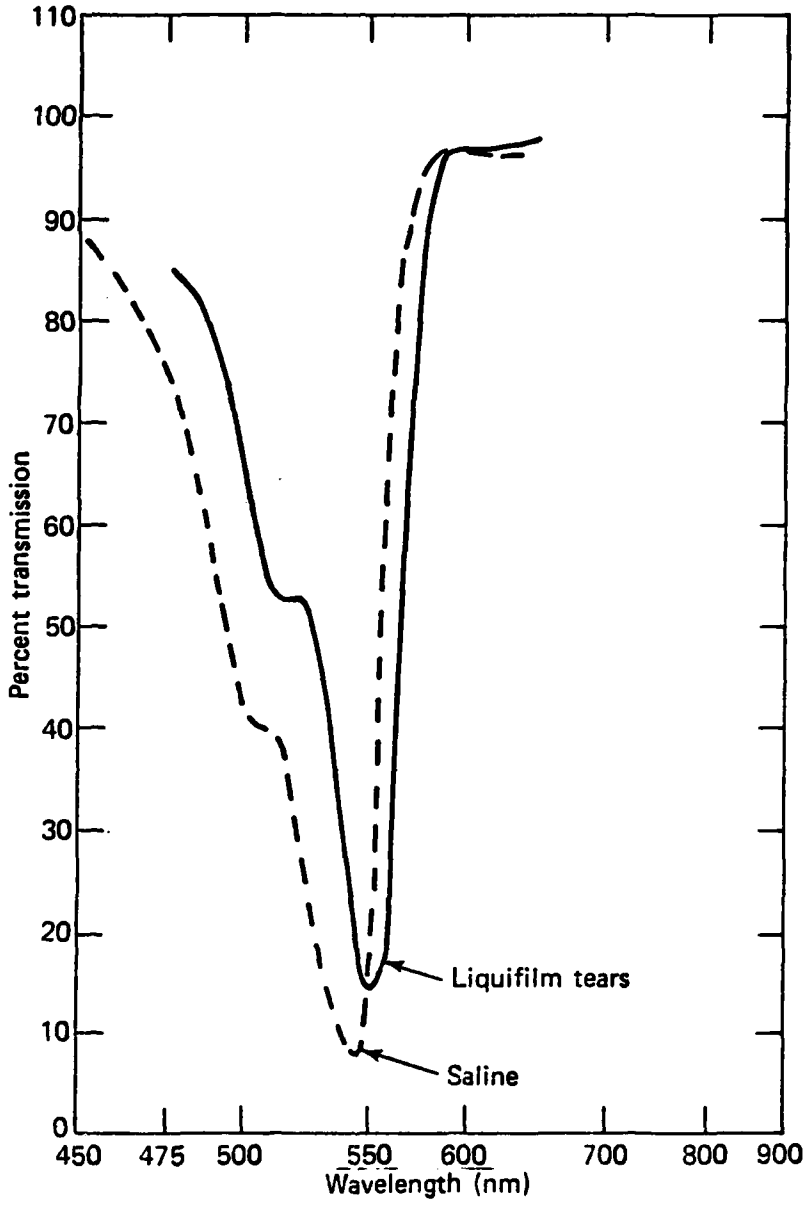

PHLOXINE - B

Fig. 1

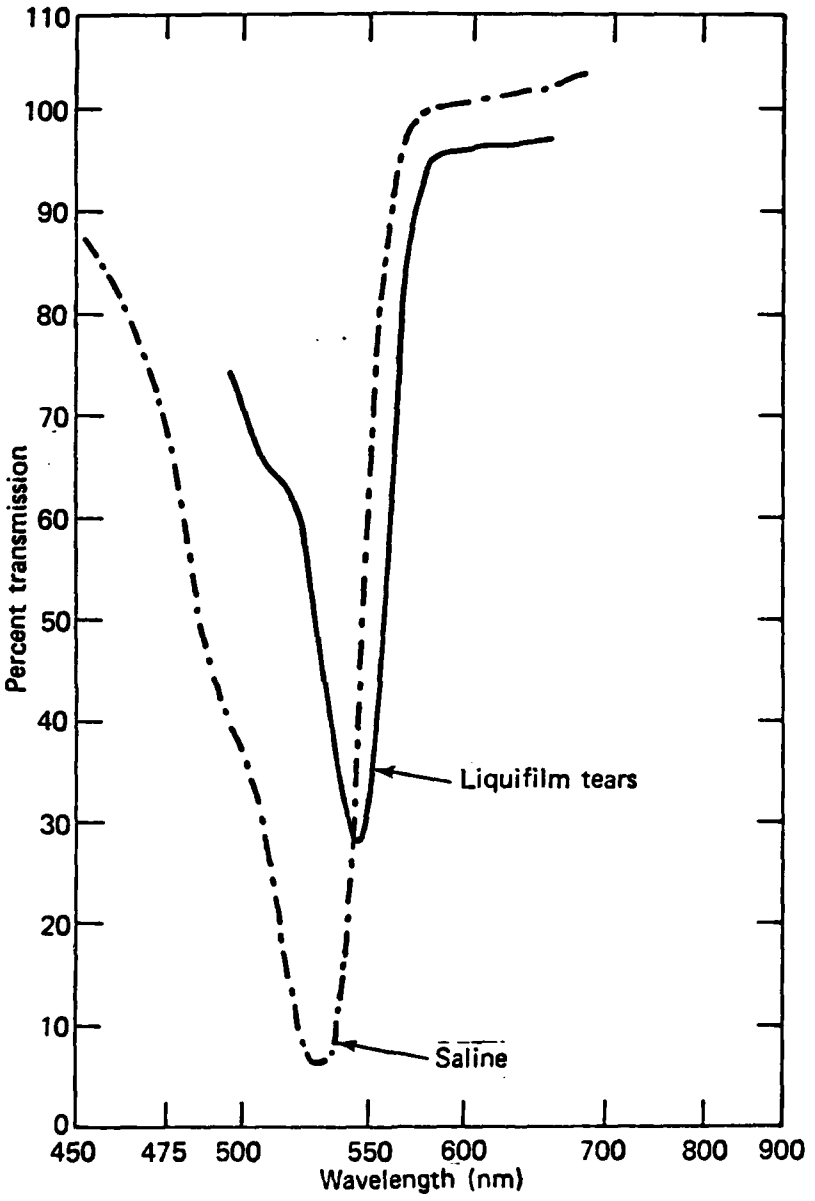

ERYTHROSIN - B

Fig. 2

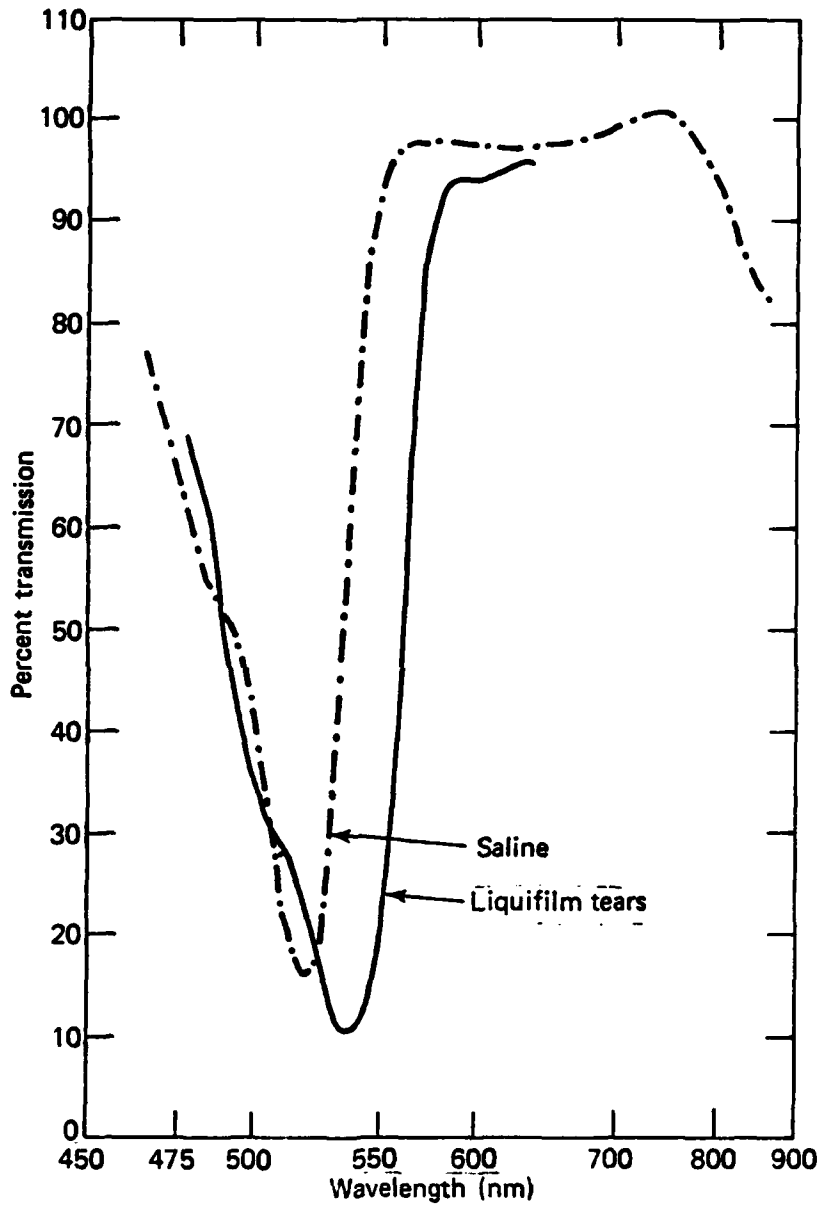
110
100
90
80
70
60
50
40
30
20
10
0
Percent transmission
450
475
500
550
600
700
800
900
Wavelength (nm)
Saline
Liquifilm tears

EOSIN - Y

Fig. 3

Improved Resolution Fluorescein Angiography

We have worked for many years at improving fluorescein angiograms by optimizing the photographic process as it is applied to this technique.[1,2]

During this past year, this optimization process was successfully used to obtain high resolution retinal fluorescein angiograms using conventional unmodified fundus cameras. The increase in resolution is approximately 2X, however, it is the improvement in contrast that is most striking. High contrast, high resolution angiograms may be obtained using Kodak #2415 Technical Pan Film (estar A-H base). This film is rated as having extremely fine grain and extremely high resolution, 400 lines/mm. #2415 film has an extended red and blue sensitivity, the green sensitivity of this film is very low compared to that of Tri-X film. However, processing this film in Kodak D-19 developer for 9 min. at 68° will yield excellent angiograms. The film should be agitated for the first 30 sec and then for 5 sec every 30 seconds. The film is then fixed in Kodak rapid fix for two minutes.

The angiograms (Figs 1,2) were obtained using a Zeiss fundus camera and a Zeiss 260-P power supply. Because of the low speed of Kodak #2415 film; the power supply must be set at flash setting #4, which has a recycle time of 2 seconds. Because of the time lost between frames, some of the transit data is lost, but in many circumstances this is not a hindrance.

Reference 1. Antoniadas, S.N. and Hochheimer, B.H.
"Developing films for high speed, high resolution and high gamma"
J. Bio Photo, 48, 167,(1980)

2. Hochheimer, B.F. and D'Anna S.A.
"Angiography with Dyes"
Exp Eye Res, 27, 1, (1978)

Fig. 1

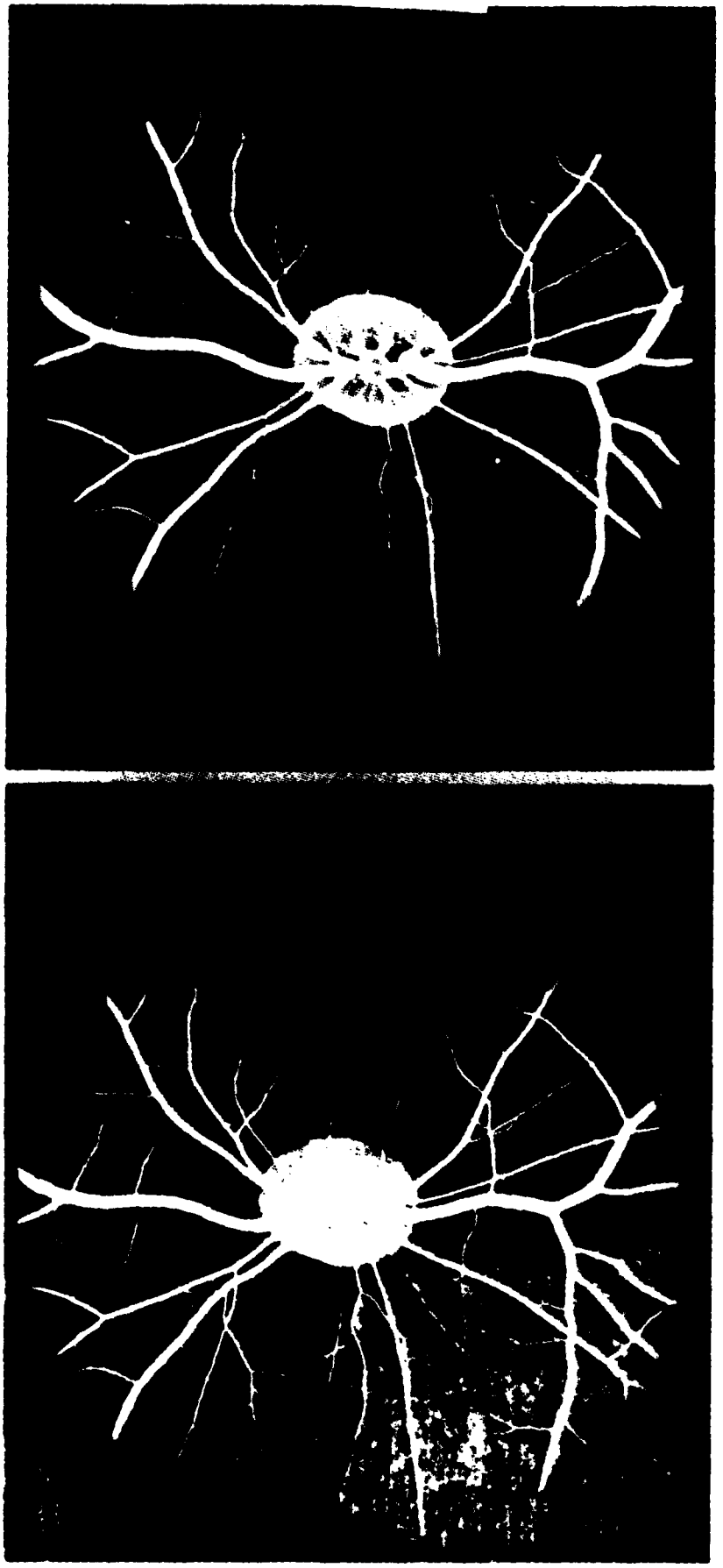

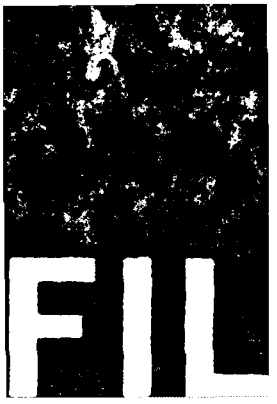
FIL